Multimodal Characterization of Microglia Heterogeneity in Aging and Alzheimer's Disease Pathology

DISSERTATION

zur Erlangung des Grades eines
Doktors der Naturwissenschaften

der Mathematisch-Naturwissenschaftlichen Fakultät
und
der Medizinischen Fakultät
der Eberhard-Karls-Universität Tübingen

vorgelegt
von

Desirée Brösamle
aus Albstadt-Ebingen, Deutschland

2024

Tag der mündlichen Prüfung: 26.01.2024

Dekan der Math.-Nat. Fakultät: Prof. Dr. Thilo Stehle
Dekan der Medizinischen Fakultät: Prof. Dr. Bernd Pichler

1. Berichterstatter: Prof. Dr. Jonas Neher
2. Berichterstatter: Prof. Dr. Kay Nieselt

Prüfungskommission: Prof. Dr. Jonas Neher
Prof. Dr. Kay Nieselt
Prof. Dr. Stefan Bonn
Dr. Nicolas Snaidero

Eidesstattliche Erklärung:

Ich erkläre, dass ich die zur Promotion eingereichte Arbeit mit dem Titel:
„Multimodal Characterization of Microglia Heterogeneity in Aging and Alzheimer's Disease Pathology" selbständig verfasst, nur die angegebenen Quellen und Hilfsmittel benutzt und wörtlich oder inhaltlich übernommene Stellen als solche gekennzeichnet habe. Ich versichere an Eides statt, dass diese Angaben wahr sind und dass ich nichts verschwiegen habe. Mir ist bekannt, dass die falsche Abgabe einer Versicherung an Eides statt mit Freiheitsstrafe bis zu drei Jahren oder mit Geldstrafe bestraft wird.

*I hereby declare that I have produced the work entitled "*Multimodal Characterization of Microglia Heterogeneity in Aging and Alzheimer's Disease Pathology*", submitted for the award of a doctorate, on my own (without external help), have used only the sources and aids indicated and have marked passages included from other works, whether verbatim or in content, as such. I swear upon oath that these statements are true and that I have not concealed anything. I am aware that making a false declaration under oath is punishable by a term of imprisonment of up to three years or by a fine.*

Tübingen, den ....
Datum / Date Unterschrift

Für meine Eltern

ACKNOWLEDGMENTS

At this point, I would like to thank all those who contributed to the success of this PhD thesis through their professional and personal support.

First and foremost, my thanks go to my supervisor, Dr. Neher, for the provision of the subject and his kind and constructive support throughout the processing time.

I would also like to thank all my colleagues of the Groups of *Neuroimmunology and Neurodegenerative Diseases (Neher Lab)* as well as from the group of *Cell Biology of Neurological Diseases (Jucker Lab)*. Especially I want to thank here Nina Hermann, who did the IHC validation for this project during her master thesis. I also want to thank Xidi Yuan, my partner for the second part of this thesis.

I also would like to thank all my collaborators of the PRECISE team of the DZNE Bonn and from the Beyer lab, especially Dr. Kristian Händler and Jonas Schulte-Schrepping for their help with sequencing and during bioinformatic analysis, Heidi Theis, who did the library preparation of all the Smart-Seq2 Plates and Dr. Collins Osei-Sarpong, who did the library preparation of the SeqWell-samples. Of course I also want to thank Rebekka Scholz, my partner in the second part of this thesis.

Finally, I would like to thank my friends and family who supported me throughout my whole studies.

Thanks to all of you!

TABLE OF CONTENTS

1 ABSTRACT

Neurodegenerative diseases such as Alzheimer's Disease remain a leading socio-economic challenge and have been intensely studied on the genetic level, demonstrating a significant contribution of the immune system to disease pathogenesis. However, how environmental factors influence pathology remains to be fully understood. As microglia are the main resident immune cell population in the brain, they have been studied intensely regarding their contribution to neurological and neurodegenerative diseases. In the last years, several transcriptomic studies independently identified different microglia subpopulations with a variety of functions in health and disease. However, despite many genetic studies, it is still not clear how microglia influence disease pathology, how they change during healthy aging and which regulatory factors drive the development of a specific microglia activation state. Therefore, the first study presented here used scRNA-Seq and scATAC-Seq to characterize microglia of wildtype and APP-transgenic mice of different ages. Single-cell transcriptomic and open-chromatin profiling revealed that microglia are a heterogenous cell population showing differences in number, gene expression and chromatin accessibility, not only with progressive β-amyloid deposition in the brain, but also during healthy aging. Furthermore, we describe for the first time an age-related decline of one homeostatic microglia population and a simultaneous increase of an aging-associated subpopulation, that develops and persists independent of Aβ pathology. Multimodal analysis of the microglia subpopulations identified several disease-relevant transcription factors, such as *Arnt* and *Hif1α*, and their candidate target genes. Finally, this study shows that *Hif1α* regulates a subset of genes that define the so-called disease-associated microglia (DAM) phenotype, and microglial knockout of *Hif1α* induced a shift in microglia subpopulations, reducing neuroinflammation and increasing plaque-compaction, which, in turn, limits neuritic damage.

The onset and progression of neurodegenerative diseases can be influenced by peripheral inflammatory insults such as certain diseases (e.g. diabetes, arthritis) or infections. As it has recently been shown in our lab that microglia can develop long-lasting immune memory effects in response to peripheral inflammatory insults, the second part of my PhD project was aimed at analyzing the molecular mechanisms of how peripheral inflammatory insults cause microglial immune memory. To this end, wildtype mice were stimulated with a set of pro- and anti-inflammatory cytokines or exposed to live bacterial infections and multiplex cytokine profiles were generated. In addition, a method was established that will allow us to profile fixed nuclei from mouse as well as post-mortem human tissue. In a proof of principle experiment, we could show that analyzing chromatin accessibility and gene expression in the same single-nucleus circumvents the issue of data sparsity and allows co-embedding of both datasets. This multi-omic analysis enables the identification of cell type-specific epigenetic and transcriptomic dysregulation in this and future studies.

2 INTRODUCTION

2.1 Microglia at a Glance

Microglia were first described as a separate cell entity in the brain in 1919 by the Spanish neuroscientist Pío del Río-Hortega [1, 2]. Using a silver carbonate staining technique, he was able to visualize and describe the morphology and distribution of microglia. However, the function of these cells remained inconclusive for a long time and even if we know nowadays that microglia are the main resident immune cell population in the central nervous system (CNS) (reviewed in [3, 4]), their exact role in brain aging and disease still needs to be elucidated.

In the mouse brain, microglia account for 5-12 % of the total cell population [5, 6] with unequal distribution across different areas. Indeed, Lawson et al. showed already in 1990 that the density can vary more than five-fold between different regions, with the hippocampus being one of the most densely populated regions and the cerebellum one of the less densely populated regions [5]. In the human brain, microglia represent between 0.5 – 16.6 % of the total cell population [7], depending on the region studied.

Microglia derive from the yolk sac, as myeloid progenitor cells migrate into the CNS and spinal cord during early embryogenesis around E9.5 [8-10]. These cells first show an amoeboid morphology with high migratory and proliferative capacity that allows them to spread and colonize the whole brain [10]. With their highly phagocytic activity, embryonic and early postnatal microglia contribute to the development of the brain by phagocytosing cell debris, supporting axon guidance and eliminating excess synapses (reviewed in [11, 12]). Around the second postnatal week, microglia adopt a more ramified morphology and as they mature, they acquire a surveillant role in the brain [10-12]. Because of the segregation of the brain from blood-borne immune cells due to the closure of the blood brain barrier (BBB) around E13.5 and due to their strong proliferation potential in the developing brain, microglia are believed to be maintained by local proliferation and self-renewal with no appreciable contribution from the peripheral hematopoietic cell pool [13, 14]. However, proliferation of mature microglia in a healthy brain environment seems to be a rather rare event. In a recent study, single cortical microglia were imaged *in vivo* for up to 15 months [15]. Using extrapolation, an average lifespan of adult microglia of around 22 months was calculated with an equal amount of dying and newborn microglia of around 13%. In contrast to the cortex, microglia from hippocampus and cerebellum show more rapid turnover [16], correlating with a higher immune-vigilance of microglia in these areas [17]. Similar studies in humans report an average microglial lifetime of 4.2 years with a median turnover rate of around 28% per year [18]. Differences in the lifespan of murine and human microglia could arise due to differences in the environment lab mice and humans live in.

However, mechanisms of microglial turnover, mode of cell division and the fate of microglial function with age remain ambiguous.

Microglia are critical regulators of neuronal function and behavior in many different areas of neuroscience, including CNS development and homeostasis as well as neurogenesis, neuroinflammation and -degeneration (reviewed in [3, 4]). In the healthy brain, microglia show a ramified morphology with thin processes that are always in motion, scanning the environment every few hours without disturbing neuronal networks [19]. Microglia can detect almost any disturbances in their environment like microbial invasion, tissue damage, apoptotic cells or protein aggregates. In addition, they can also respond to very subtle alterations in their microenvironment including changes in pH or ion composition [20]. The microglial "sensome", a collection of more than 100 proteins and receptors on the cell surface, allows microglia to fulfill this task. The sensome genes appear to be expressed uniformly in all microglia throughout the brain, suggesting that all microglia share these sensing functions [20, 21]. Upon sensing any disturbance, microglia adapt an activated phenotype characterized by an amoeboid shape, migrate to the site of the event and mediate the immune response. This includes the release of cytokines and other inflammatory mediators that help clear invading pathogens or other toxic factors as well as damaged cells and tissue debris and to recruit other immune cells [22, 23].

Besides scanning the microenvironment for any disturbances, microglia also maintain neuronal networks by formation and control of synaptic plasticity [24]. Recent studies also suggest roles in neurogenesis and synaptic pruning [24, 25] in the developing, as well as in the adult brain. The role of microglia in remodeling of neuronal circuits indicates an influence of microglia in learning and memory in the adult brain [26]. And with their longevity and slow turnover rate, microglia are also capable of developing long-term immune memory for multiple inflammatory or neurodegenerative events [27]. However, the complex network of microglial functions and the mechanisms behind are still incompletely understood.

In this context, the hypothesis that microglia consist of several subpopulations has gained more attention in recent years and has been addressed on the cellular as well as molecular level. However, the full complexity of microglial heterogeneity in the brain could only be grasped with the development of single-cell technologies such as single-cell RNA sequencing (scRNA-seq) and mass cytometry. Indeed, using these approaches, several subpopulations in healthy and diseased brains have been identified, with specific subtypes found to be associated with brain development, homeostasis and aging [28-30], as well as neuropathological conditions such as amyloid aggregation and Alzheimer's Disease (AD) [31, 32]. Our current knowledge about these subtypes will be summarized in the following.

2.2 Microglia and the Aging Brain

Age-related changes can be found in all parts of the body, including the brain. Signs for brain aging cannot only be found at the anatomical level (e.g. shrinking volume of certain brain regions), but also on psychological level with obvious symptoms (e.g. depression, memory deficits) in the elderly [33]. But these negative effects of aging do not affect all people equally. Indeed, there are so called "cognitive super agers", people beyond their 80s but with brain function comparable to people 20-30 years younger [34]. Although brain biology and chemistry in these people seem to differ from their age-matched normal agers, little is known about the causes and mechanisms behind their superior cognitive performance.

Not only does the brain as an organ age, but its cells also undergo an aging process. Long-lived cells with a low turnover rate, such as microglia, seem to be especially susceptible to these aging processes resulting in selective age-dependent alterations (reviewed in [3, 21, 35]). The first evidence of microglial aging was found based on morphology and immunohistochemistry in human tissue sections [36], showing a dystrophic phenotype with cytoplasmic fragmentation, process deramification, spheroid formation and gnarling. Other changes found in aging microglia are shortening and decreased motility of processes, indicating a decreased capacity to survey their surrounding brain parenchyma, impaired synaptic contact and poor injury response [37, 38]. Possibly compensating for their age-related dysfunction, microglial turnover and total microglial numbers are increased with age [38]. However, this hypothesis is still under debate, as different studies present conflicting results. Noteworthy, it is possible that these differences may depend on the investigated brain region [39, 40], the sex of the animals [41] or on techniques used to visualize and score microglia in the studies.

As the brain ages, microglia accumulate lipofuscin (an accumulation of undegradable phagocytic cargo) in their cytoplasm [3, 42], possibly indicating deficient phagocytic activity [43]. Interestingly, the motility of processes of these microglia is significantly reduced [37, 38]. Thus, in the aging brain, signaling processes between microglia and neurons as well as immunological responses might be impaired.

The longevity of microglia also makes them prone to cellular senescence, which is characterized by a permanent cell cycle arrest [44] and a senescence-associated secretory phenotype (SASP) [45, 46]. Senescent microglia show increased SASP-production, including pro-inflammatory cytokines such as IL-1β and IL-6, reactive oxygen species (ROS) and other factors with negative impact on surrounding cells [45]. Besides a more pro-inflammatory cytokine profile, aged microglia also display alterations of several pathways related to immunity [35], showing regional differences in the gene expression pattern of immune-amplifying genes like Sirpb1a, Trem3, Cd300ld [17]. However, as these pathways are also often activated in disease, it's difficult to distinguish between physiological and pathological activation of immune-related pathways.

2.3 Alzheimer's Disease

Alzheimer's Disease (AD) is one of the most common neurodegenerative diseases (NDDs) and causes about 60-70 % of all dementia cases [47, 48]. With old age being the primary risk factor for AD and dementia, the increasing human life expectancy will also increase the number of people affected. By 2050, it is thought that the number of people living with dementia will almost double, reaching 3% of the total population in Europe [47].

AD is a progressive neurodegenerative disease which eventually results in cognitive decline. In the end stages of AD dementia, patients often have difficulties in performing their daily lives [49]. The two hallmarks of AD, first described by Alois Alzheimer in 1907, are extracellular amyloid-beta (Aβ) deposition (senile plaques) and intraneuronal inclusions of hyperphosphorylated tau (neurofibrillary tangles, NFTs) [50, 51]. It is a widely accepted assumption that AD starts with abnormal processing of the amyloid precursor protein (APP), leading to misfolding and aggregation of Aβ already 15-20 years before the onset of cognitive symptoms [51, 52]. Indeed, all known forms of autosomal-dominant AD (also called familial AD, FAD) involve mutations or polymorphisms either in genes encoding APP itself or related to the cleavage of Aβ from APP (*PSEN1 or PSEN2*) [52-55]. Due to misbalance in production and/or clearance rate, Aβ forms multimeric aggregates, which then leads to a pathological cascade characterized by accumulation of neurofibrillary tangles, synaptic dysfunction and neuronal loss, finally leading to dementia (reviewed in [53, 55]). However, the precise mechanisms behind this so-called amyloid cascade hypothesis [56] are still unknown, but probably are a result of the toxic effects of Aβ-oligomerization [52].

However, FAD only accounts for about 1% of all AD cases, while the remaining ~99% occur sporadically, usually after a mean age of 65. Sporadic late onset AD (LOAD) is more complex then FAD with genetic and environmental influences (reviewed in [54]). One of the strongest genetic risk factors for LOAD is the ε4-allele of the Apolipoprotein E (*APOE ε4*), which also increases the risk for cerebral amyloid angiopathy (CAA) and age-related cognitive decline during healthy aging [54, 57]. However, it is not yet clear how APOE is involved in AD pathogenesis. Recent studies also showed epigenetic dysregulation at different timepoints of AD pathology, but it is not clear which role epigenetic changes play in disease development and progression [58]. Since Aβ is continuously produced throughout life, aging is probably the main risk factor for developing sporadic AD as it increases the chance of accumulating misfolded Aβ. Together with the before mentioned age-related impairments of cellular functions (particularly decreased process motility and phagocytic activity of microglia), this may initiate the development of neurodegenerative diseases like AD.

2.3.1 Microglia, Aβ and Neuroinflammation in Alzheimer's Disease

Aβ-plaques and NFTs are the main hallmarks of AD and the prevailing Amyloid-Cascade Hypothesis suggests that Aβ-deposition initiates the disease. However, many aspects of AD pathogenesis cannot be explained by this hypothesis and several studies showed that Aβ burden alone does not correlate with cognitive decline [59, 60]. Philippens *et al.* showed that intracranial injection of Aβ fibrils alone was not enough to induce amyloid pathology in marmosets [61]. However, co-injection with lipopolysaccharide (LPS) or injection into animals with chronic systemic inflammation resulted in Aβ-plaque formation and an early AD immune blood cell expression profile. This suggests that Aβ-deposition itself is not enough to trigger AD and that neuroinflammation plays an essential role in the pathogenesis and severity of neurodegenerative diseases (reviewed in [51, 62, 63]). This is further supported by the fact that an increase in inflammatory marker expression was shown to be correlated with the development and severity of dementia [60].

The observations in clinical studies are supported by findings from preclinical studies that Aβ can activate the brain's immune system, primarily microglia and astrocytes [64], which in turn internalize and degrade Aβ. Microglia are able to bind soluble Aβ as well as Aβ-fibrils via a variety of cell-surface receptors, such as CD36 and Toll-like receptors (TLRs) [64, 65]. However, while soluble Aβ can be degraded by extracellular proteases and pinocytosis, fibrillar Aβ is mostly resistant to enzymatic degradation (reviewed in [66]) and accumulates in lysosomes after phagocytosis [67]. Excessive accumulation of Aβ in microglia can even lead to destabilization of the lysosomal membrane and eventually to cell death, releasing Aβ into the extracellular space and thereby contributing to plaque growth [67]. Furthermore, preclinical studies showed that microglial activation by Aβ is accompanied by the release of potentially neurotoxic substances, such as pro-inflammatory cytokines and chemokines (reviewed in[51, 62, 63]), including but not restricted to tumor necrosis factor alpha (TNF-α), Interleukin 6 (IL-6), IL- 1β, reactive oxygen species (ROS) or nitrogen monoxide [68]. This shift to a more inflammatory environment may propagate further amyloid deposition, NFT formation and neuronal damage [51, 55].

Another important modulator of neuroinflammation is the complement system, a major constituent of the innate immune system and involved in various physiological and homeostatic processes. However, during AD it can be directly activated by Aβ leading to chronic inflammatory responses and aberrant synaptic pruning by microglia [69, 70]. Consistent with this finding, the knockout of complement C3 in an aged transgenic mouse model of AD protected against loss of synapses and neurons and cognitive decline despite Aβ-plaque deposition, probably by an altered glial response to plaques [71]. Similarly, APP mice lacking C1q, the initializing component of the classical complement activation pathway, were also shown to have less neuronal damage although the total amount of amyloid and Aβ-fibrils was comparable to APP animals with *C1q* expression [72].

The inflammatory environment in AD pathogenesis also dysregulates cellular crosstalk between microglia, astrocytes and neurons, resulting in a positive feedback loop between neuroinflammation and neurotoxicity [73, 74].

The fact that Aβ is constantly produced throughout life and that Aβ deposits can be detected in the brain years before the onset of cognitive symptoms suggests that exogenous or endogenous factors might influence the microglial immune response induced by Aβ (reviewed in [51]). Thus, local inflammatory insults (e.g. traumatic brain injury) [75], as well as co-morbidities with a systemic inflammatory component (e.g. diabetes mellitus, obesity, smoking) [76, 77] as well as peripheral infections [78, 79] might increase the risk to develop AD and influence the course of the disease. This is supported by studies in mice and humans showing that non-steroidal anti-inflammatory drugs (NSAIDs) lower the risk of developing AD or dementia [80, 81]. However, the efficacy of these drugs is still debated as they were shown to be ineffective in several clinical trials [82, 83], indicating that they may act only in the context of peripheral inflammatory disease.

Findings of clinical and epidemiological studies that connect inflammation and microglia to AD development and progression are further supported by GWAS that have linked several immunity-related gene variants, including in the genes encoding Triggering receptor expressed on myeloid cells 2 (*TREM2*) [84] and *CD33* [85], to an increased risk of developing LOAD (reviewed in [58, 86]. Although AD-related mutations of *TREM2* are rather rare, it is proposed that AD-associated *TREM2* mutations (e.g. R47H) decreases binding to its ligands and therefore may result in reduced microglial activation and phagocytic clearance as well as impaired clustering of microglia around amyloid-plaques, thereby enhancing neuritic dystrophy [84, 86, 87]. Mutations or variations of the microglial cell surface receptor CD33 result in accumulation of activated microglia with impaired phagocytic capacity [85, 86]. Although rarely analyzed so far, some studies also indicate epigenetic changes in immune-related genes in AD (reviewed in [88]), highlighting the importance of epigenetic mechanisms in AD pathogenesis and opening up new possibilities for treatment strategies.

2.3.2 Mouse Models for Preclinical Studies of Alzheimer's Disease

AD is a progressive neurodegenerative disease that probably starts already 15-20 years before the first clinical symptoms. After AD is diagnosed in a patient, only symptomatic treatment is currently possible, but the disease itself, up to date, cannot be cured. Recent approaches using passive immunization against Aβ have shown promise to at least halt progression of the disease (reviewed in [89, 90]). However, due to the complexity of the disease and age-linked decline of the immune system, many ongoing clinical studies are still failing and vaccines might be more effective as a prevention rather than a treatment strategy [89]. Therefore, it is important to understand the underlying mechanisms and to find possible intervention points even in pre-clinical states of the disease. While current animal models do not reproduce all features of AD, transgenic (Tg) animal models have been generated that recapitulate certain hallmarks of AD, namely amyloid and/or tau pathology (reviewed in [91]). According to Alzforum, there are around 200 murine models for AD [92], most of which are overexpressing human genes identified in FAD mutations. As mutations in *PSEN1* or *2* are the most common cause of early onset FAD, monogenic models expressing these mutations were created. However, although they showed an altered processing of murine APP, they failed to develop plaques [93]. In contrast, overexpression models of human APP with FAD mutations such as the Swedish (K670N/M671L), the Indiana (V717F) and the London (V717I) mutations [94] develop plaques as well as synaptic dysfunction, neuro-inflammation and cognitive impairment [95]. The second generation of transgenic mouse models for AD carried a combination of mutated *APP* and *PSEN1/2*, amongst them the APPPS1 [96] and 5x FAD [97] lines. These bigenic models show stronger and earlier Aβ-pathogenicity, neuronal death and cognitive deficits [91].

However, the before-mentioned mouse-models do not recapitulate NFT-pathology which in AD brains was shown to correlate with cognitive decline more closely than Aβ-deposition [91, 98]. Therefore, based on mutations identified in patients with primary tauopathies, single tg-lines with mutated human microtubule-associated protein tau (*MAPT)* have been created to reproduce tau-pathology in mice. Yet, as most of these models produce endogenous tau, they show an undesired combination of mutated human and murine tau protein and give rise to pathology in brain areas that are not necessarily relevant for AD [91]. With htau, a model was developed that exclusively expresses human tau, showing a spatio-temporal distribution of NFT-like pathology similar to humans [91, 99].

In a third generation of mouse models of preclinical AD, Aβ-overexpression and tau-pathology was combined to better recapitulate the complexity of AD neuropathology. For example, the 3x Tg-AD mouse model combines the Swedish mutation of APP and a mutated form of *PSEN1* (M146V) with a mutant form of *MAPT* (P301L) [100]. Nevertheless, although it not only shows plaque-deposition and NFTs but also learning and spatial memory deficits, the results gained with this mouse model are hard to interpret as it represents a combination of two distinct pathologies that may develop

independently in mice, while tau pathology is likely downstream of Aβ deposition in LOAD patients. More mixed models have been developed, including knock-out lines or models expressing mutations found in sporadic AD such as *TREM2.* While no model has been able to fully reproduce human pathology so far, they can still be useful for studying different pathological aspects of AD. A comparison of some of the most widely used Tg-mouse models for preclinical AD-studies is shown in Table 1.

In this thesis, the APP23 mouse model was used which carries the human Swedish mutation (K670N/M671L) under the murine Thy1 promoter causing an overproduction of Aβ [101]. Aβ-deposits can first be observed at 6-7 months of age and plaques increase in size and number thereafter, with females developing plaques faster than males [102]. APP23 animals also develop astrogliosis and microgliosis and hyperphosphorylated tau near plaques, although NFTs and global neuron loss are lacking. APP23 mice also develop cerebral amyloid-β angiopathy (CAA) and at later stages microhemorrhages occur [101, 102]. Cognitive impairment also emerges with aging: at three months of age, these mice already show a deficit in performance in Morris water maze that becomes more severe with age and in 25 months old animals memory deficits in passive avoidance can be observed [103]. Thus, APP23 mice represent a suitable mouse model to study β-amyloidosis-related changes in the brain, allowing us to examine transcriptomic changes in adult mice during the pathogenesis of AD and even before plaque onset.

Tab. 1: Comparison of selected AD mouse models *(adapted from [91, 92])*

Strain	Genetic Background	Mutation	Promoter	Neuro-pathology
APP transgenics				
PDAPP (line 109)	C57B6 x DBA2	APP^{V717F}	Human PDGF-β	Aβ-plaques, gliosis, synaptic loss
APP23	C57BL/6	$APP^{KM670/671NL}$	Murine Thy1	Aβ-plaques, gliosis, neuronal loss in CA1, cerebral amyloid-β angiopathy
J20	C57BL/6	$APP^{KM670/671NL,V717F}$	Human PDGF-β	Aβ-plaques, gliosis, neuronal loss in CA1, synaptic loss
APP/PS1 transgenics				
APPPS1	C57BL/6	$APP^{KM670/671NL}$ $PS1^{L166P}$	Murine Thy1	Aβ-plaques, gliosis, neuronal loss in dentate gyrus, synaptic loss, enlarged pial vessels
5x FAD	C57BL/6	$APP^{KM670/671NL,I716V,V717I}$ $PS1^{M146L,L286V}$	Murine Thy1	Aβ-plaques, gliosis, neuronal loss in cortical layer V, synaptic loss
Tau transgenics				
JNPL3	C57BL/6, DBA/2, SW Mixed Background	$MAPT^{P301L}$	Murine Prp	NFTs, body inclusions, neuronal loss
htau	C57BL/6	Wildtype MAPT	Human Tau	NFTs, neuronal loss
PS19 line (with humanized TREM2)	C57BL/6	$MAPT^{P301S}$ (4R/1N)	Murine PrP	NFTs, gliosis, synaptic loss, brain atrophy
APP/PS1/Tau transgenics				
3x Tg-AD	C57BL/6	$APP^{KM670/671L}$ $MAPT^{P301L}$ $PSEN1^{M146V}$	Murine Thy1.2 (APP, MAPT), Endogenous (PSEN1)	Aβ-plaques, gliosis, NFTs in CA1 and Ctx, synaptic loss, neuronal loss in Ctx

2.4 Omics-Technologies in Microglia Research

As mentioned above, microglia are a heterogenous cell population depending on region, age and health status. They comprise several subpopulations and can adapt their phenotype in response to a variety of cellular or extracellular triggers [3, 4]. However, despite rapid advances in the field of microglia research, it is still not completely understood whether their function in neurodegenerative diseases is initially beneficial but eventually becomes insufficient to combat disease or even becomes detrimental in later stages of disease [104, 105].

Because neither morphology nor the expression profile of cell-surface markers can identify all microglial phenotypes and functions, recent studies focus on the molecular characterization of different microglia activation states. Thereby, omics-technologies (genomics, transcriptomics, epigenomics, proteomics, metabolomics/lipidomics) offer the possibility to identify underlying disease mechanisms, discover novel diagnostic biomarkers and develop new therapeutic strategies [106].

2.4.1 Transcriptomics

Transcriptomics explores differences in mRNA expression to investigate the function of genes and their associated pathways [107]. First attempts for global transcriptomic studies began in the early 1990s with the development of SAGE (serial analysis of gene expression) [108] and microarrays [109]. SAGE is based on Sanger sequencing of concatenated short transcript fragments, while microarrays use fluorescently labeled cDNA-fragments that bind to synthetic probes fixed on the surface of a bio-chip producing a fluorescent signal. However, the main limitation of this technique is the required prior knowledge of the cDNA sequences which often restricts its usage to well-studied model organisms [107]. In 2012, microarrays were used to generate the first murine core microglia signature in the Immunological Genome (ImmGen) project [110].

With emerging high-throughput technologies, especially next generation sequencing (NGS), previous limitations could be overcome. RNA sequencing (RNA-seq) allows the study of the entire transcriptome, can provide additional information (e.g. splice variants, allele-specific gene expression) or detect previously unannotated genes [111]. Using direct RNA-seq, Hickman *et al.* identified the before mentioned microglial “sensome” [20, 112]. Other studies followed, leading to the description of the core gene expression signature of homeostatic microglia (reviewed in [113]) and to the identification of age- [114], region- [17], sex- [115] and disease-dependent [116] heterogeneity of microglia in humans. However, bulk RNA-seq data just provides an average gene expression level across a population of cells. As described above, this can be useful for comparative transcriptomics or quantifying gene expression signatures in disease studies, but it might mask biologically relevant

cellular differences, particularly in underrepresented cell populations. Hence, it is insufficient for studying heterogenous cell populations like microglia.

Bulk RNA-seq has been quickly adapted for analyzing single cells [117] and only two years later, in 2009, the first transcriptome study on single-cell level was published [118]. From then on, interest in this technology has grown steadily as it allows the identification of rare cell-populations, the study of heterogeneous cellular responses or the inference of gene regulatory networks [117, 119]. Indeed, single-cell (scRNA-seq) and single-nuclei RNA-seq (snRNA-seq) led to new discoveries in almost every field of biomedicine, including microglia and AD research. For example, by using the 5x FAD mouse model and performing MARS-Seq, a plate-based scRNA-seq approach, Keren-Shaul *et al.* identified a subpopulation of microglia associated with AD, termed Disease associated microglia (DAM) [31]. These cells are characterized by upregulation of genes associated with lipid metabolism or phagocytosis, such as *Apoe*, *Trem2* and *Tyrobp*, while homeostatic genes, such as *Tmem119* or *P2ry12*, are downregulated. Notably, this phenotype is (at least partially) conserved in humans, where DAMs are localized near Aβ-plaques, suggesting a protective role in Aβ-clearance [31]. This phenotype was later confirmed several times, amongst others by Hammond *et al.* [28] and Sala Frigerio *et al.* [120], who suggested the name activated response microglia (ARM), because of its existence even in healthy aged mice [31, 120]. This group was also able to identify a second reactive phenotype with genes enriched for interferon response (e.g. *Ifit3*, *Oasl2*, *Irf7*), calling them interferon response microglia (IRM). They describe this phenotype as less affected by the presence of Aβ-pathology than the ARMs, suggesting a physiological role during aging [120]. Hammond *et al.* investigated murine microglial transcriptomes at different stages of development, aging and disease [28]. They found the greatest heterogeneity during early development, but several populations expanded during aging and/or emerged after demyelinating injury.

Recent studies also described distinct microglia subpopulations in humans, that only partially overlap with the described gene signatures in mice, such as the DAM and IRM phenotype [121, 122]. However, microglia heterogeneity in humans is still poorly explored, especially in healthy aging, and the significance of the results are often inconsistent. For example, there are snRNA-seq studies showing no detectable substructure in human microglia [123, 124], while other scRNA-seq studies found diverse numbers of subpopulations involved in homeostasis, proliferation, interferon response and antigen presentation [121, 122].

Taken together, single-cell transcriptomics can be a powerful tool for characterizing microglial cells. However, results are largely influenced by sample size and data quality and the method used. All of the above-mentioned studies used either living cells or nuclei of fresh-frozen tissue. Therefore, in order to study, for example, the role of microglia proliferation during healthy aging and disease, new

methods are needed that 1) allow using a small sample size and 2) can handle fixed material to allow enrichment via intracellular staining.

2.4.2 Epigenomics

Epigenomics is the study of epigenetic modifications of the DNA of a cell, including DNA methylation, histone modifications, chromatin remodeling as well as regulation by non-coding RNA expression (e.g. microRNAs) [125]. These modifications can alter gene expression and cellular function without changing the DNA sequence itself and have been shown to be important for cell differentiation [126], aging and disease [88, 127], but also in learning and memory formation [128].

In microglia, epigenetic mechanisms are important in their activation and in controlling their proinflammatory response (reviewed in [129, 130]). For example, it has been suggested that DNA methylation in aging microglia plays a crucial role in regulating inflammation in the aging CNS, as it directly regulates *IL-1β* expression [131, 132]. Indeed, hypomethylation of specific CpG sites on the *IL-1β* proximal promoter leads to increased IL-1β expression and impaired cognitive function in aged mice or animals with tau pathology [131].

Some therapeutic approaches focus on the use of histone deacetylase (HDAC) inhibitors to ameliorate neuroinflammation in NDDs, since histone acetylation was shown to modulate inflammatory responses in different cell types, including microglia [133, 134]. A recent study demonstrated, that *HDAC1* and *HDAC2* differentially affect microglia during development, homoeostasis and AD [135]. Indeed, while prenatal depletion of both genes reduced microglia survival during development, its depletion in adult microglia did not affect cell number or morphology under homeostatic conditions. However, in an AD mouse model, *Hdac1+2* deletion resulted in enhanced microglial amyloid phagocytosis and improved cognitive function [135]. Similar findings exist for microRNAs (miRNAs), whose dysregulation can contribute to the pathogenesis of different NDDs by sustaining neuroinflammation, hyperactivation and abnormal polarization of microglia [136-142].

In addition to the contribution to microglia polarization towards a specific activation state or to their inflammatory response, it has been proposed that epigenetic modifications can help microglia memorize particular events. Indeed, it has been shown that after exposure to a priming stimulus, microglia respond differently to the same or a different second challenge [143]. This acquired epigenetic memory is also observed during development and aging. For example, in a rat model of drug addiction, increased maternal care reduced methylation of the microglial *IL-10* gene in newborns, leading to an enduring anti-inflammatory response and reduced microglial reactivity after drug exposure [144]. Recently, Wendeln *et al*. also observed immune memory in microglia after inflammatory stimuli, resulting in either immune training or tolerance, that is enhanced or reduced

immune activation, respectively [145]. They also suggest that this immune memory is due to epigenetic changes and that these might also be involved in the differential responses to neuropathology. Similarly, by using different omics-approaches on bulk microglia, Zhang *et al.* identified distinct gene networks activated by inflammatory stimuli and aging, which in turn affect epigenetic signatures and functional phenotypes (desensitized vs primed) of the cells [27]. Specifically, the enrichment of permissive epigenetic marks at enhancer regions may explain the hyper-responsiveness of trained microglia, while immune tolerance might be induced by loss of these epigenetic marks. However, not much is known yet about long-term regulation of microglia by epigenetic modifications and if or how they affect different microglia subpopulations.

2.5 Relevance and Aims of the Project

Despite the fact that aging is the biggest risk factor for neurodegenerative diseases (NDDs), such as Alzheimer's Disease (AD), research often focuses on studying the disease rather than aging itself. However, to be able to find the causal parameters that shift the balance from healthy aging to disease or to understand the causes of regional specificity of neurodegeneration, it is crucial to understand the process of and cellular responses to healthy brain aging.

In recent years, omics studies especially of human brains, have provided evidence that neuroinflammation is a critical component of AD pathogenesis and that microglia, as the main resident immune cells in the brain, could be an effective target to influence disease progression. However, despite many studies on this topic, little is known about the role played by the different activation states of microglia. First, we still lack knowledge about the function of microglial subtypes during normal aging and second, we do not understand the interplay of systemic aging and pathology. Hence, it is not only important to define microglia subsets on transcriptomic level, but to understand their functional roles and to identify regulatory factors that drive the development of specific microglia subpopulations.

This study therefore aimed to better understand physiological changes of microglia during healthy aging and AD pathology by using the following approaches:

- Single-cell profiling of microglia during aging and AD pathology in mice to understand how different microglia subpopulations react to aging and Aβ-pathology and if there is a synergy between these states.
- Characterization of the impact of peripheral inflammation on healthy aging and AD-pathology and investigating if different peripheral inflammatory insults can induce long-term changes in microglia (on transcriptomic and/or epigenetic level).

3 MATERIAL AND METHODS

3.1 Experimental Animals

C57BL/6J (WT), APP23 transgenic mice (with Aβ pathology) or APP23 transgene-negative littermates (WT) were obtained from in house breedings and housed in the animal facility of the Hertie Institute for Clinical Brain Research (University Clinics Tübingen) with 12 hours light/dark cycle and unlimited access to water and food. The animal protocols used in this study were approved by local authority (Regierungspräsidium Tübingen) and all animal work was performed in accordance with the animal experimentation regulation of Baden-Württemberg.

For experiments analyzing the immune response after peripheral stimulation and for validation experiments, both male and female mice were used. All other experiments only used male mice.

3.1.1 Transgenic mice

For studies of AD pathology, the APP23 transgenic mouse model was used [98]. These mice contain human transgenes for *APP* (isoform 751) with the Swedish mutation (KM670/671NL) under Thy1 control of their murine *Thy1* promoter [98, 99].

For the *Hif1α* knockout study, a conditional knockout model was used on WT or APP23 background. *Hif1α-ko* mice were obtained by crossing *Cx3Cr1-Cre^{ER}* mice with *Hif1α$^{fl/fl}$* mice to generate *Cx3Cr1-Cre^{ER}:Hif1α$^{fl/+}$* which were then mated to *Hif1α$^{fl/fl}$* mice to generate *Cx3Cr1-Cre^{ER}:Hif1α$^{fl/fl}$* mice (Fig. 1). KO-mice were generated on C57BL/6J and on APP23 background for healthy vs. diseased conditions. Knockout of *Hif1α* was induced by subcutaneous tamoxifen injection at 7 months of age.

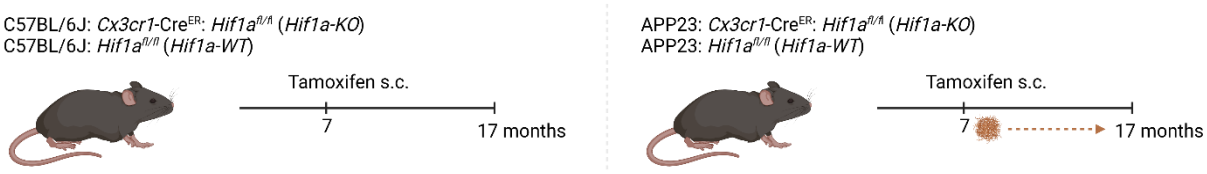

Fig. 1: Strategy for generating Hif1α-ko mice on C57BL/6J and APP23 background. *Cx3Cr1-Cre^{ER}* mice were mated with *Hif1α$^{fl/fl}$* mice to generate *Cx3Cr1-Cre^{ER}:Hif1α$^{fl/+}$* which were then mated to *Hif1α$^{fl/fl}$* mice to generate *Cx3Cr1-Cre^{ER}:Hif1α$^{fl/fl}$* mice. Conditional knockout of *Hif1α* was induced by subcutaneous Tamoxifen injection. [Created with Biorender.com].

3.1.2 Peripheral immune stimulation

3 months old male and female C57BL/6J mice were randomly assigned to the following treatment groups:

- 1x LPS (0.5 µg/g body weight)
- 4x LPS (0.5 µg/g/ body weight on four consecutive days)
- Poly(I:C) (5 µg/g body weight)
- 4x IL-10 (0.1 µg/g body weight on four consecutive days)
- 4x TGFβ (0.1 µg/g body weight on four consecutive days)
- High dose TNFα (0.2 µg/g body weight)
- Low dose TNFα (0.1 µg/g body weight)
- PBS Control (100 µl once or on four consecutive days, depending on the treatment)

All injections were done intraperitoneally and always at similar times in the morning to decrease circadian fluctuations. The acute immune response was analyzed 3 hours or 1 day post injections (3 hpi, 1 dpi). To determine possible long-term effects on the brain's immune response, mice were restimulated after 4 weeks with either 1 µg/g LPS (lipopolysaccharide from *salmonella enterica* serotype typhimurium, Sigma) or 5 µg/g Poly(I:C) (Polyinosinic-polycytidylic acid, InvivoGen) or 100 µl PBS (phosphate buffered saline, sterile) and prepared 3 hpi or 1 dpi after restimulation.

For bacterial live infections, 2-3 months old female mice were intravenous (tail vein) injected with either $1x10^6$ of the gram-negative bacteria *Yersinia eneterocolitica* (*Y.e.*), $1x10^6$ of the gram-positive bacteria *Staphylococcus aureus* (*S.a.*), $1x10^3$ of the live vaccine *Bacillus Calmette-Guérin* (*BCG*) or PBS. Sampling was done as described before either 1, 3 or 7 days post infection (dpi) or 3 hpi or 24 hpi after restimulation with either 1 µg/g LPS, 5 µg/g Poly(I:C) or PBS. Live infection experiments were performed in the lab of Prof. Dr. Stella Autenrieth in Tübingen and Heidelberg.

3.2 Tissue Sampling

For all experiments, mice were prepared in the morning (until latest 11:30) to decrease circadian fluctuations. Mice were deeply anaesthetized with Ketamin-Xylazin, blood was collected from the right ventricle and mice were transcardially perfused with ice cold PBS. The brain was removed and hemispheres separated sagitally. One hemisphere was always fixed with 4% paraformaldehyde (PFA) for 24 hours and cryopreserved with 30% Sucrose in PBS before freezing and storing at -80°C for histological validation experiments later on. The other hemisphere was either fresh frozen on dry ice (for peripheral immune stimulation experiments) or directly used for microglia isolation (all other experiments). All samples were stored at -80°C until further use.

3.3 Microglia Isolation and Cell Sorting

All procedures were carried out at 4°C and with cold solutions if not indicated otherwise. Mice were deeply anesthetized with Ketamin-Xylazin and transcardially perfused with ice cold PBS before collection of Hippocampus (Hp), Cerebellum (Cbm) and prefrontal Cortex (Ctx). The finely minced tissue was dissociated into single-cell suspensions using a well-established purely mechanical dissociation protocol as described previously [15, 145]. Briefly, the brain tissue was subjected to mechanical dissociation using two different sizes of glass dounce homogenizers (7 ml and 5 ml). The homogenized tissue was applied on a 70 µm strainer and rinsed with 1x HBSS before centrifuging for 20 min at 300 g and 4°C without brake and gentle acceleration. Removing of myelin and cell debris and enrichment of brain leukocytes was carried out using a 3-layer percoll gradient (Fig. 2A). After transferring and washing of the cells from the interphase, Fc-receptors were blocked for 10 min with 1:400 anti-CD16/32 (BD) and live microglia were stained with Zombie Violet Dye (BioLegend, 1:200). Afterwards, cells were fixed with CellCover (Anacyte) for 1h at 4°C to ensure that the microglial phenotype corresponds to the *in vivo* situation and that cells were not activated due to the time-consuming SeqWell procedure. Compatibility of this fixation with both sequencing methods, SeqWell and SmartSeq2, was confirmed experimentally beforehand. Live microglia were then purified by fluorescence-activated cell sorting (FACS) based on low fluorescence intensity of Zombie Violet Dye (BioLegend, 1:200), CD11b^{high} (anti-mouse CD11b-BV785, BioLegend, 1:200) and CD45^{int} (anti-mouse CD45-AF700, BioLegend, 1:100) using a Sony SH800Z cell sorter (Fig. 2B).

As the intention was to analyze differences between plaque-associated and plaque-distant microglia, the amyloid-binding dye Methoxy-XO4 (MX04, abcam) [146] was added additionally into the single cell suspension to allow the enrichment of Aβ-phagocytosing microglia (MX04+) (Fig. 2B), which comprise only around 1-5 % of the total microglia population. MX04 positive and negative microglia were then sorted into 384-Well plates for SmartSeq2 library preparation and sequencing.

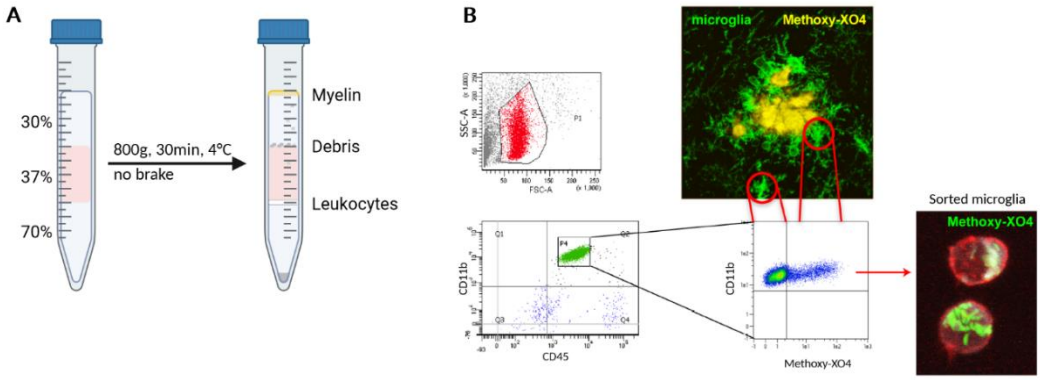

Fig. 2: Microglia isolation and sorting strategies. (A) After density gradient centrifugation, leukocytes are visible as a white thin halo at the 37/70 % - interphase of the 3-layer percoll gradient. [Created with Biorender.com]. **(B)** Separation of single cells based on granularity (SSC) and size (FSC) is shown in the upper left panel. Live Microglia (center) are identified as CD45^{int}, CD11b^{high} (bottom). **(C)** Identification of MX04 positive (Aβ-phagocytosing microglia) and negative microglia (plaque-distant microglia) are shown from a representative sort. Confocal images show the staining of Aβ-plaques with MX04 and its uptake by microglia through phagocytosis of aggregated Aβ.

3.4 Nuclei isolation and Sorting

Single nuclei from fresh frozen brain tissue were isolated by homogenizing fine minced cortical tissue was using a 7 ml and 5 ml glass Dounce homogenizer and fixed with 0.5% Paraformaldehyde for 5 min at RT under rotation. After stopping fixation for 5 min at RT under rotation (1.17 M glycine, 0.84% BSA in 419 mM Tris-HCl, pH 8.0), the single nuclei suspension was purified with a 2-layer sucrose density gradient centrifugation at 3000 g for 45 min at 4°C (protocol adapted from Sigma-Aldrich, NUC-201, Technical Bulletin No. MB-735). The nuclei pellet was then washed and stained with a neuronal (anti-mouse NeuN, EMD Milllipore, 1:50) and microglial marker PU.1 (clone 9G7, Rabbit mAb, Cell Signaling, 1:50) for 1 hour at 4°C on a rotation wheel in the dark. Secondary antibody staining (goat anti-rabbit AF-488 and goat anti-mouse AF-633, Inivitrogen, 1:200) was performed for 20 min at 4°C on a rotation wheel in the dark with additional 10 min of DAPI staining. Microglia nuclei, NeuN negative and whole cell population were purified by FACS using a Sony SH800Z cell sorter.

Note: This protocol describes the final version and a series of pilot experiments were carried out beforehand to test for best possible compromise between fixation condition and RNA, DNA and library quality, including

1) Testing different fixation methods (Formaldehyde (FA) vs. RAID (single-cell RNA and Immunodetection) [147]) and fixation stop solutions
2) Optimizing the FA-concentration and fixation time of the single-nucleus suspension
3) Adding RNase Inhibitor to all steps after FA-fixation
1) Removing Triton X-100 from the staining buffer

3.5 Single-cell Sequencing Procedures, Library Preparations and Sequencing

To do transcriptomic and epigenetic profiling of microglia in healthy aging and AD pathology, different single-cell solutions were used which are described in the following chapters. Sequencing was always performed on a NextSeq500 at the PRECISE facility at DZNE Bonn.

3.5.1 SeqWell

20,000 fixed Microglia were sorted into CellCover-10 + 10% FBS and used for high-throughput scRNA-Seq according to manufacturer's instructions [148]. In brief, cells and barcoded mRNA capture beads were co-loaded into an array of sub-nanoliter wells. The array was closed with a special plasma-treated semipermeable membrane, transferred to an Agilent clamp and incubated at 37°C for 30 min. Afterwards, cells were lysed for 20 min and the liberated mRNA was hybridized to bead-bound barcoded poly(dT) primer. After washing, beads were removed from the array and reverse transcription (RT) was performed. The cDNA was sent to collaboration partners at the DZNE Bonn for final library preparation, quality control and sequencing.

3.5.2 SmartSeq2

MX04+ and MX04- microglia were sorted into 384-Well plates containing SmartSeq2 (SS2) lysis buffer. Plates were centrifuged quickly and stored at -80°C until RT and whole transcriptome amplification (WTA), library preparation and sequencing was performed as in the published protocol [149] by the PRECISE team in an automated manner.

3.5.3 scATAC-Seq (10X Chromium)

10,000 Microglia were sorted (as described in chapter 3.3) and nuclei were isolated according to the low-input protocol suggested by 10X Genomics [150]. Briefly, sorted microglia were washed with PBS + 0.04% BSA. The cell pellet was lysed, washed and the nuclei pellet was diluted in 7 µl 1x Nuclei Dilution Buffer and counted in a Neubauer chamber. Nuclei were then diluted to the corresponding stock concentration [151] based on a targeted nuclei recovery of 2,500 nuclei per sample. 5 µl of each sample was then incubated with 10 µl Transposition mix and transposed nuclei were loaded on a Chromium Next GEM Chip H and into the Chromium Single Cell Controller to generate nanodroplets containing single nuclei and reagents. After breaking the droplets, the open chromatin was bead-purified. During library construction, Illumina primers needed for bridge amplification and sample specific indices were added via PCR. After quality check, libraries were quantified and sequenced on a NextSeq500 according to 10X recommendations.

3.5.4 Establishment of SHARE-Seq on microglia nuclei

To analyze the influence of peripheral inflammatory insults on the brain's immune response, the SHARE-Seq method (simultaneous high-throughput ATAC and RNA expression with sequencing) [152] was established, a multiomics approach that allows measuring chromatin accessibility and gene expression in the same single-cell. For using this technique on microglia nuclei, some issues had to be overcome (e.g. small amount of RNA, limited number of nuclei, FA-fixation). Therefore, some modifications of the protocol were needed to improve nuclei and RNA recovery as well as library quality.

A series of pilot experiments were carried out to test various modifications of the original SHARE-Seq protocol to improve recovery and library/data quality, including

1) Adapting the PFA fixation step in our nuclei isolation protocol
2) Adding stopping points, as the whole procedure takes at least three complete days
3) Testing minimal number of nuclei input needed
4) Optimizing Tn5 concentrations
5) Optimizing the settings for reverse transcription and KAPA-PCR
6) Testing different RNase Inhibitors
7) Testing FA-fixed nuclei vs nuclei isolated from CellCover-fixed and sorted microglia
8) Optimizing the pre-processing pipeline for data analysis

In the following, the final adaptations of the original SHARE-Seq protocol [152] are described (see also [153] for a detailed step by step instruction).

Single nuclei from fresh frozen brain tissue were isolated by homogenizing finely minced cortical tissue using a 7 ml and 5 ml glass Dounce homogenizer and fixed with 0.5% formaldehyde (FA) for 5 min at RT under rotation. After stopping fixation for 5 min at RT under rotation (1.17 M glycine, 0.84% BSA in 419 mM Tris-HCl, pH 8.0), the single nuclei suspension was purified with a 2-layer sucrose density gradient centrifugation at 3000 g for 45 min at 4°C (protocol adapted from Sigma-Aldrich, NUC-201, Technical Bulletin No. MB-735). The nuclei pellet was then washed and stained with a neuronal (anti-mouse NeuN, EMD Milllipore, 1:50) and microglial marker PU.1 (clone 9G7, Rabbit mAb, Cell Signaling, 1:50) for 1 hour at 4°C on a rotation wheel in the dark. Secondary antibody staining (goat anti-rabbit AF-488 and goat anti-mouse AF-633, Invitrogen, 1:200) was performed for 20 min at 4°C on a rotation wheel in the dark with additional 10 min of DAPI staining. Microglia nuclei and NeuN negative cell populations were purified by FACS using a Sony SH800Z and a BD FACSymphony S6 Cell sorter.

Isolated and FACS sorted nuclei were directly applied to transposition reaction using 42.5 µl transposition reaction mix (38.8 mM Tris-acetate, 77.6 mM potassium acetate, 11.8 mM magnesium acetate, 18.8% DMF, 0.12% NP-40 (Thermo Scientific), 0.68 U/µl Enzymatics RI, 0.4% protease inhibitor

cocktail (Sigma-Aldrich)) and 2.5 µl of the appropriate double-loaded Tn5 for each 5 µl nuclei suspension at 37°C for 30 min with shaking at 500 rpm.
Note: Tn5 concentration might have to be adjusted for every new batch and therefore has to be tested beforehand.

After reverse transcription (18.75% PEG6000, 625 µM dNTPs (NEB), 12.5 µM biotinylated RT primer, 25 U/µl Maxima H Minus RT (Invitrogen), 0.3 U/µl Enzymatics RI, 0.3 U/µl SUPERase RI (Invitrogen) in RT buffer) samples were washed twice with 300 µl NIB (10 mM NaCl, 3mM MgCl2, 0.1% NP-40, 0.1 U/µl Enzymatics RI, 0.05 U/µl SUPERase RI in 10 mM Tris-HCl, pH7.5) and stored at 4°C overnight in 200 µl NIB.

After three rounds of split-pool-barcoding, reverse crosslinking was performed for 1 h at 55°C. Proteinase K was inactivated with 2.5 µl of 100 mM PMSF for 10 min before RNA and chromatin fragments were separated using MyOne Streptavidin C1 Dynabeads (Invitrogen) for separate library preparation. RNA (bound to beads) was subjected to a Template Switch reaction, first for 30 min at RT with rotation, then additional 90 min at 42°C with shaking at 300 rpm and pipet mixing every 30 min to avoid settling and clumping of beads. In the meanwhile, chromatin fragments (supernatant) were cleaned up with the MinElute PCR cleanup kit (Qiagen) following manufacturer's instructions and transposed DNA was eluted twice in 11 µl EB Buffer.
Note: DNA samples can be stored overnight at 4°C or at -20°C for several days.

RNA library Preparation:

After Template Switch, cDNA samples were subjected to 5 cycles KAPA-HiFi (Roche) PCR. Afterwards, these samples could also be stored at 4°C over night.
Note: Longer storage might be possible, but is not recommended at this step.

After 5 cycles of PCR, qPCR (SYBR Green) was performed to determine the optimal number of additional PCR cycles needed as ⅓ of the maximum fluorescence intensity. The additional PCR cycles were run without the initial denaturation step and samples were purified using 0.6X AMPure XP beads (Beckmann Coulter). cDNA was eluted in 10.5 µl EB Buffer and quality checked with a HS D5000 Tape (Agilent). Depending on the concentration, tagmentation of libraries was carried out in 20 or 50 ng reactions. Note: Again, the final Tn5 concentration has to be tested beforehand for every new batch.

For Tagmentation reaction, 25 µl of 2x Tris-DMF and 5 µl of the appropriate single-loaded Tn5 dilution was added to each 20 µl cDNA and mixed by pipetting. After 5 min at 55°C with shaking at 300 rpm, the tagmented cDNA was immediately purified with the MinElute PCR purification it (Qiagen) and eluted twice in 10.5 µl EB buffer. 7 cycles of tagmentation PCR (NEB Next High-Fidelity PCR Master Mix, NEB) with the library specific Ad1 primer was run and the final library was purified with 0.7X AMPure XP beads.

ATAC library Preparation:

After 5 cycles of ATAC-PCR (NEB Next High-Fidelity PCR Master Mix, NEB), a qPCR (SYBR Green) was run to determine the optimal number of additional PCR cycles needed as ⅓ of the maximum fluorescence intensity. The additional PCR cycles were run without the initial step, libraries were purified using 1.2X AMPure XP beads (Beckmann Coulter) and eluted in 10.5 µl EB Buffer.

After quality check and optional additional size selection of ATAC- or cDNA library using AMPure XP beads, libraries were pooled and sequenced on a Illumina NovaSeq 6000 platform (aimed for at least 25000 reads/nucleus): Read 1: 49 cycles, Index 1: 99 cycles, Index 2: 8 cycles, Read 2: 49 cycles

3.6 Data Analysis and Biological Interpretation

3.6.1 Transcriptomics (scRNA-Seq)

Raw reads were demultiplexed and aligned to the mm10-1.2.0 mouse reference transcriptome using `Kallisto` [154] and gene expression matrices were further processed using the R package `Seurat v3` and `v4` [155]. After removing low quality cells, data was normalized and scaled for number of genes per cell and proportion of mitochondrial genes using regularized negative binomial regression (`sctransform`) [156]. Subsequently, the individually pre-processed libraries were integrated into a common dimensionally-reduced space using principal component analysis (PCA) and a canonical correlation analysis (CCA)-reduction up to 30 dimensions. Stochastic neighbor embedding (tSNE) and uniform manifold approximation and projection (UMAP) was performed using the integrated dataset and dimensions 1:11. Clustering was performed by constructing a KNN graph with the Louvain algorithm using dimensions 1:11 and a resolution of 0.8. Major cell-type annotations were assigned using `singleR` [157] with Immgen and MouseRNA-Seq databases as references and by manual inspection of canonical marker gene signals, DEGs and GO enrichment results. Differential expression analysis between cell types as well as between APP23+ and WT microglia was assessed using Seurat's `FindMarker` function and FDR-corrected p-values were used to determine significance at an absolute average log fold-change > 0.1. Enrichment analysis was performed using `clusterProfiler` [158] and the following databases: Gene Ontology (Biological Processes), Kyoto Encyclopedia of Genes and Genomes (KEGG), WikiPathways.

Conensus Co-expression network analysis of microglia in Alzheimer's disease was performed using `hdWGCNA` [159]. To this end, genes expressed in at least 5% of cells in any of the three different sequencing runs were retained. The final network was visualized using UMAP with the top 10 hub genes (ranked by kMEs) per module as input features and annotated together with some additional selected genes. `enrichR` [160] was used to perform enrichment analysis on the top 100 genes per

module ranked by kME using the following databases: `GO_Biological_Processes_2021`, `KEGG_2019_Mouse`, `WikiPathways_2019_Mouse`.

To model transcriptional dynamics regulating the shift from homeostatic to activated microglia in AD pathology, pseudotime analysis with `Monocle3` [161] was performed to build a continuous trajectory between microglia subpopulations. Module dynamics throughout the trajectories was assessed by grouping microglia into 50 evenly-sized bins throughout each major trajectory and averaging MEs of each module in these bins by applying loess regression.

3.6.2 Open chromatin Profiling (scATAC-Seq)

Raw reads were demultiplexed and aligned to the mm10-1.2.0 mouse reference transcriptome using `cellranger-atac` (10X Genomics). The reads of all libraries were then aggregated without depth normalization and further processed with `Signac v1.10` [162], a companion package of `Seurat v4`. After removing low quality nuclei, sample-specific ATAC peaks were called with `MACS3`. The data was then normalized with term-frequency inverse-document-frequency (TFIDF) with default parameters and dimensional reduction was performed using singular value decomposition (SVD). Batch effect was corrected by using `Harmony` on the latent semantic indexing reduction (lsi) and tSNE, UMAP and clustering were performed on the integrated embedding using dimensions 2:13. Clustering was performed by constructing a KNN graph with the Louvain algorithm using dimensions 2:13 and a resolution of 0.4. A gene activity matrix was constructed using protein-coding genes annotated in the Ensembl database. After log-normalization, this matrix was used for label transfer with the integrated scRNA-seq dataset and CCA. However, as neither this nor other integration methods gave satisfying results, no integrated analysis of scRNA- and scATAC-data was performed, but the datasets were rather analyzed separately.

Differential chromatin accessibility (differential accessible regions, DAR) between cell types as well as between APP23 and WT microglia was assessed using Signacs `FindMarker` function and FDR-corrected p-values were used to determine significance at an absolute average log fold-change > 0.1. Enrichment analysis was performed using `clusterProfiler` [158] and `enrichR` [160] with the following databases: Gene Otology (Biological Processes), Kyoto Enzyclopedia of Genes and Genomes (KEGG), WikiPathways.

Peaks were annotated to genomic regions with `ChIPSeeker` and `clusterProfiler` using Ensembl and `FANTOM` [163] databases in the mm10 reference genome. Motif enrichment within DARs was assessed using Signac's `FindMotif` function for cell-specific accessible peaks matched for GC content with `TFBSTools` [164] and `motifmatchr`. `chromVAR` [165] TF motif activities were calculated using

the `JASPAR2022` [166] database adjusted for the number of fragments in peaks for each nucleus. *Cis*-Co-accessibility Networks (CCANs) and gene-links were computed using `cicero` [167, 168] in Signac with default parameters.

To link co-accessible chromatin regions to likely target genes, an accessibility-expression correlation strategy was used, stratified by major cell type (here: all microglia combined) and genotype of each sample, according to Morabito et al. [169]. Briefly, pairs of co-accessible peaks overlapping with promoter regions were identified and the Pearson correlation between expression of candidate target gene in the scRNA-Seq dataset with the chromatin accessibility of the linked candidate *cis*-regulatory-element (cCRE) from the snATAC-Seq dataset was computed. This step was performed iteratively for all promoter-cCRE-co-accessible links identified in microglia with regard to genotype. Links with a Pearson correlation coefficient in the 95th percentile and with a p-value < 0.01 were defined as genomic regions with a significant correlation to at least one target gene. Genes with a significant correlation to at least one cCRE were defined as cCRE-linked genes [169].

TF-regulatory networks in microglia were constructed using both the snATAC-Seq and scRNA-Seq dataset and the R package igraph, with each vertex representing a TF or target gene and each edge representing a promoter or linked cCRE binding event (code adapted from [169]).

3.7 Validation of Marker Genes on Protein Level via IHC

To validate some marker genes of important microglia subpopulations on protein level, their fluorescent staining intensities were analyzed on histological brain sections. Therefore, three matched sagittal brain sections per animal were selected based on anatomical structures (Fig. 3A). The sections were washed 3x10 min in PBS, blocked for 60 min at room temperature with 0.3 % Triton X-100 and 5 % donkey serum (Fisher scientific) in PBS and stained with the respective primary antibodies diluted in PBS with 0.3 % Triton X-100 and 2 % donkey serum over night at 4 °C (Tab. 2). After another 3x washing with PBS, autofluorescence caused by endogenous lipofuscin was quenched for 10 sec with TrueBlack^{R} (Biotium) and subsequently washed 3x 10 min in PBS (this step was only done for P2ry12 co-stainings). Afterwards, sections were incubated with the respective secondary antibodies (Tab. 2) for 3 h at RT before washing and mounting on coated slides. Dried sections were coverslippped with fluorescent mounting medium (Agilent) and dried again overnight at room temperature in the dark before transferring to 4°C.

Z-stack images from three consistent subregions of cortex, cerebellum and hippocampus (Fig. 3B) were taken using a Leica TCS SP8 confocal microscope (Leica Microsystems) and analyzed using Imaris v9.3.1 and v9.7.5. Statistical analyses were performed using R 4.3 software and the `ggpubr` package.

A non-parametric independent-samples median test (namely Kruskall-Wallis) was performed for comparisons across different groups, followed by post-hoc testing with Dunn's test and BH-correction for significant-main effects ($p < 0.05$).

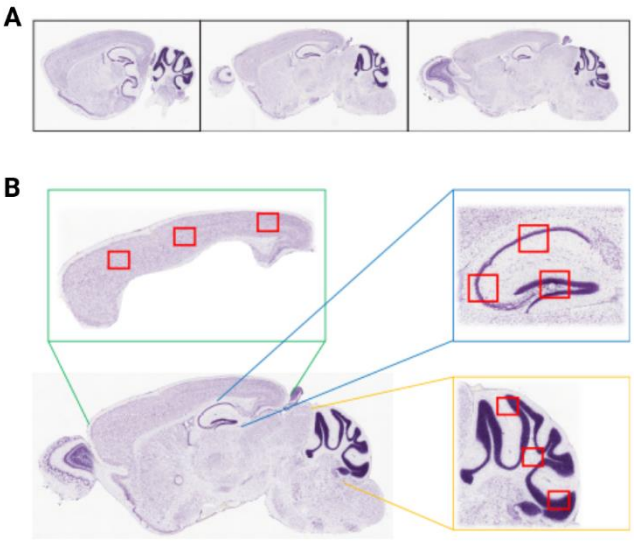

Fig. 3: Sagittal brain sections and regions used for validation of marker gene expression. Three matched sagittal brain slices were chosen per animal **(A)** and images were taken from three consistent subregions (red boxes) of cortex (green box), hippocampus (blue box) and cerebellum (yellow box) **(B)**. *(Images taken and adapted from Allen Mouse Brain Atlas [170])*.

Tab. 2: Antibodies overview.

Antibody	Manufacturer	Used dilution
Primary antibodies		
Chicken anti-Iba1	Synaptics Systems GmbH	1:500
Goat anti-Iba1	Novus	1:400
Goat anti-ApoE	EMD Millipore	1:1500
Rabbit anti-B2M	abcam	1:250
Rabbit anti-Tmem119	abcam	1:2000
Rat anti-P2ry12	BioLegend	1:250
Secondary antibodies		
AF488 donkey anti-rabbit IgG	Jackson Immuno Research	1:250
AF488 donkey anti-chicken IgG	Jackson Immuno Research	1:250
AF647 donkey anti-goat IgG	Jackson Immuno Research	1:250
AF647 donkey anti-rabbit IgG	Jackson Immuno Research	1:250
Cy™ 3 donkey anti-rat IgG	Jackson Immuno Research	1:250

3.8 Cytokine Measurements

For cytokine measurements after peripheral immune stimulation, fresh frozen brain pieces were homogenized using a Precellys 24 Tissue Homogenizer (Bertin) with 1.4 mm ceramic beads for soft tissue homogenization (Bertin). 25 % brain homogenates were prepared in homogenization buffer (0.1 % Triton X-100 in PBS) containing phosphatase and protease inhibitor (Pierce). Homogenates were fuged for 15 min at 18.000 g and aliquots of supernatant were frozen on dry ice and stored at -80°C until measurement (usually within 1-2 weeks).

Cytokines of serum and brain homogenates were measured using the 13-plex Mouse Macrophage/Microglia LEGENDplex panel (BioLegend), which allows to measure pro-inflammatory (CXCL1 (KC), IL-18, IL-23, IL-12p70, IL-6, TNF-α, IL-12p40, IL-1β) and anti-inflammatory cytokines (Free Active TGF-β1, CCL22 (MDC), IL-10, G-CSF, CCL17 (TARC)). In short, fluorescent capture beads in different sizes bind to their specific analytes. After washing, a biotinylated antibody detection cocktail is added to form capture bead-analyte-detection antibody sandwiches and Streptavidin-phycoerythrin (SA-PE) provides fluorescent signal intensities proportional to the amount of analyte bound to the beads [171]. Samples were measured on a FACSLyric™ flow cytometer (BD) where analytes were differentiated by size and internal fluorescence intensity, while analytes are distinguished by the PE signal intensities. Concentrations are then calculated from the standard curves for each analyte using the software provided by BioLegend.

On each measured plate, a standard sample consisting of pooled brain homogenate from different C57BL/6J mice (male and female) was added. This sample was used for inter-plate normalization of cytokine concentrations. Statistical analyses were performed using R 4.3 software and the `ggpubr` package. As most cytokine data showed inequality of variance as well as skewedness, a non-parametric independent-samples median test (namely Kruskall-Wallis) was performed for comparisons across different treatment groups, followed by post-hoc testing with Dunn's test and BH-correction for significant-main effects ($p < 0.05$).

4 MICROGLIA REPROGRAMMING DURING AGING AND AD-PATHOLOGY

In this project, single-cell RNA sequencing and single-nucleus ATAC sequencing were performed to characterize different microglia subpopulations during healthy aging and Aβ-pathology. Therefore, three different age groups were analyzed:

- young adult: 6 months of age, very start of amyloid plaque deposition and gliosis in APP23 mice
- adult: 17 months with pronounced and still increasing Aβ-plaque deposition
- very old: 27 months, close to the end of the mouse' lifespan, with plateaued Aβ deposition.

4.1 Transcriptomic Shifts in Microglia Subtype Distribution with Aging and Disease

To identify age-, region- and disease-specific microglia subpopulations on transcriptomic level, isolated and FACS-sorted microglia from cortex (Ctx), cerebellum (Cbm) and hippocampus (Hp) of male C57BL/6J (WT) and APP23 mice of 6, 17 and 27 months of age were used for scRNA-Seq (Fig. 4A). Considering the combinations of genotype, age and brain region, we analyzed 27 different experimental conditions within 45 samples. After quality control and filtering, we retained 12,428 cells for downstream analysis.

Unsupervised clustering of the quality-controlled cells identified six microglia subpopulations and two macrophage/monocyte clusters with different frequencies between genotypes and age groups (Fig. 4B and D). About 73% of the total microglia population was made up by three clusters expressing high levels of homeostatic marker genes (*Tmem119*, *Cx3cr1*, *P2ry12*) [110, 112, 172], called homeostatic microglia 1 (HM1), HM2 and HM2b. Similar to a previous study [120] but more pronounced, HM2 decreased substantially with age (showing a striking reduction from ~30-35 to ~5-10% of the total population at 27 months of age), independent of pathology (Fig. 4D), while the number of HM2b microglia was not affected by healthy aging and the number of HM1 increased slightly in WT animals at 27 months of age. However, in APP23 positive animals, the latter populations also decreased with pathology, especially HM2b (reduction of ~ 15% in 27 months old animals), and only a comparably little fraction of plaque associated-microglia (MX04+) are homeostatic at all. Thus, HM2 and HM2b seem to be more sensitive to aging and amyloid pathology than HM1. Although HM2 and HM2b are quite similar in their gene expression profile and do not show specific expression signatures, they do show subtle differences in the expression of immune genes (e.g. complement system genes like *C1qa*, *C1qb* and *C1qc* are higher expressed in HM2) or genes related to lysosomal activity and synapse pruning (e.g. *Ctsd*, *Lyz2*, *Glmp*, *Acp2*), suggesting different functions of these homeostatic microglial subtypes.

HM1 shows a less activated phenotype compared to HM2 and HM2b, with significant downregulation of genes involved in the complement system or in antigen presentation via MHC-II, compared to HM2 and HM2b, but increased expression of genes involved in tissue repair (*Gpnmb*, *Dkk2*).

While HM2 is reduced with aging, another cluster increases independent of amyloid-pathology by about 20% (Fig. 4D) between 17 and 27 months of age. This so-called aging associated microglia subpopulation (AAM) has not been described so far and indicates a new microglial phenotype that only starts to become apparent at the end of the lifespan. Although this cluster doesn't display a specific gene signature, it shows increased expression of activation markers and genes involved in immune response such as *C1qa*, *C1qb*, *C1qc, Jun* and *B2m* (Fig. 4C and D). Another cluster is strongly associated with Aβ-pathology and comprises almost half of the plaque-associated microglia (MX04+, see Fig. 4C). It's gene signature and responses are strongly overlapping with the response of disease-associated microglia (DAM) described by Keren-Shaul *et al.* [31]. It shows upregulation of known AD risk factors (*Apoe* [173], *Ctsd* [174], *Trem2* [84]) and is characterized by increased expression of *Apoe* and inflammation markers (*Cst7*, *Itgax*), while the expression of homeostatic genes is reduced. However, this cluster is also found in the brain of WT-mice, especially in aged animals, indicating that it is not only restricted to pathology, but also is part of physiological aging. Therefore, calling them activated response microglia (ARM) as suggested by Sala Frigerio *et al.* [120] might be a better fit. Nevertheless, the name DAM will be kept in this work, as this is the name first given to this subpopulation and it's also the most commonly known name for this microglial subtype.

Two other clusters only show a small enrichment with the development of plaques (~2-3% increase compared to 6 months old mice) and are either enriched for genes involved in TNF-α response (and are therefore called TNF-α response microglia, TRM, here), such as *Tnf*, *Il6*, *Nfkbia* and *Mapk1* or interferon response (interferon-responsive microglia, IRM [120]), such as *Ifit3*, *Oasl2* and *Irf7*. Interestingly, TRMs also show upregulation of some known AD risk genes (*Lpl* [175], *Tyrobp* [176], *Trem2* [84]), although the average expression of *Apoe* is much lower compared to DAMs/ARMs.

Altogether, these findings suggest that aging alone is enough to drive the development of transcriptionally diverse microglia subpopulations and that Aβ-deposition does not induce a unique pathological microglial state but might rather induce a shift in the differentiation of microglia towards more active phenotypes, especially DAMs/ARMs (see also chapter 4.4).

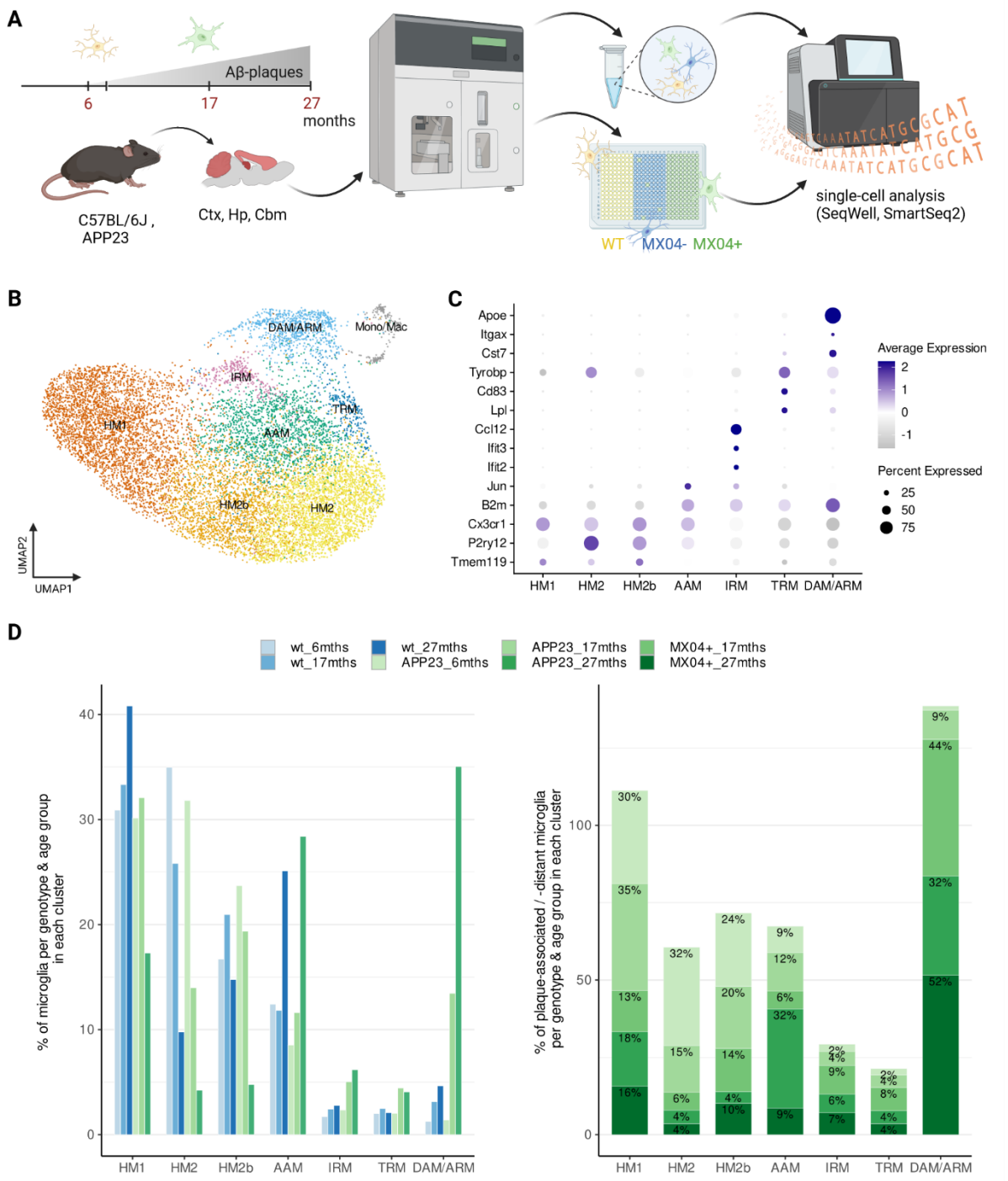

Fig. 4: Microglia subtype distribution with aging and Aβ-pathology. **(A)** Schematic diagram of the microglia isolation workflow from mouse cortex (Ctx), hippocampus (Hp) and cerebellum (Cbm) for scRNA-Seq (SeqWell and SmartSeq2). See Materials and Methods for more details. [Created with Biorender.com] **(B)** UMAP plot of the 12,428 cells passing quality control (*n* = 24 mice). Cells are colored according to clusters identified with Seurat's k-nearest neighbors (kNN) approach. In total, 7 microglia clusters and 2 monocyte/macrophage (Mono/Mac) clusters were identified. HM1 and HM2/2b = homeostatic microglia; DAM/ARM = disease associated / activated response microglia; AAM = aging associated microglia; IRM = interferon response microglia; TRM = TNF-α response microglia. **(C)** Dot plot of normalized expression values of some cluster marker genes. The size of the dot indicates the percentage of cells expressing this gene in this cluster. The color intensity corresponds to the normalized mean expression value of this gene over all cells within this cluster. Negative expression values (grey dots) correspond to expression values below the mean expression across the dataset. **(D)** Percentage of cells per microglia cluster from each genotype-age group. Cells from WT animals are indicated in shades of blue, while cells from APP23 positive mice are indicated in shades of green.

4.2 Validation of Marker Genes via Immunohistochemistry

We used immunofluorescent staining to validate some marker genes for the main identified microglia subtypes (Fig. 5 and Fig. 6) in male and female mice, confirming that these subpopulations are also valid in females. *P2ry12* was chosen as a marker for homeostatic microglia, especially HM2/b, while *Apoe* and *B2m* marked DAMs and AAMs respectively. As we noticed differences in gene expression profiles of plaque-associated compared to plaque-distant microglia, analysis of APP23 positive animals was also done separately for these groups. Therefore, we used Methoxy-X04 (MX04) to fluorescently label Aβ-plaques, as it shows a high binding affinity and specificity for Aβ-fibrils *in vitro* [177]. All markers of interest were co-stained with general microglia markers (*Tmem119* and/or *Iba1*) to identify and reconstruct individual microglia, based on which the expression of the proteins of interest were quantified. Fig. 5 shows the mean fluorescent intensities of individual microglia normalized to either Tmem119 (in case of P2ry12) or Iba1 (in case of B2m and Apoe). As seen in the transcriptomic data, Tmem119 and P2ry12 show only very low intensities around plaques. Hence, comparably few MX04+ microglia could be analyzed. Overall, P2ry12 intensities showed a bell-shaped distribution with decreasing intensities during aging (Fig. 5B) and increasing intensities with plaque load and proximity in hippocampus. Interestingly, microglia in the cerebellum had higher intensities in all conditions compared to the other brain regions, together with a generally flatter and wider distribution, indicative for higher variance. Additionally, P2ry12 staining showed significantly higher intensities in APP23+ cells compared to WT cells, even in 6 months old animals. Together these data support the observations of single-cell transcriptomics showing that the proportion of HM2/b declines with age, independently of pathology. The higher intensities in cerebellum could reflect a stronger basal phagocytic clearance capacity of cerebellar microglia, as shown by Ayata *et al.* on transcriptomic level [178], which could be beneficial during disease and might be a reason why this brain area is not affected by most hallmark features of AD (e.g. Aβ-plaques).

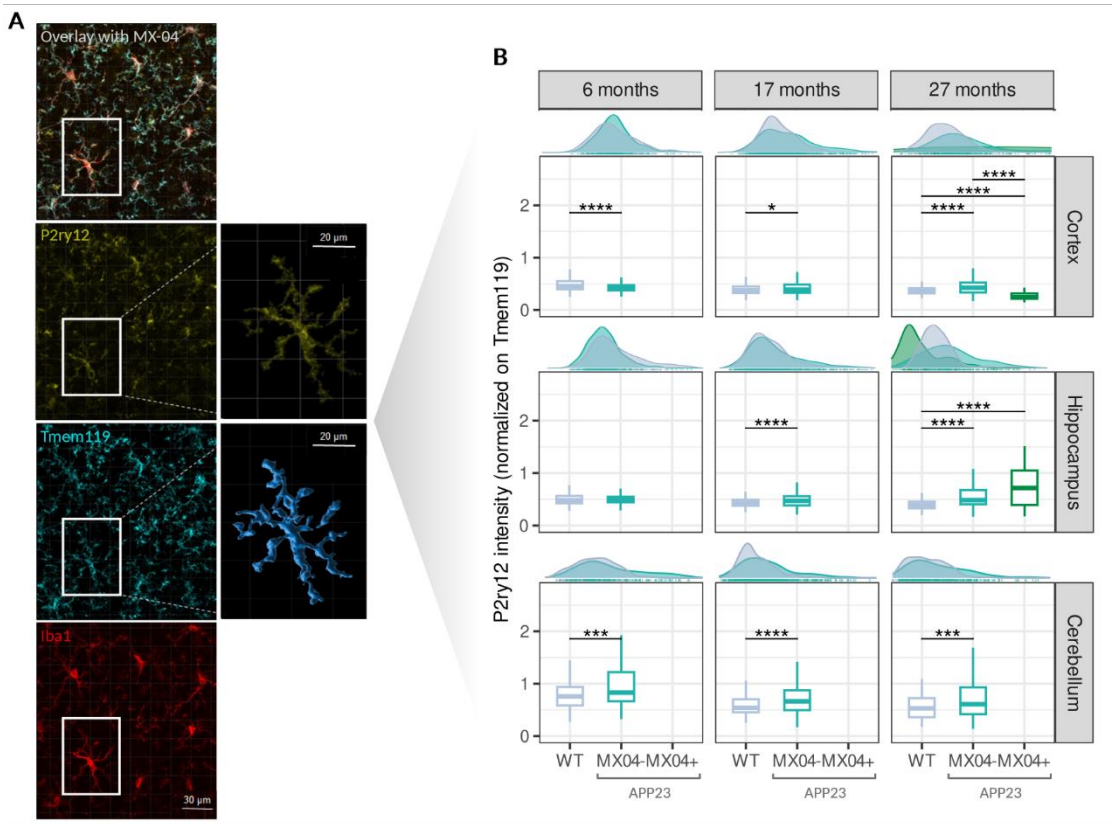

Fig. 5: Histological validation of P2ry12 gene expression. (A) Exemplary co-staining of Iba1, Tmem119, P2ry12 and Methoxy-XO4 as a marker of Aβ-plaques (left, from bottom to top). Single microglia were reconstructed based on Tmem119 (right, bottom) and the P2ry12 signal was masked on the 3D reconstruction (right, top; images and data provided by Nina Hermann). **(B)** Boxplots showing the normalized mean intensities of the 2,371 reconstructed microglia in WT animals and 3,379 microglia in APP23 animals (56 of which were plaque-associated, MX04+). Note: Only few plaque-associated microglia (PAM) could be identified, because of very weak Tmem119 signal in vicinity of plaques and one PAM (MX04+) can contain more than one individual microglia, because of clustering around plaques (see **A**). Statistical comparison was performed using Kruskall-Wallis test with post-hoc Dunn's test and Benjamini Hochberg (BH) correction for significant main effects ($p < 0.05$). ns (not significant): $p>0.5$, *$p<0.5$, **$p<0.01$, ***$p<0.001$, ****$p<0.0001$. Density plots on the top show the mean intensity distribution for each condition.

Apoe is important in cholesterol metabolism and the main marker of disease associated microglia (DAM/ARM). Interestingly, on protein-level, we observed almost no difference between WT and APP23 microglia in the cortex of each age group (Fig. 6D). However, values increase in microglia in close contact to Aβ-plaques, especially in the very old animals. Notably, while intensities are slightly increasing in the cerebellum of WT animals with aging, they are decreased in APP23 animals compared to WT animals. A similar pattern can be seen in cortex and hippocampus of 6 months old mice that do not yet show overt pathology. The role *Apoe* in AD pathogenesis is not well understood, but increasing evidence suggests that it does not only influence microglial function in AD, but also directly influences Aβ clearance and aggregation in the brain [179].

B2-microglobulin (B2m) is a component of the major histocompatibility complex I (MHC I) and therefore important for antigen presentation to cells of the immune system. It was previously found to be enriched in elderly humans and mice, negatively regulating cognition and regenerative functions in an age-dependent manner [180]. Interestingly, while its gene expression increases drastically in 27 months old mice, the increase on protein level is not very pronounced (Fig. 6C). Still, for the WT animals there is a steady increase in B2m intensities in all three brain regions, whereas intensities go down with increasing plaque-load. And even though microglia in close contact to plaques (MX04+) show higher B2m intensities than plaque-distant microglia, intensities were still lower than in WT microglia from age-matched animals. This may reflect the release of B2m from the cell surface and its integration in Aβ plaques, as recently demonstrated [181]. Overall, immunohistochemistry confirms age- and Aβ pathology-associated microglial phenotypes, but highlights the need to study differentially expressed genes also at protein level, as some may be released from microglia, interacting with Aβ-plaques in the extracellular space.

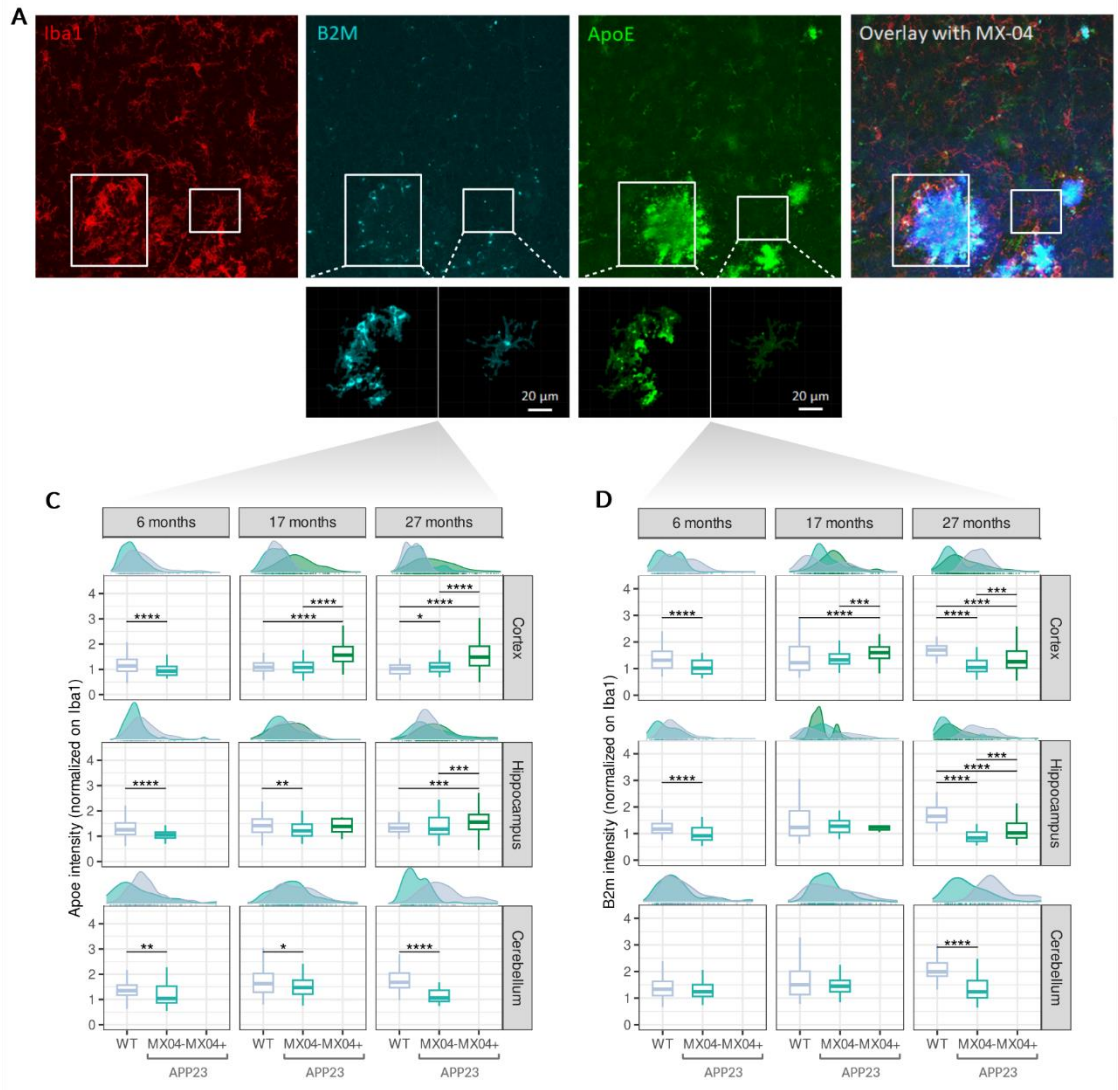

Fig. 6: Histological validation of B2m and Apoe gene expression. (A) Exemplary co-staining of Iba1, B2m, Apoe and Methoxy-XO4 as a marker of Aβ-plaques (top, from left to right). Single microglia were reconstructed based on Iba1, and the B2m and Apoe signals were then masked on the 3D reconstruction (bottom; images and data provided by Nina Hermann). **(B)** Boxplots showing the normalized mean intensities of the 1,200 reconstructed microglia in WT animals, 766 not plaque-associated (Methoxy-X04 negative, MX04-) and 616 plaque-associated microglia (MX04+) in APP23 animals. Note: One PAM (MX04+) can contain more than one individual microglia, because of clustering around plaques (see **A**). Statistical comparison was performed using Kruskall-Wallis test with post-hoc Dunn's test and Benjamini Hochberg (BH) correction for significant main effects ($p < 0.05$). ns (not significant): $p>0.5$, *$p<0.5$, **$p<0.01$, ***$p<0.001$, ****$p<0.0001$. Density plots on the top show the mean intensity distribution for each condition.

4.3 Transcriptional Heterogeneity of Microglia in the healthy, aging brain

To further explore microglial heterogeneity in the healthy brain, differential gene expression (DEG) and overrepresentation analysis of microglia from wildtype animals was performed. Although PCA did not show a separation by age or brain region, unique subsets of variable genes could be identified for both biological factors.

Comparisons of differentially expressed genes (DEGs) between brain regions in each microglia subpopulation resulted in almost 3,000 significant DEGs (FDR corrected p-value < 0.05, $|\log_2 FC| > 0.1$), with the largest number found in cortex (4,685 DEGs, of which 1,324 are unique for this region), whereas the hippocampus revealed the fewest (1,198 DEGS, of which 25 are unique for this region). Interestingly, over 97 % of the significant DEGs in the cerebellum and over 99% in hippocampus derived from homeostatic microglia, especially the HM2b cluster. In the cortex, DEGs in all subpopulations could be identified, but the main proportion still derived from homeostatic microglial subtypes HM1 and HM2b. Gene ontology enrichment was performed for the uniquely expressed DEGs and results support regional heterogeneity of microglia under steady state. No major differences could be identified between hippocampal and cerebellar microglia, but the transcriptomes of cortical microglia differ in terms of upregulation of genes involved in mitochondrial and oxidative functions as well as phagocytosis and immune regulation. These findings are in line with previous studies demonstrating regional differences in microglial gene expression profiles in mice [17, 29, 182] and humans [29, 116, 183].

As microglia are extremely long-lived cells, it is assumed that they undergo an aging process similar to systemic aging of the whole body. Therefore, the same analysis was performed for WT microglia from young adult, adult and aged brains. Over 6,000 DEGs could be identified, over half of which are unique to the 27 months old cohort (Fig. 7B). The 17 months old cohort did not show any uniquely expressed DEGs, suggesting that these cells are in a transitional state between young adult and aged microglia. Similar to what was seen in the analysis of WT brains, most DEGs derive from homeostatic microglia, especially HM2b (68.6 % in 6 months, 45.5 %in 27 months old animals). Again, the uniquely expressed DEGs were annotated to biological functions using Gene Ontology, KEGG and WikiPathways. Compared to the younger animals, microglia from the 27 months old animals showed altered expression of genes involved in autophagy, mRNA processing, DNA damage repair and Golgi vesicle transport.

Several reports highlight an age-related increase in genes involved in innate immune activation in microglia, both, in mice and humans. And indeed, aged microglia showed upregulation of complement components (e.g. *C1qa*, *C1qb*, *C1qc*) and *Apoe*, compared to young adult cells. Other upregulated DEGs in microglia from aged animals belong to the Toll-like receptor family (e.g. *Tlr1*, *Tlr2*, *Tlr4*, *Tlr9, Myd88*) or MHC family (e.g. *H2-M3*, *H2-Q4*). This data is in accordance with other studies describing an

upregulation of pro-inflammatory genes in healthy aged microglia (reviewed in [175]), supporting again the theory of “inflammaging” as a phenomenon of the normal aging process.

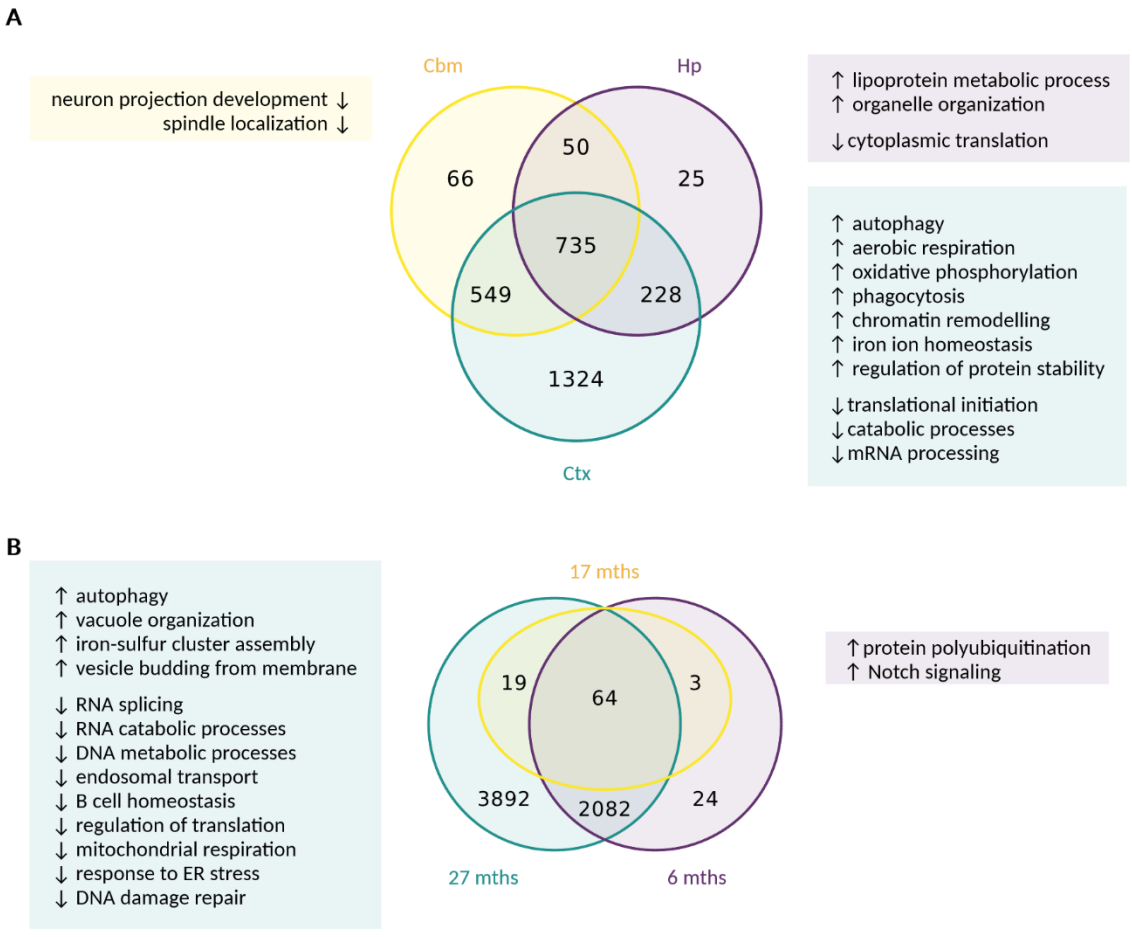

Fig. 7: Regional and age-dependent overlap of DEGs from WT animals. (A) Pairwise comparison of microglial DEGs (FDR adjusted p-value ≤ 0.05, |log2FC| > 0.1) of WT animals in cortex (Ctx), cerebellum (Cbm) and hippocampus (Hp) with enriched GO terms for significant DEGs that are unique for this brain region. **(B)** Pairwise comparison of microglial DEGs (FDR adjusted p-value ≤ 0.05, |log2FC| > 0.1) of WT animals in 6, 17 and 27 months old animals with enriched GO terms for significant DEGs that are unique for this age group. Color code according to the Venn Diagrams; enrichment results are listed according to the q-value (lowest q-value on the top).

4.4 Impact of Aβ-pathology on Microglial Heterogeneity

To assess the impact of Aβ pathology and its synergy with aging processes of microglia in different brain regions, APP23 cells were compared to WT cells in each microglia cluster. Not surprisingly, six months old animals did not show significant differences in gene expression profiles (Fig. 8A). This was expected, as these animals do not yet show strong signs of Aβ-pathology. With aging and development of pathology, terms related to immune activation and peripheral immune cell invasion became enriched in microglia from APP23 mice, especially in the homeostatic microglial clusters and in the cortex.

Interestingly, most significant DEGs could be found in 17 months old animals, independent of brain region. At that age, even in the cerebellum, which does not develop Aβ-pathology in APP23 mice, has 40 uniquely upregulated DEGs between APP23 and WT animals. Yet, no significant enrichment result could be found. In comparison, the hippocampus, one of the main affected areas in the AD-brain only has 19 unique DEGs in adult and aged microglia. In contrast, the cortex did not only show the highest number of DEGs spread across almost all microglia subpopulations, but it also showed a general upregulation of genes involved in immune response compared to the other regions examined, probably reflecting that it carries the highest Aβ burden in APP23 animals.

In particular, several microglia populations showed an increase in translational processes, especially in 27 months old animals, similar to what was found before in the WT animals only. This might indicate an accumulation of aberrant protein composition at aged synapses in the healthy brain because of aberrant translational processes, which then might lead to proteostatic burden and increased levels of damaged or aggregated proteins leading to unhealthy brain environment prone to neuropathological cascades [184, 185]. Another common feature that was shared between different conditions was a downregulation of genes involved in the TCA cycle and a heightened pro-inflammatory response in microglia from APP23 animals. Other pathways that were altered in AD pathology are for example oxidative phosphorylation, respiratory burst and regulation/generation of superoxide anions, all of which were shown to be related to highly active microglia exposed to (fibrillar) Aβ and jointly responsible for neuron loss in AD [186-188].

There was one cluster of genes upregulated in APP23 microglia that were shared between 17 and 27 months old cortical microglia as well as 27 months old hippocampal microglia (Fig. 8B). Interestingly, these genes were also upregulated in old WT animals, although not as strongly as in AD pathology. This suggests similar transcriptomic processes in microglia of late-stage Aβ pathology and very old healthy brains, possibly explaining the low numbers of DEGs found in old animals. Pathway enrichment analysis (KEGG, WikiPathways) showed enrichment of genes related to glycolysis, TYROBP Causal Network and Hypoxia-inducible factor-1 (Hif1)-signaling. Enrichment of mitochondrial DEGs in old animals and upregulation of HIF-1 signaling in aging as well as in AD pathology indicates a metabolic switch from

oxidative phosphorylation to aerobic glycolysis. Thus, prolonged activation of the Hif-1α signaling pathway due to chronic exposure to hypoxia, as it is found in aged and AD brains, might result in compromised cellular bioenergetics and metabolic dysfunction [189]. Together this data suggests cluster-specific transcriptomic changes in AD resulting in distinct dysregulation of biological pathways, especially related to energy production and metabolic processes.

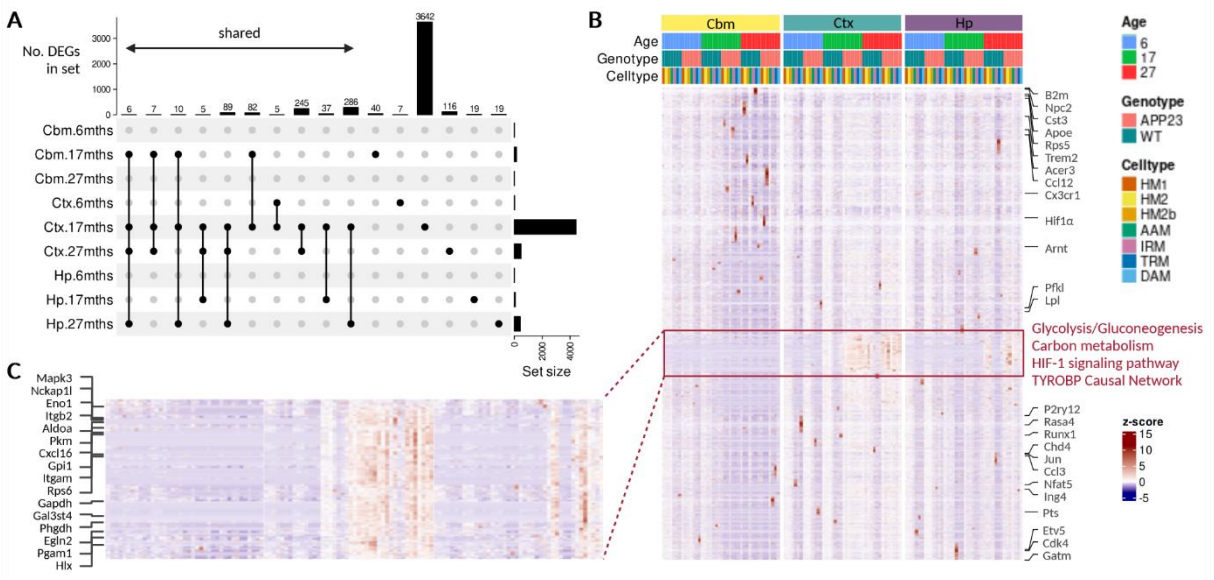

Fig. 8: Impact of Aβ pathology on the microglial transcriptome. (A) UpSet plot showing up- and downregulated DEGs of each microglia cluster (FDR corrected p-value < 0.05, $|\log_2 FC| > 0.1$) unique for or shared between conditions. **(B)** Heatmap of the 4,645 DEGs associated with AD pathology in each condition (FDR corrected p-value < 0.05, $|\log_2 FC| > 0.1$). Color code represents the z-score of median expression of each gene (row) averaged by celltype and condition (genotype, brain region and age). **(C)** Zoom into red box (B) with selected genes annotated to the pathways labeled in (B).

To identify differences in microglia directly responding to amyloid-plaques, the SmartSeq2 dataset was analyzed separately, as it contains the information for every microglia cell if it was interacting with Aβ (Methoxy-positive, MX04+) or not (Methoxy-negative, MX04-). Plaque-associated microglia (PAM) still separated from the other microglia in PCA, tSNE and UMAP and showed a strong enrichment for pathology-related clusters, especially the DAM/ARM subcluster (Fig. 9A), with almost no homeostatic microglia. Differential expression and gene set enrichment analysis show a strong upregulation of AD risk genes (e.g. *Cts7*, *Apoe*, *Lpl*) and metabolic pathways like carbon or cholesterol metabolism in these PAMs (Fig. 9B, C), similar to what was seen in our larger dataset and corroborating previous studies [190]. This indicates that the genes identified before (Fig. 8B) as strongly Aβ pathology-related are mainly due to plaque-associated microglia. PAMs also showed alterations in lipid metabolism and energy production as well as an increased *Hif1α* expression, indicating a switch from mitochondrial respiration to glycolysis. Metabolic dysfunction is a common feature in AD and other neurodegenerative diseases and alterations of glucose and lipid metabolism are early biomarkers for

AD that are linked to cognitive impairment [191, 192]. Interestingly, many DAM signature genes are HIF-1α-responsive genes (e.g. *Spp1*, *Igf1*) and many genes that drive KEGG pathway enrichment are also important players in the HIF-1α -signaling pathway (Fig. 9D), suggesting *Hif1α* as a key regulatory element of plaque-associated microglia.

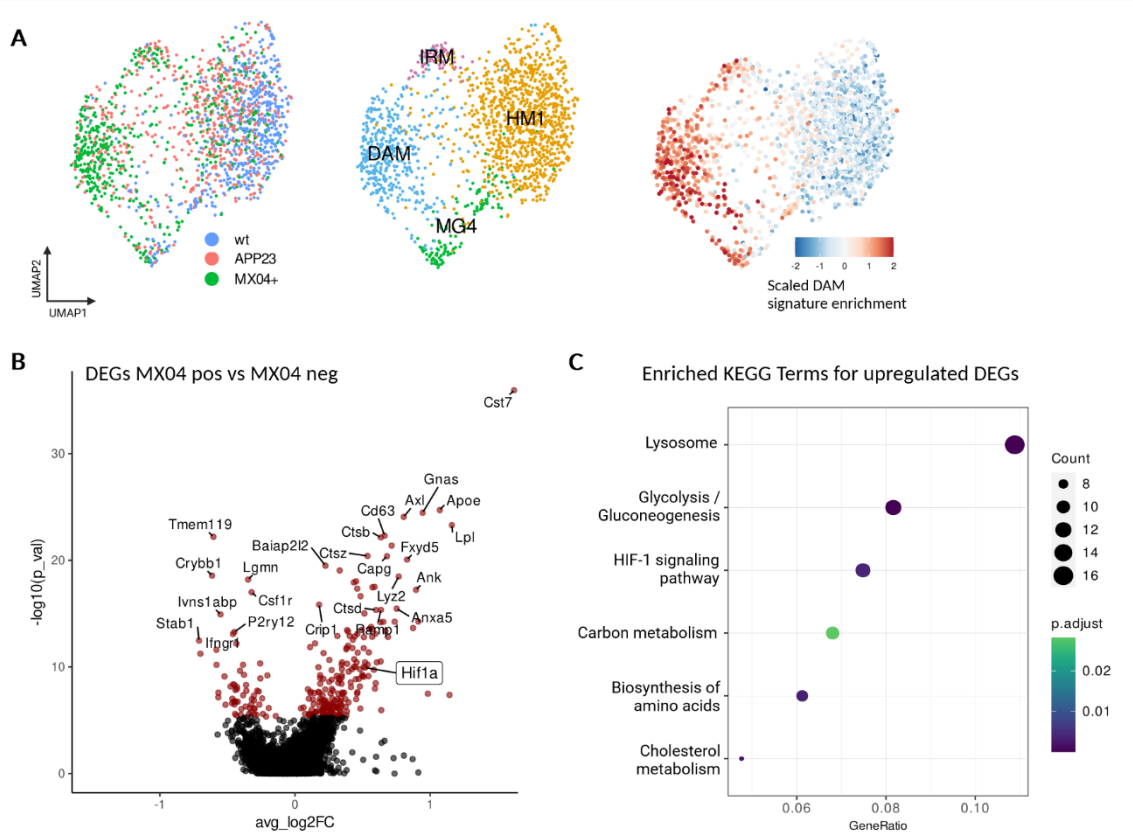

D

KEGG pathway	Gene
Cholesterol metabolism	*Apoe, Lpl, Npc2, Nceh1, Lrpap1, Tspo, Scarb1*
Biosynthesis of amino acids	*Pkm, **Gapdh**, **Eno1**, **Aldoa**, **Pgk1**, **Pfkl**, Psat1, Tpi1, Pgam1*
Carbon metabolism	*Pkm, **Gapdh**, **Eno1**, **Aldoa**, **Pgk1**, **Pfkl**, Psat1, Tpi1, Pgam1, Gpi1*
HIF-1 signaling pathway	*Igf1, Gapdh, Eno1, Aldoa, Pgk1, Hif1a, Cybb, Ldha, Pfkl, Egln3, Slc2a1*
Glycolysis / Gluconeogenesis	*Pkm, **Gapdh**, **Eno1**, **Aldoa**, **Ldha**, **Pgk1**, **Pfkl**, Tpi1, Akr1a1, Pgam1, Gpi1, Aldh2*
Lysosome	*Cd63, Ctsb, Ctsz, Ctsd, Cd68, Npc2, Hexa, Ctsl, Glb1, Gusb, Ctse, Gba, Gm2a, Ctsa, Fuca1, Lamp1*

Fig. 9: Gene expression changes in Plaque-associated Microglia. (A) Plaque-associated microglia (MX04+) are mostly composed of DAM/ARM cells. **(B)** Differential gene expression of plaque associated vs plaque distant microglia. Volcano plot shows up- (average $\log_2$ Fold change > 0) and downregulated DEGs (average $\log_2$ Fold change < 0). DEGs with a Bonferroni adjusted p-value < 0.1 are marked in red. **(C)** KEGG- enrichment for DEGs (marked red in (B)) upregulated in plaque-associated (MX04+) vs plaque-distant (APP23+) microglia. The color indicates the significance value (Bonferroni adjusted p-value), the size of the dots refers to the gene counts. Genes responsible for this enrichment results are shown in **(D)**. Interestingly, the bold printed genes are all part of the HIF1-signalling pathway.

4.5 Co-expression Network Analysis and Cell Fate Decisions in Microglia

Biological systems are highly complex with tightly-regulated interactions between all functional units. Therefore, analyzing individual genes may oversimplify the underlying biology [159]. To further examine the molecular phenotypes of the identified microglia subtypes and their roles during healthy aging and Aβ pathology, consensus co-expression network analysis with `hdWGCNA` [159, 169] was performed, yielding five co-expression modules (Fig. 10A). The module eigengenes (MEs) show that some modules are primarily confined to a special subpopulation (e.g. MG-M5) while others are spread across multiple clusters (Fig. 10B). Furthermore, differential ME analysis (DME) revealed significant differences between MEs in microglia from APP23 vs. WT animals for all modules, with the largest differences being found in the DAM cluster (Fig. 10B).

To model the developmental process of microglia subtypes, `monocle3` pseudotime analysis [161] was applied. This analysis ordered microglial phenotypes along a four-branched trajectory (Fig. 11A) that starts from HM1 (the less activated homeostatic phenotype) and ends either in HM2, AAM, DAM or IRM. Interestingly, cells from the TRM cluster seem to only transition into DAMs, while the AAMs can either be an endpoint or transition into the IRM stage, which again shows that aging itself might prime microglia into a more activated phenotype, making them more prone to develop into reactive phenotypes during pathology.

Comparison of the ME dynamics throughout the different trajectory arms uncovered gene co-expression modules critical for cell fate decisions (Fig. 11B). Increased expression of the yellow module MG-M4, which contains marker genes of the IRM phenotype (e.g. *Ifit2*, *Oasl2, Irf7*), is associated with the transition from homeostatic into the IRM phenotype. The red module MG-M1 contains classical markers of homeostatic microglia (*P2ry12*, *Cx3cr1*) and its expression decreases along all trajectories and pseudotime (Fig. 11B, C), suggesting its association with the HM1 cluster, the starting point of all microglial trajectories. GO-enrichment analysis also associates MG-M1 with homeostatic microglia functions such as regulation of cell motility or Rho signaling, which is important for synaptic plasticity, spine formation and memory (reviewed in [193]). The other modules also contain genes associated with key microglial processes like phagocytosis, synapse pruning and various immune activity related functions (Fig. 10A, C). However, they also show enrichment for disease-associated processes like microglia activation, Aβ-response, cytokine production and activation of different pathways involved in neuropathology (Fig. 10C). This also suggests that these modules contain gene-networks underlying microglia activation in AD, while MG-M1 represents the homeostatic gene network.

Interestingly, both, the green and the blue modules (MG-M3 and MG-M4) contain genes associated with the DAM-signature and AD risk (e.g. *Apoe*, *Trem2*, *Lpl*, *Tyrobp*) and their expression also increases throughout the DAM-lineage (Fig. 11B). However, when looking closer into the genes and

GO-enrichment results of MG-M3, this module could be either a mixture of different microglia subtypes, especially AAM, TRM and DAM, or it could form a subpopulation of DAMs, possibly related to plaque-associated microglia (see also upregulated DEGs in Fig. 9B).

Altogether, our transcriptomic data corroborate specific aspects of previous studies, namely microglia heterogeneity in aging and pathology and increased *Hif1α* in MX04+ microglia, and demonstrate for the first time the increase of an aging-associated subpopulation while simultaneously a homeostatic microglia population diminishes.

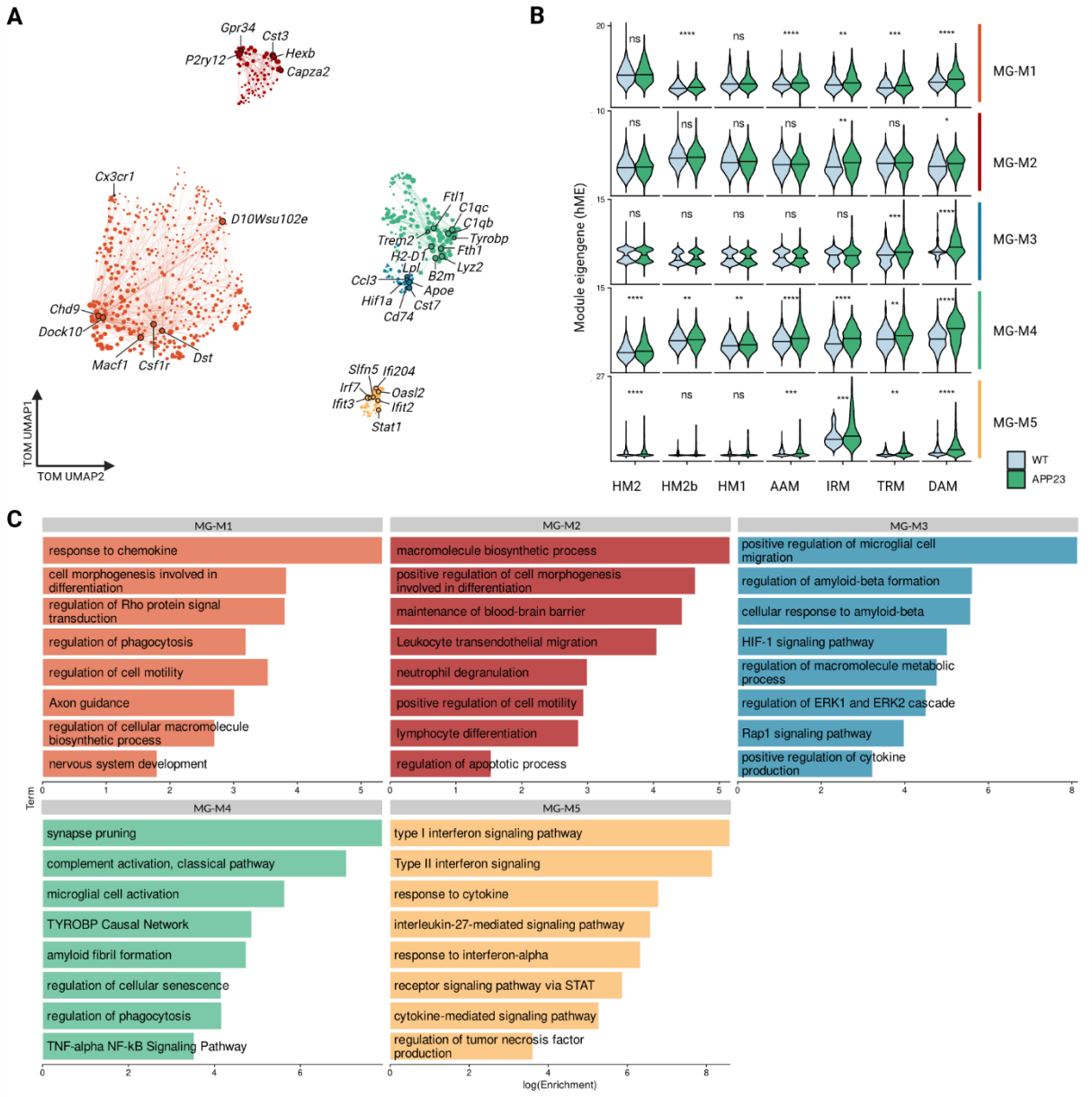

Fig. 10: Co-expression network analysis of microglia. (A) UMAP-Plot of the microglia co-expression network. Nodes correspond to genes (colored by co-expression module assignment), edges represent co-expression links between genes and module hub genes. Point size is scaled by kME. The top 3 hub genes per module and additional genes of interest are labelled and network edges were downsampled for visual clarity. **(B)** Violinplots of differential module eigengene analysis in each microglia cluster comparing cells from APP23 vs WT animals using two-sided Wilcoxon test, indicating up- or downregulation of co-expression modules in each microglia population. ns (not significant): p>0.05, *p<0.05, **p<0.01, ***p<0.001, ****p<0.0001. **(C)** Barplots of selected GO enrichment results (log-scale) for each co-expression module

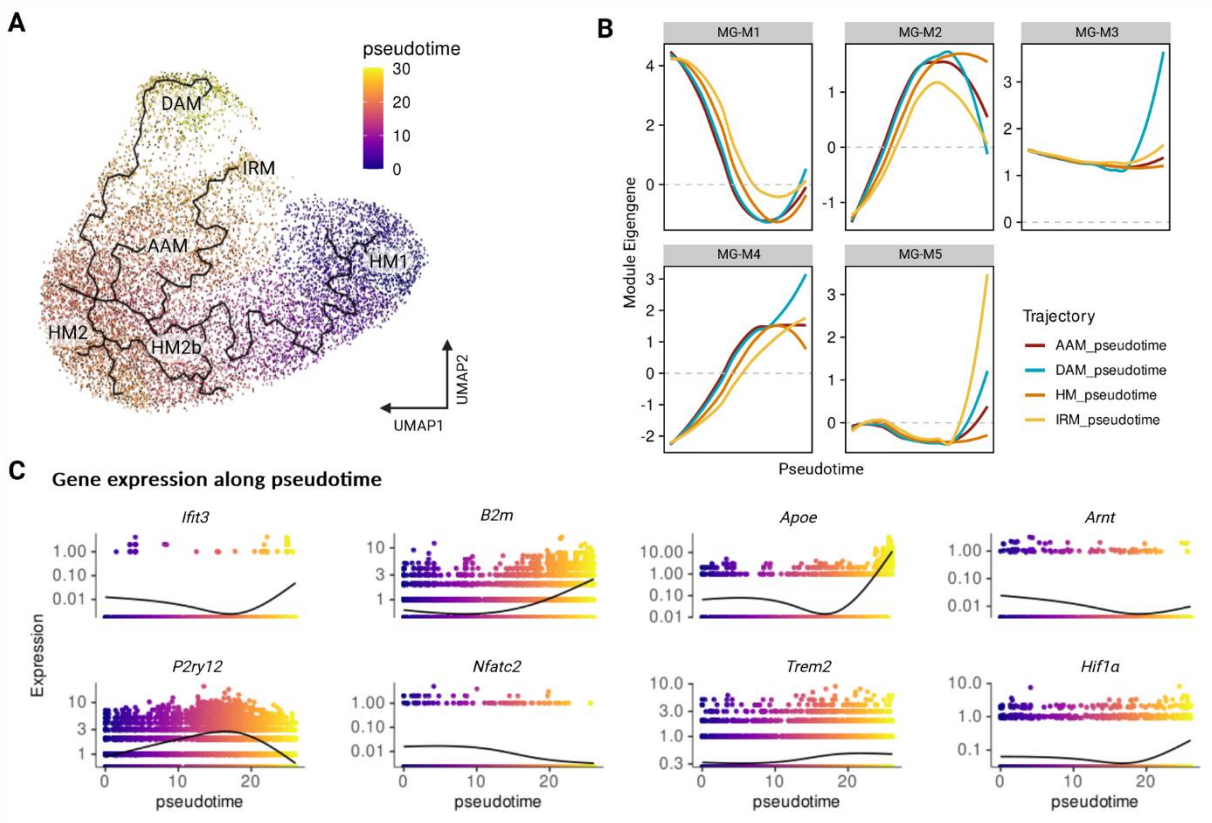

Fig. 11: Pseudotime analysis in microglia. (A) UMAP-plot of microglia, colored by monocle3 pseudotime assignment. Black line indicates trajectories identified by `monocle3`. Microglia transition from HM1 over HM2 to either AAM, DAM (over TRM) or IRM (over AAM). **(B)** Co-expression module dynamics for each trajectory arm. Plotted are the loess regressions of module eigengenes (MEs) as a function of pseudotime for each co-expression module in each trajectory arm. **(C)** Gene expression changes of some selected marker and hub genes in pseudotime. Each Dot represents the expression of the according gene in a single microglia cell, the black line represents the smooth expression curve generated by spline-line fitting.

4.6 Open Chromatin Profiling of Microglia during Aging and Disease

A few years ago, our lab demonstrated at cell population level that epigenetic changes occur in microglia in response to Aβ-pathology [140]. To see if these changes are driven by specific microglial subtypes and to better understand if and what kind of synergy exists between aging and Aβ-pathology, open chromatin profiling via scATAC-Seq was performed. To this end, nuclei from isolated and FACS-sorted cortical microglia of male C57BL/6J (WT) and APP23 mice of 6, 17 and 27 months of age were used, matching scRNA-seq data. After quality control and filtering, 31,865 nuclei from 17 samples were retained for downstream analysis.

Interestingly, scATAC-Seq identified more clusters than scRNA-Seq (Fig. 12B) and not all clusters could be clearly identified via label transfer or RNA imputation from the scRNA-Seq dataset. This suggests that scATAC-Seq provides additional information on microglia subtypes that is not detected by scRNA-Seq. Indeed, the majority of cell type-specific open chromatin regions (Differentially Accessible Regions, DARs) are located not only in promoter but also in intergenic and intronic regions (Fig. 12C), indicating the importance of regulatory elements, such as enhancers, in the adaptation of a specific microglial activation state.

Similar to the scRNA-seq analysis, the most abundant cell type were homeostatic microglia, which constituted over 60% of all microglia cells and comprised of 3 subtypes, two of which (HM1 and HM2) were identifiable via label transfer from the scRNA-Seq dataset. The smallest of the homeostatic clusters (HM) showed strong activity of homeostatic marker genes and GO enrichment analysis of its differentially accessible chromatin regions (DAR) indicate an important immune regulatory function and phagocytic activity. Similar to what was seen in transcriptomics, the number of HM2 cells decrease with age, in WT as well as in AD pathology, while no obvious change in numbers could be seen for HM (Fig. 12D). AAM cells, which were also identifiable by label transfer, however, differed in their distribution, being not found in 6 months old animals but found at much lower proportion in aging animals compared to transcriptomic data. In general, this data suggests that despite their overall similarity, microglia do show differences in their open chromatin profile. However, these differences are either not completely correlated with transcriptomic differences, or are limited by the high sparsity of scATAC-Seq data. Interestingly, overall, the number of open chromatin regions decreases with age in microglia from both wildtype and APP23 animals (Fig. 12E, top). However, in the end stage of Aβ pathology, chromatin seems to be again more accessible. The number of transcribed genes (Fig. 12E, bottom) supports this finding, yet there's also an increase in gene transcription in 27 months old WT animals. This again supports the hypothesis that aging itself might lead to microglia dysfunction, where poor chromatin accessibility might prevent the activation of genes involved in immune regulatory processes.

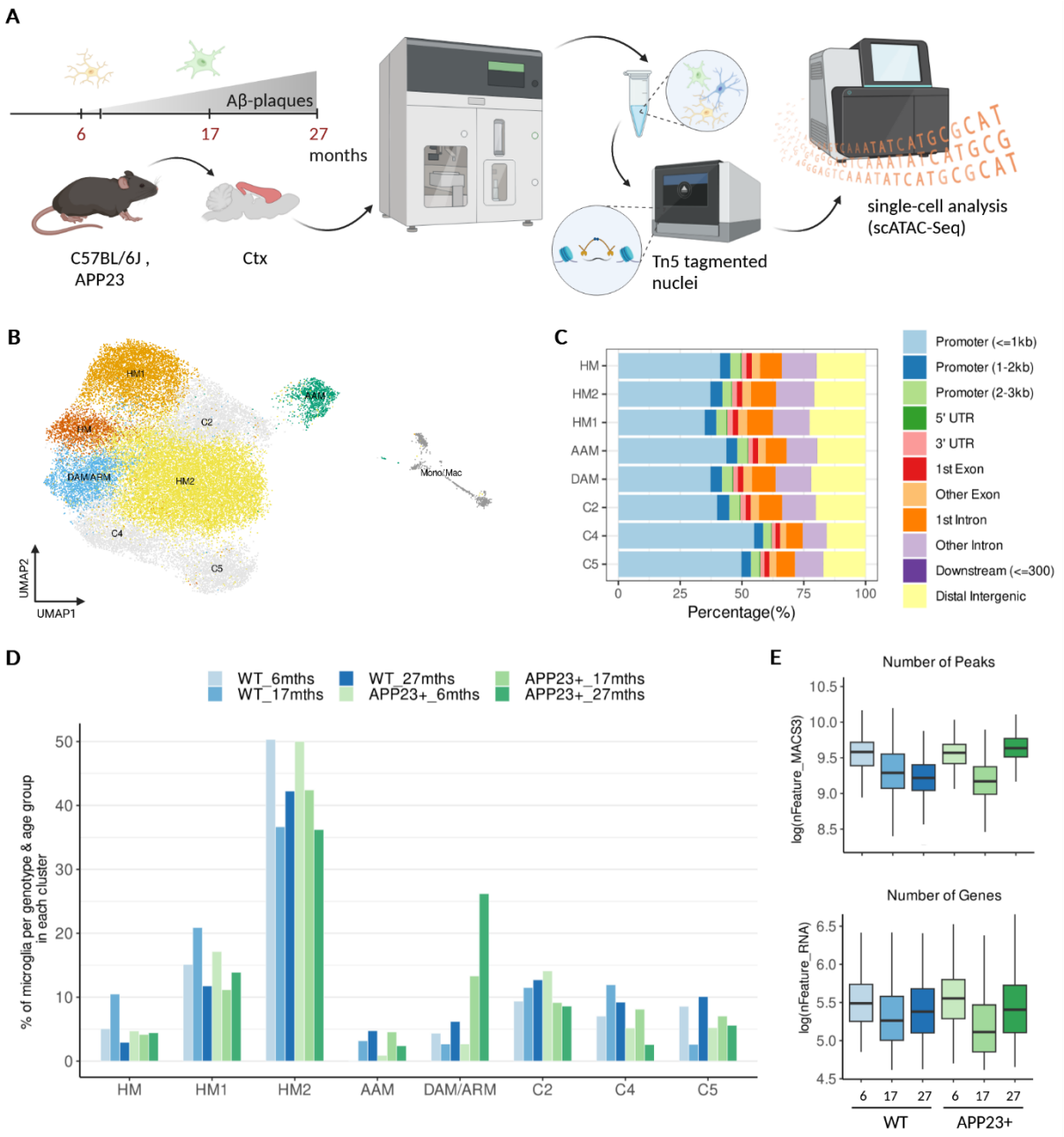

Fig. 12: snATAC-Seq of microglia with aging and Aβ pathology. (A) Schematic diagram of the microglia isolation workflow from mouse cortex (Ctx) for scATAC-Seq (10X chromium technology). See materials and Methods for more details. [Created with Biorender.com] **(B)** UMAP plot of the 31.865 nuclei passing quality control (*n* = 17 mice). Cells are colored according to clusters identified with Seurat's k-nearest neighbors (kNN) approach. In total, 8 microglia clusters and 2 monocyte/macrophage (Mono/Mac) clusters were identified. HM, HM1 and HM2 = homeostatic microglia; DAM/ARM = disease associated / activated response microglia; AAM = aging associated microglia; C2, C4 and C5 = microglia clusters with yet unidentified functions. **(C)** Number of detected open chromatin (peaks, right) and transcribed genes (left) in the different conditions. Cells from WT animals are indicated in shades of blue, while cells from APP23 positive mice are indicated in shades of green. **(D)** Percentage of cells per microglia cluster from each genotype-age group. Cells from WT animals are indicated in shades of blue, while cells from APP23 positive mice are indicated in shades of green.

To check if there are cell subtype-specific changes in open chromatin regions during healthy aging, cluster-specific DARs between the three age groups were identified. In contrast to the transcriptomics data, the number of protein-coding genes close to significantly regulated DARs (FDR corrected p-value < 0.05, $|\log_2 FC| > 0.1$) was highest in the young animals and decreased with age. This is in accordance to what was seen when comparing number of genes and number of peaks (Fig. 12E). Interestingly, although a large number of DARs unique to each age group could be identified, they did not show particular pathway enrichments, possibly reflecting the fact that not all regulatory regions can be properly assigned to their respective genes.

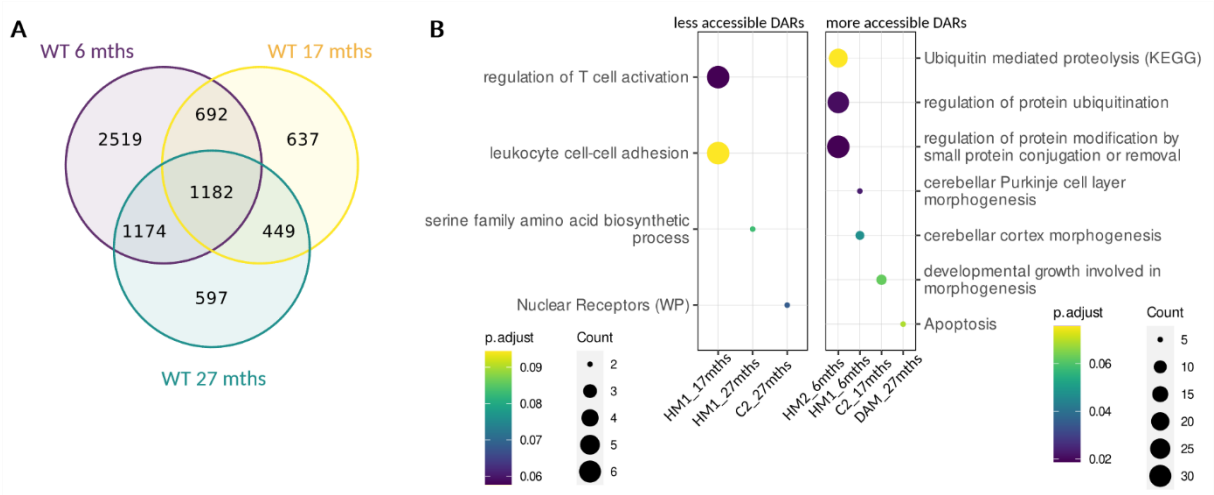

Fig. 13 Temporal Overlap of DARs from WT animals. (A) Pairwise comparison of microglial DARs (FDR adjusted p-value ≤ 0.05, |log2FC| > 0.1) of WT animals in 6, 17 and 27 months old animals with enriched GO terms **(B)** for genes close to significant DARs that are unique for this age group.

Comparing APP23 and WT samples identified 16,016 cell subtype-specific DARs (FDR corrected p-value < 0.05, |log2FC| > 0.25), most of which were located in promoter (~35 %) or intergenic regions (~26 %) with a median distance of ~25 kb from the nearest Transcription start site (TSS) (Fig. 14A). Around 70 % of these intergenic DARs (3,006 of 4,265) and around 57 % (2,648 of 4,649) of intronic DARs were mapped to a FANTOM [163] enhancer. Most DARs showed increased accessibility in Aβ pathology (10,446 vs 5,570), especially in the DAM/ARM cluster, which in general has most DARs (*n* = 5,264) followed by C2 (*n* = 1,529) and HM1 (*n* = 753) (Fig. 14B). Less abundant cell types had less DARs, reflecting either limited power to detect them or indicating that these microglia phenotypes do not undergo significant molecular changes due to Aβ-pathology in mice. Gene ontology enrichment analysis of the nearest protein-coding genes of the unique DARs identified upregulation of developmental processes in the homeostatic clusters and downregulation of inflammatory processes. Especially HM in APP23 cells show drastically decreased chromatin accessibility near genes involved in immune cell activation (Fig. 14C), indicating that this microglia population might be important for

maintaining tissue homeostasis in Aβ pathology. Less accessible DARs in microglia from APP23 animals in cluster C2 are close to genes involved in response to insulin stimulus and glucose import into the cell, both of which were shown to be impaired in AD patients and related to cognitive decline (reviewed in [194-197]). In contrast, DAM show higher chromatin accessibility near genes related to ion transport and response to insulin stimulus, peptides or hormones, which might support the hypothesis that DAMs are a beneficial microglia phenotype during AD, trying to ameliorate the disease outcome [31]. There were chromatin regions that were less accessible during AD pathology in all microglia subpopulations identified. Genes close to these shared DARs were enriched for MAPK-signaling, especially p38 MAPK, which is one of the most important regulators of Aβ-toxicity (reviewed in [198]). This data suggests that reduced activity of MAPK pathways in general might be involved in the pathogenesis of AD and could be another interesting therapeutic target that may warrant further investigation.

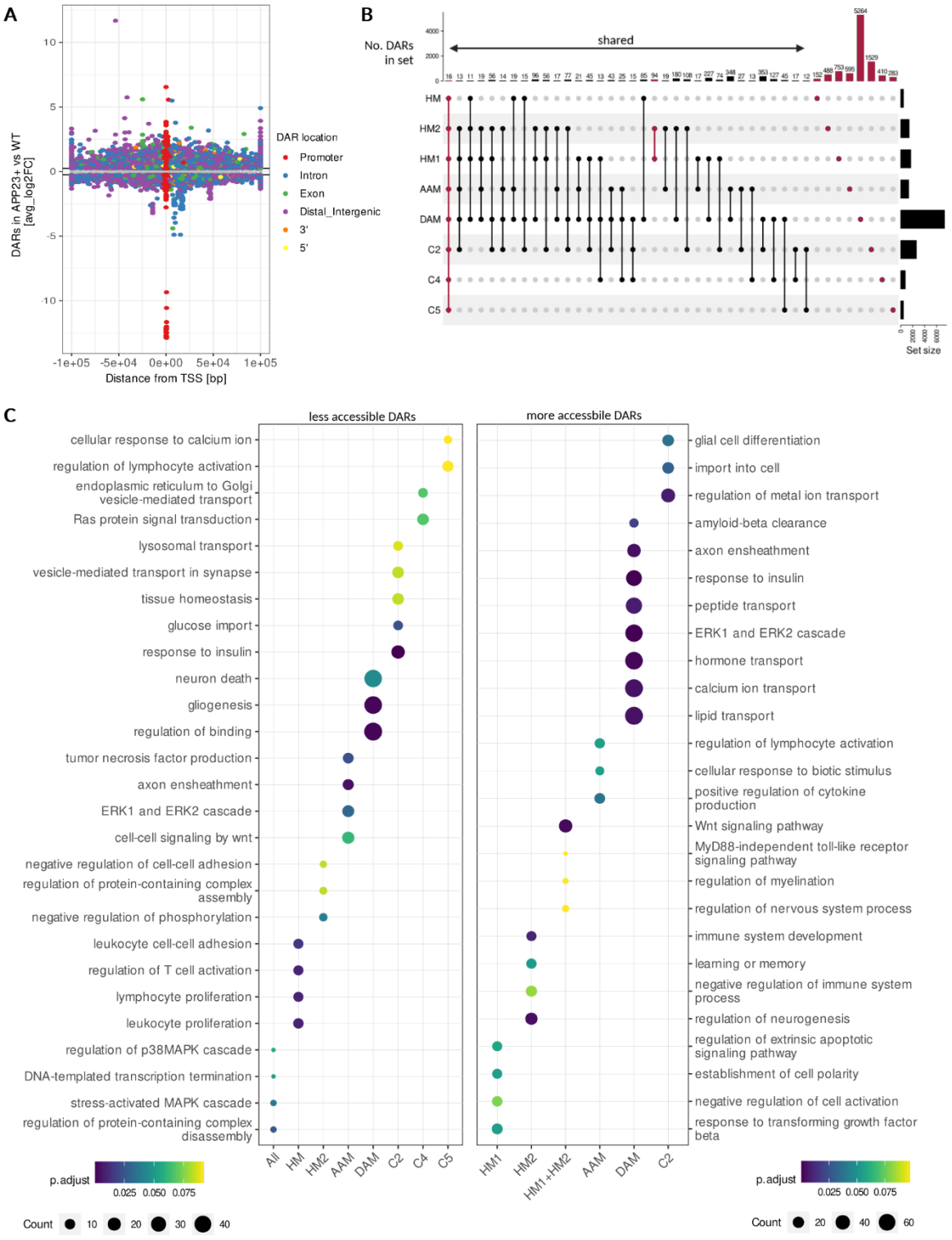

Fig. 14: Microglia-specific DARs with Aβ pathology. (A) Location and Effect size of significant DARs in APP23 vs WT microglia (fdr corrected p-value < 0.1, logFC threshold = 0.1). Cell-specific DARs were annotated relative to the nearest TSS. **(B)** Upset Plot showing DARs unique for or shared between microglia subpopulations. DAR sets for which the GO enrichment results are shown in (C+D) are marked in red. **(C)** Dotplot of selected top GO enrichment results for genes close to significant DAR sets (marked red in (B)). The color indicates the significance value (Bonferroni adjusted p-value), the size of the dots refers to the gene counts.

4.7 Microglia-specific Transcription Factor Motif Enrichment in response to Aβ pathology

Transcription Factors (TFs) are key determinants of cell fate and differentiation and have been implicated in neurodegeneration. Therefore, overrepresented transcription factor motifs in cluster-specific scATAC-peaks and in APP23 vs WT microglia were identified using the JASPAR database [166]. Microglia subtypes could be defined by individual TF-motif activities, suggesting that specific TFs regulate chromatin accessibility in different microglia subpopulations. TFs that are enriched within DARs could provide insight into alterations of microglia signaling pathways in aging and Aβ pathology. Interestingly, motif variability in DARs of all microglia populations was increased in APP23 compared to WT cells. This was also supported by chromVAR [165], a tool to infer TF associated chromatin accessibility and therefore predict TF activity in an unbiased way compared to motif enrichment as it does not need a pre-specified list of cell-specific DARs. Increase in motif variability and chromatin accessibility in Aβ pathology may explain why the majority of microglia clusters in all conditions showed upregulation of translational processes. For example, both methods show an enrichment of *Hif1* binding motifs (*Hif1α* and its heterologous binding partner *Arnt* or *Hif1β*) within the DAR of DAM-cells (Fig. 15, motif activity), that was supported by increased *Hif1α* expression in the scRNA-Seq dataset (Fig. 15B, target gene expression) and upregulation of gene expression throughout the pseudotime trajectory (Fig. 11C), suggesting that *Hif-1α* acts as a transcriptional activator in microglia. Interestingly, while the motif variabilities of *Arnt and Hif1α* were significantly increased in HM2 of 27 months old APP23 positive animals, target genes in the RNA-Seq data were slightly downregulated in this group, indicating that *Arnt* may act as a repressor in this cluster or that other epigenetic modifications prevent HIF-1α binding. We made similar observations for *Nfatc1* and *c2* and *Nfe2l2* which show high motif variability in aged mice or with Aβ-pathology, especially in HM2 and DAMs, with a slightly decrease in target gene expression. Nfat, nuclear factor of activated T cells, is a family of pro-inflammatory TFs and especially the isoforms c1 and c2 are highly expressed in microglia [199]. Constituent expression also during healthy aging can support a neuroinflammatory environment prone to neurodegeneration. Indeed, knocking out *Nfatc2* in a mouse model of Aβ-pathology attenuated cytokine levels and reduced microgliosis and astrogliosis but did not have an effect on plaque-load [200]. In contrast, *Nfe2l2* (nuclear factor 2 erythroid 2 like 2, also referred to as Nuclear respiratory factor 2, NRF2) represses inflammation and has been shown to counteract neurodegeneration in mice-models of Tau-pathology as well as in AD patients [201, 202].

Several other TFs implicated in inflammatory responses (e.g. Stat2, *Stat4*, *Stat5a*, *Stat5b*, *Stat6*) (reviewed in [203]) or in microglia proliferation and differentiation (e.g. *Runx1 [10]*) showed increased TF activity and target gene expression in the DAM cluster, but also in AAM (*Runx1*, *Stat2*) and in HM2 (*Stat2*, *Stat4*, *Stat5a*, *Stat5b, Stat6)*. To gain further insight into microglial TF-mediated gene expression

during AD pathology, a TF regulatory network was generated (Fig. 15C). Within this network, several of the DEGs associated with Aβ-pathology (Fig. 8) could be identified, including *B2m*, *Jun* and *Pfkl*.

Together, these data support the hypothesis that Aβ-pathology leads to microglia subtype-specific changes in chromatin accessibility during the progression of Aβ deposition, providing insight into how these subpopulations might contribute to AD pathology.

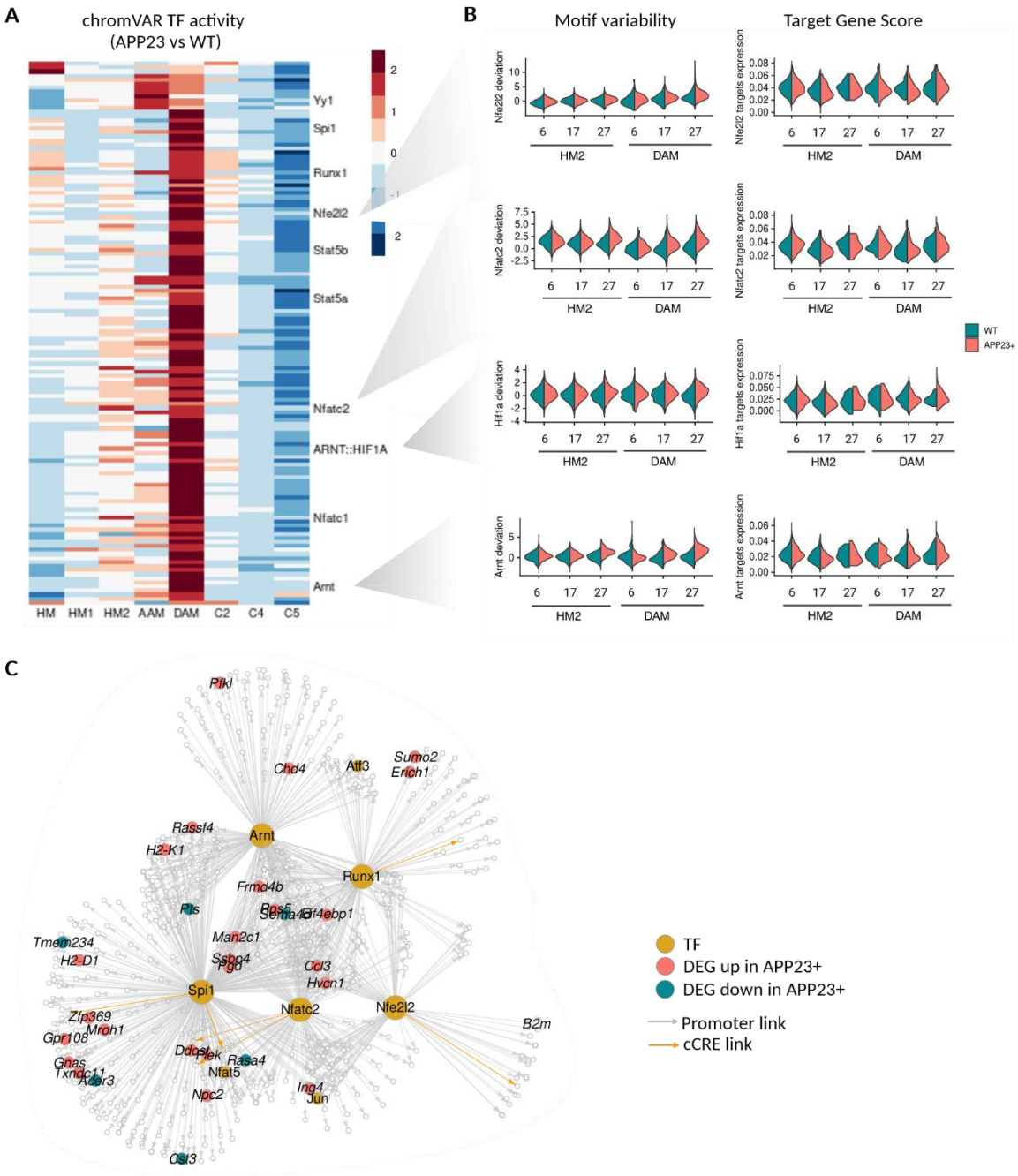

Fig. 15: ChromVAR motif activity identifies key regulatory elements in AD pathology. (A) Heatmap of average chromVAR motif activity for APP23 vs WT for each cell type, colored by z-score and scaled by row. **(B)** Violin plots displaying motif variability in snATAC-Seq microglia cluster that showed significant differences between APP23 and WT microglia in the Chromvar Heatmap in (A) and the according target gene expression in scRNA-Seq data (right) of *Nfe2l2*, *Nfatc2, Hif1α* and *Arnt*, split by genotype. **(C)** TF-regulatory network showing some predicted candidate target genes for the following TFs: *Spi1*, *Arnt*, *Runx1*, *Nfatc2*, *Nfe2l2*. Only highly significant DEGs are shown (FDR corrected p-value < 0.01, $|\log_2 FC| > 0.25$).

4.8 The role of Hif1α in AD pathology

We encountered the HIF-1α-signaling pathway again and again during the course of this project, firstly as a strong marker for the DAM/ARM cluster, secondly as highly expressed in plaque-associated microglia and finally also in the epigenetic analysis. This data suggests that HIF-1α may be a key regulatory element that drives Aβ pathology-associated microglial responses. Indeed, several recent reports have demonstrated an upregulation of HIF-1α-signaling in AD, pointing to concurrent activation of *Hif1α* and genes related to oxidative phosphorylation as a common feature for microglia responding to Aβ plaques in mice as well as in humans [190, 204]. However, it is not clear yet which aspects of microglia activation are regulated by *HIF1α* and if HIF-1α-signaling is deleterious or beneficial for the progress of AD. To examine these aspects, our lab generated a conditional knockout of *Hif1α* in microglia (using Cx3cr1-CreER-mediated recombination) on WT as well as APP23 background. Knockout of microglial *Hif1α* resulting in increased proliferation of microglia around Aβ-plaques, enhanced plaque compaction and reduced neuritic damage while leaving plaque load unchanged (Fig. 16; data generated and provided by Ann-Christin Wendeln and Lisa Steinbrecher), suggesting that HIF-1α signaling might impair microglia barrier function. To further characterize the effects of *Hif1α* knockout on amyloid-responding microglia, single cell RNA-seq analysis was performed, including enrichment of MX04+ cells (Fig. 17A).

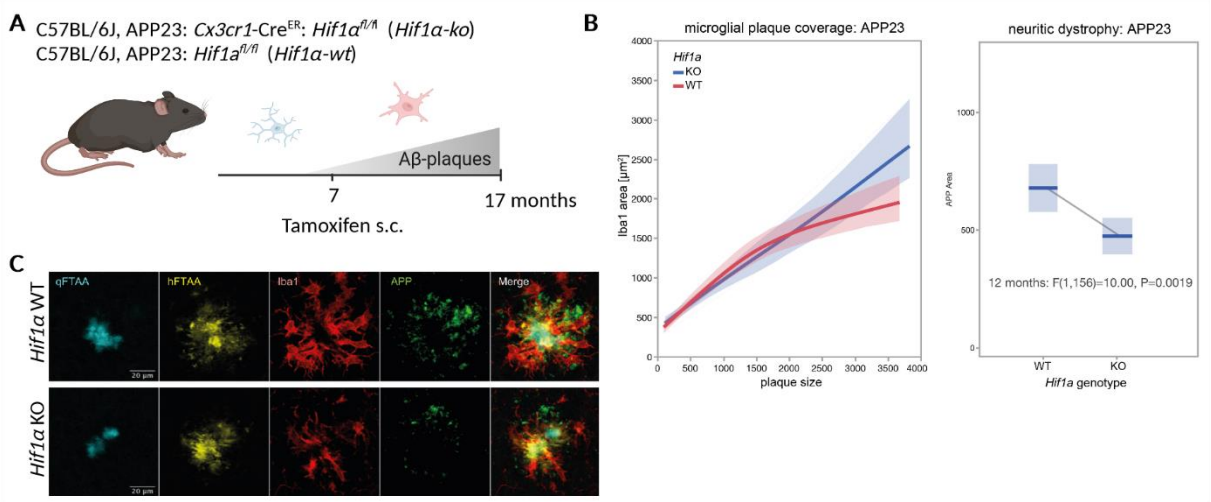

Fig. 16: Hif1α-ko enhances microglial barrier function. (A) Schematic diagram of the conditional Hif1α-knockout mouse model used in this part of project. See Materials and Methods for more details. [Created with Biorender.com] **(B)** *Hif1α*-ko enhances microglial plaque coverage (left) and reduces neuritic damage (right) while leaving plaque load unchanged (data generated and provided by Ann-Christin Wendeln und Lisa Steinbrecher). **(C)** Exemplary staining of Aβ-plaques with luminescent conjugated oligothiophenes (LCOs) surrounded by microglia in *Hif1α*-wt (top) and Hif1α-ko (bottom) animals. Co-staining of the LCO qFTAA (quatroformylthiophene acetic acid) that stains the compact Aβ-plaque core, hFTAA (heptaformylthiophene acetic acid) which stains more diffuse plaques and APP which stains dystrophic neurites [205]. Microglia are labelled with Iba1.

Single-cell transcriptomics with SmartSeq2 of plaque-associated and -distant microglia shows a shift in subpopulations of *Hif1α*-ko animals to a more homeostatic phenotype in APP23 mice, with almost complete loss of the IRM cluster (Fig. 17D). Both together suggests a role of *Hif1α* in activating the interferon response and pro-inflammatory cytokine production, similar to what was seen in monocytes before (reviewed in [206]). Interestingly, such a strong reduction in cell numbers could not be seen in DAM/ARMs, although many of the DAM signature genes are HIF-1α-responsive and *Hif1α* itself is a DAM-signature gene. However, when comparing DAM cells in *Hif1α*-ko vs. *Hif1α*-wt cells, the expression of genes related to metabolic pathways like glycolysis and cholesterol metabolism was found to be reduced (Fig. 17C), indicating that *Hif1α* might only regulate a specific part of the DAM response that does not affect their clustering. Pathway enrichment further indicated a reduction of genes involved in the formation of phagosomes and lysosomes, which might be an explanation for the previously mentioned constant number of plaques due to reduced Aβ-phagocytosis and enhanced plaque compaction.

Comparing *Hif1α*-ko *vs Hif1α*-wt in all microglia clusters for all conditions (Fig. 18) showed decreased expression levels of genes related to immune system activation and inflammatory processes, whereas homeostatic marker genes and functions (e.g. synapse pruning) are upregulated in knockout animals. In addition, some genes well-known to be related to Aβ-pathology like *Apoe* and *Trem2* show reduced expression in the absence of microglial *Hif1α*, again indicating reduced neuroinflammation in *Hif1α*-ko brains. Interestingly, *Tyrobp,* one of the early signature genes during the transition from homeostatic to stage 1 DAMs [31] and a modulator of *Apoe* transcription even in the absence of *Trem2* [207], was upregulated in *Hif1α* knockout microglia. Together, this data suggests that the knockout of *Hif1α* induces a selective shift in the activation state of different microglia subpopulations to a less inflammatory and neurotoxic phenotype, probably ameliorating disease.

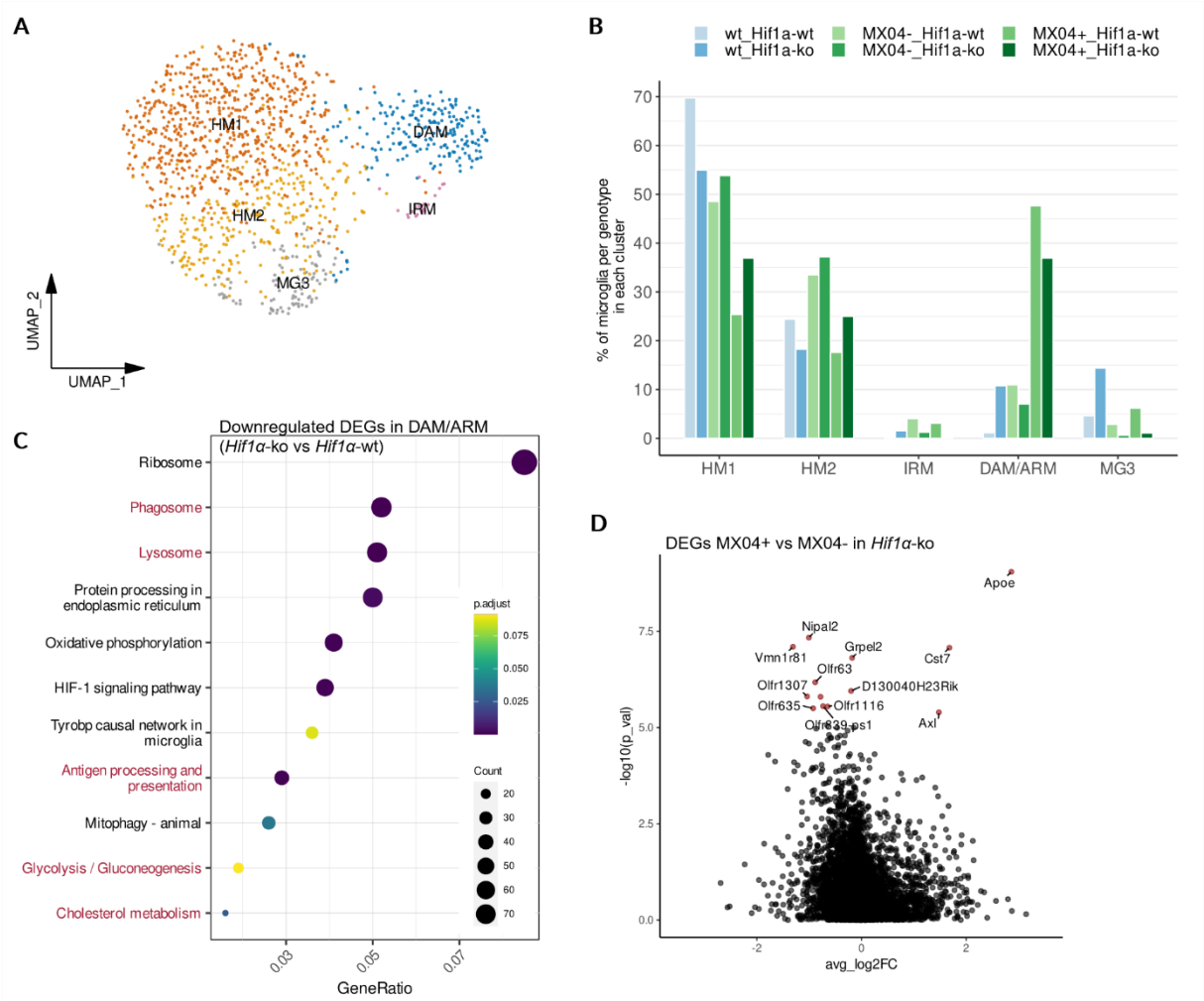

Fig. 17: *Hif1α*-ko induces transcriptional shifts in microglial subpopulations. (A) UMAP plot of the 1,306 cells passing quality control (*n* = 10 mice). Cells are colored according to clusters identified with Seurat's k-nearest neighbors (kNN) approach. In total, 5 microglia clusters were identified. HM1 and HM2 = homeostatic microglia; DAM/ARM = disease associated / activated response microglia; IRM = interferon response microglia. **(B)** Percentage of cells per microglia cluster from each condition. Cells from WT animals are indicated in shades of blue, while cells from APP23 positive mice are indicated in shades of green. **(C)** Dotplot showing selected top enrichment results (KEGG, WP) for downregulated DEGs (FDR corrected p-value < 0.05, $\log_2$FC < -0.1) between *Hif1α*-ko and *Hif1α*-wt animals in the DAM/ARM cluster. The color of the dots indicates the Bonferroni adjusted p-values. Terms marked in red are of particular interest, as these terms are not only strongly upregulated in DAM cells, but also in plaque-associated microglia. **(D)** In APP23 animals, plaque-associated (MX04+) and plaque-distant (MX04-) microglia from *Hif1α*-ko animals do not show strong differences in their gene expression profile. DEGs with a Bonferroni adjusted p-value < 0.1 are marked in red.

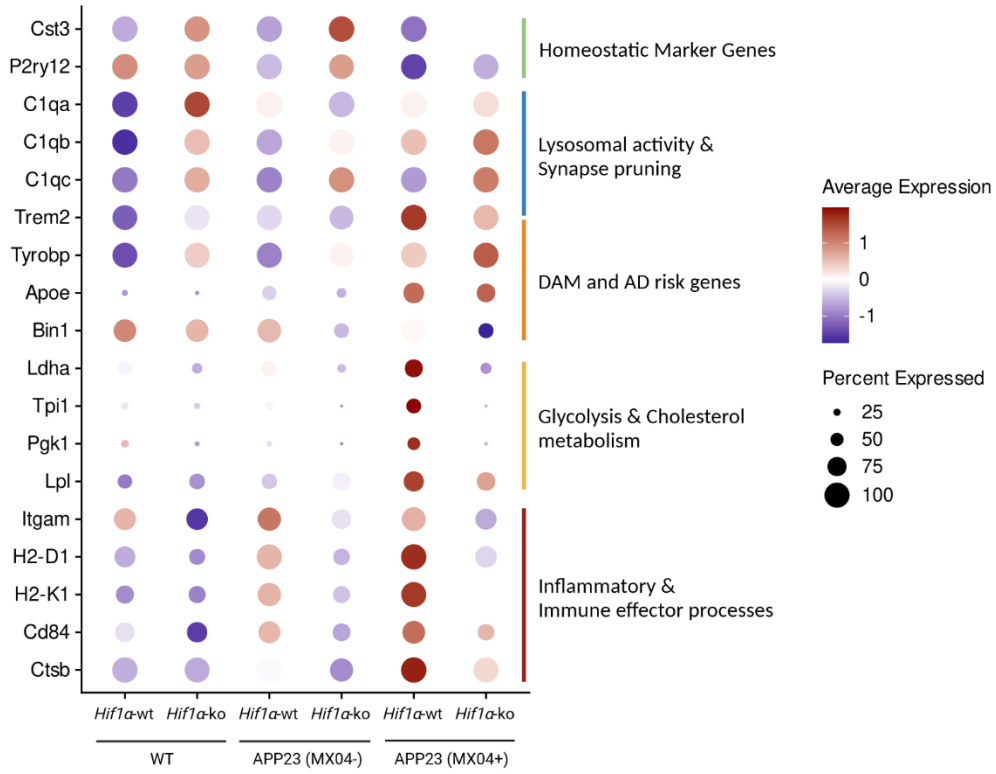

Fig. 18: Impact of *Hif1α*-ko on the microglial transcriptome. DotPlot of selected DEGs between *Hif1α*-ko vs *Hif1α*-wt of each Genotype with associated pathways. The color of the dots indicates up- (red) or downregulation (blue) of the gene in this group of cells, the size of the dots refers to the percentage of cells expressing this gene in this condition.

4.9 Discussion

In the beginning, this study aimed at identifying and characterizing microglia subpopulations on transcriptomic level during aging and AD-pathology. In the meanwhile, it is well accepted that these subpopulations exist, especially during development and disease (reviewed e.g. in [4, 208]). However, little is known about their role and function and a mix of detrimental and beneficial roles have been suggested for different microglial subtypes.

In this study, single cell transcriptomic and open chromatin profiling of microglia during aging and AD-pathology showed that heterogeneity of microglia does not only develop in response to Aβ-pathology, but also during healthy aging. Indeed, aging itself can lead to shifts in microglia subtype distribution, giving rise to an aging-associated microglia subpopulation (AAM) that was not described so far, but could be confirmed on protein level here. Given its occurrence only at very old age, this microglia population could reflect a senescent phenotype, which could be highly relevant for age-related neurodegenerative diseases. Yet, this needs further validation as transcriptomic senescence markers are hard to identify and AAMs did not clearly show a senescent gene signature as published recently by Hu et al. [209]. In addition, homeostatic microglia could be further divided into 3 subgroups, one of which declines significantly during aging and with Aβ-pathology, indicating a transition of these microglia to more activated phenotypes. This finding could be confirmed by pseudotime analysis, indicating that most of the microglia populations identified originate from this homeostatic cluster and may transition into DAM/ARM [31] or through AAM into IRM [120], indicating that the aging-associated phenotype might also represent a molecular state that can more easily transition into disease-associated subtypes.

While differentially accessible chromatin regions provided only limited information with regards to biological pathways due to the poor annotation of regulatory regions to their target genes, open chromatin profiling could be used to identify several transcription factor binding sites that were more accessible in microglia from APP23 animals. For example, binding sites for several Stat TFs were highly enriched in DAMs in late stage Aβ-pathology. Accordingly, activation of *Stat*-genes is important for various biological processes (e.g. cell growth, differentiation, development and apoptosis (reviewed in [203, 210]) as well as regulation of inflammatory and immune responses, with overaction of the STAT-signaling-pathway also being associated with numerous diseases, including AD. Indeed, *Stat5* is essential for IL-3 induced microglial activation [211] and it was also recently shown to be involved in the detrimental effect of the R47H-*TREM2* variant in patients with late onset AD [212]. Another TF binding motif highly enriched in APP23 DAM cells is *Nfatc2*, which also functions as a regulator of proinflammatory gene expression [199]. These data support the hypothesis that Aβ-pathology leads to microglia-subtype-specific overaction, leading to an increased neuroinflammatory environment.

Aβ plaques and phosphorylated tau are two pathological hallmarks of AD and they are both considered to be related to cholesterol metabolism and glycolysis [213-215]. Indeed, metabolic dysfunction has long been recognized as a preclinical anomaly in AD and can be measured by the cerebral metabolic rate of glucose (CMRglc), an indicator of neuronal and synaptic activity (reviewed in [216]). Both pathways were upregulated in plaque-associated microglia from this study, especially in DAMs. This is in line with previous reports showing an abnormal accumulation of cholesterol in cores of mature plaques in mice as well as in patients [215]. As both cholesterol and glycolytic metabolism are essential for proper brain functioning, they could be an interesting target to bolster brain metabolic resilience and as such alter the course of brain aging and/or disease development to reduce or prevent the risk for developing NDDs such as AD. Thinking of how this could be achieved, we checked the genes underlying these pathways and found an enrichment of genes related to the HIF-1α-signaling pathway in plaque-associated microglia (Fig. 9). An independent analysis of the open chromatin profiles in microglia during Aβ pathology also revealed changes in gene regulation and biological pathways involved in AD-pathogenesis (Fig. 14 and Fig. 15), similar to the ones identified on gene expression level. Together, both methods suggest *Hif1α* and its heterologous binding partner *Arnt* as key regulatory elements in the pathogenesis of AD, in accordance with previous findings from our lab, showing *Hif1α* expression to be correlated with disease severity [145]. *Arnt* motif variability was increased in DAM cells in late-stage Aβ pathology (Fig. 15B), suggesting more accessible binding sites. Gene expression of *Hif1α* was also increased with Aβ-pathology and both genes show upregulation throughout pseudotime trajectory (Fig. 11C)), suggesting that the TF HIF-1α acts as a transcriptional activator in disease associated microglia.

To further characterize the role of *Hif1α* in Aβ-pathology, a conditional knockout model was generated. Although no reduction of plaque load could be found upon microglial *Hif1α* knockout, histological data suggests increased proliferation of microglia around Aβ-plaques, enhanced plaque compaction and reduced neuritic damage. Transcriptomics shows a selective shift of microglia subpopulations to more homeostatic phenotypes. For example, the expression of *Apoe* and *Trem2*, two well-known AD risk genes, was reduced in *Hif1α*-ko animals, while *Tyrobp* expression was increased. Emerging evidence suggests a beneficial role of *Tyrobp* in Alzheimer's disease, as it can repress microglia-mediated cytokine production and secretion and therefore suppresses neuroinflammation. It's upregulation upon amyloid deposition could therefore be a compensatory mechanism that attempts to limit the pro-inflammatory function of microglia. In addition, it can enhance phagocytic activity of microglia and therefore enhance clearance of Aβ and apoptotic neurons (reviewed in [217]). Together this data supports the hypothesis that *Hif1α* induces a detrimental microglial phenotype and impairs microglia barrier function. Reducing HIF-1α activation might therefore be a therapeutic strategy to selectively shift microglia activation states in AD pathology, which could be beneficial for disease pathology due to reduced Aβ-neurotoxicity and neuroinflammation.

5 THE IMPACT OF PERIPHERAL INFLAMMATORY INSULTS ON BRAIN MICROGLIA

A separate part of this project built on our lab's previous finding that microglia are capable of developing immune memory in response to peripherally applied bacterial lipopolysaccharide (LPS) [145]. As this original study was performed at cell population (bulk) level, it remains unclear, if specific subpopulations of microglia are driving long-lasting memory effects. Moreover, it remains unclear if and how different stimuli modify the molecular responses of microglia. Therefore, to broaden our understanding of immune memory in microglia, various peripherally applied immunological stimuli (recombinant cytokines, bacterial lipopolysaccharide and the viral mimetic Poly(I:C)) were here characterized for their ability to induce immune memory effects in the brain of young adult mice based on multiplex cytokine measurements. In addition, it was investigated to which extent living pathogens (*Yersinia enterocolitica*, *Staphylococcus aureus*, *Bacillus Calmette-Guérin*) can induce immune memory effects. These experiments served to select conditions with strong immune memory effects for further analysis using single cell multi-omic profiling, which was also established as part of this thesis and which will be described in section 5.2.

5.1 Cytokine Measurements

To examine immune memory effects in the brain, C57BL/6J mice were either injected with isolated immunological stimuli (LPS, Poly(I:C), TNF-α, IL-10, TGF-β) or infected with living pathogens (*Y. enterocolitica*, *S. aureus*, *BCG*). The animals immune response was evaluated by measuring thirteen cytokines (TNF-α, KC/CXCL1, IL-18, IL-23, IL-12p70, IL-6, IL-12p40, IL-1β, TGF-β, IL-10, G-CSF, TARC/CCL17, and MDC/CCL22) in serum and brain homogenates either during the acute phase of the immune reaction after the first stimulation or after a second challenge 4 weeks later with bacterial lipopolysaccharide (LPS) or Poly(I:C), the latter of which mimics viral RNA. For reasons of clarity, only selected cytokines are shown below.

Already three hours after the first insult an increase of cytokine levels could be detected, which was more pronounced in serum than in brain homogenates (Fig. 19). Matching the previous study [145], LPS injections on four consecutive days (4x LPS) led to reduced blood levels of certain pro-inflammatory cytokines (e.g. KC, TNF-α), while their levels in the brain were still elevated. Anti-inflammatory cytokines, such as IL-10 and G-CSF, remained elevated in both brain and serum, indicating immune-tolerance. Together with the fact that these animals only showed strong phenotypical effects until the second LPS injection and started recovering from day 3 on, this may indicate a stronger and/or faster peripheral tolerance-effect induced by 4x LPS injections. Repeated peripheral application of anti-inflammatory cytokines (4x TGF-β and 4x IL-10) did not induce acute cytokine release in the brain;

however, 4x IL-10 injections significantly reduced certain interleukin-levels (e.g. IL-12p70, IL-1β; not shown) in the brain but not in serum, confirming that cytokines can directly affect the brain and that the brain's immune response is to some extent uncoupled from the periphery.

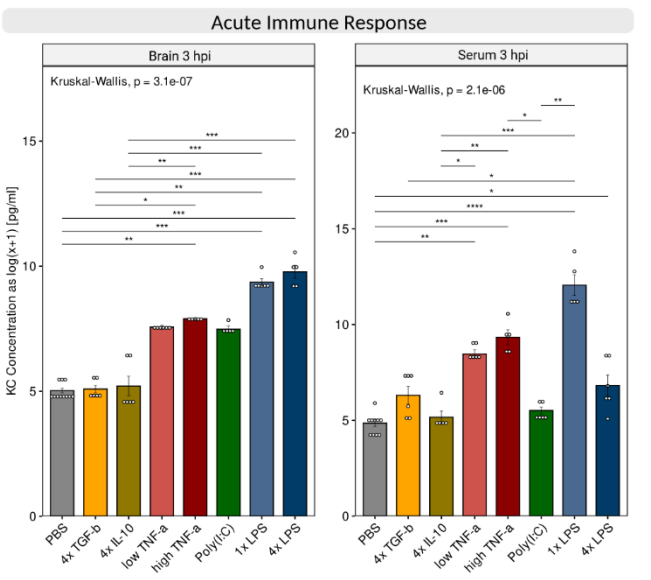

Fig. 19: Acute immune response after stimulation with recombinant cytokines. Barplots for measured KC concentration in serum (left) and brain homogenates (right) 3 hours after stimulation. Single samples are shown as dots, error bars show standard error of the mean. Statistical comparison was performed using Kruskall-Wallis test with post-hoc Dunn's test and Benjamini Hochberg (BH) correction for significant main effects ($p < 0.05$). ns (not significant):p>0.5, *p<0.5, **p<0.01, ***p<0.001, ****p<0.0001.

To further evaluate the training and tolerance effects in the brain, mice were peripherally challenged with either a high dose of LPS or with Poly(I:C) four weeks after the first peripheral stimulation of the immune system. In both cases, the proinflammatory cytokine release returns mostly back to baseline within 1 day in serum. However, this effect is less pronounced in the brain. Indeed, for some pre-treatments, such as repeated application of LPS, TGF-β or IL-10, levels of certain cytokines (e.g. TARC, IL-6) were still elevated 1 day after the second peripheral insult, while other cytokines (e.g. TGF-β, IL-10) were reduced. In contrast, pre-treatment with a single dose of LPS or with the viral Toll-like receptor 3 agonist Poly(I:C) resulted in a general cytokine increase in serum and brain, indicating immune training. In addition, similar to what was described before for LPS [145, 218, 219] this data indicates dose-dependent immune training (low dose) and tolerance (high dose) effects for TNF-α after restimulation with LPS.

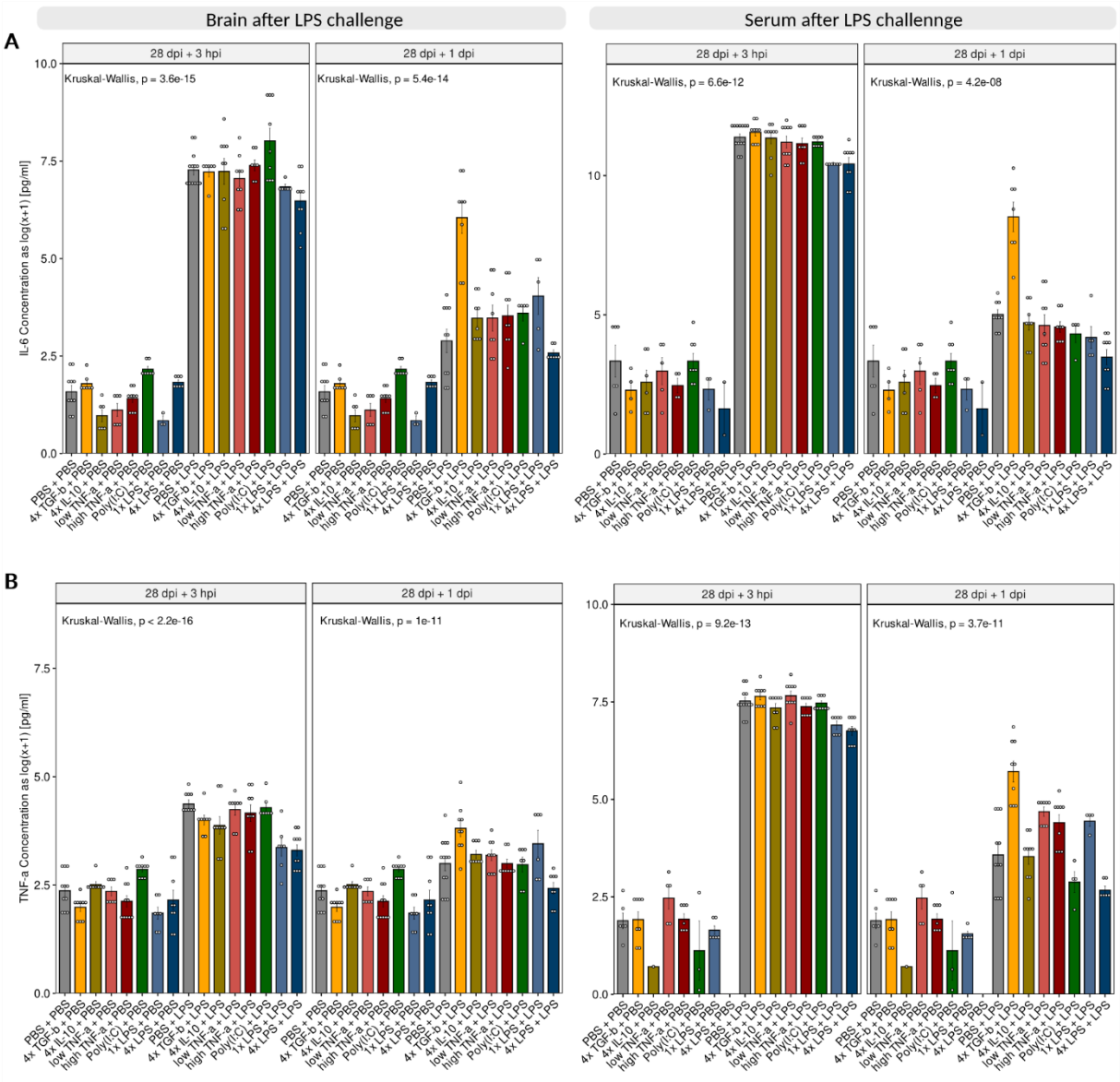

Fig. 20: Immune response after stimulation with isolated cytokines and re-challenge with LPS. Barplots for IL-6 **(A)** and TNF-α **(B)** levels in serum (right panels) and brain homogenates (left panels) 3 hours and 24 hours after challenge with LPS. Concentrations are shown as log(x+1). Single samples are shown as dots, error bars show standard error of the mean. Statistical comparison was performed using Kruskall-Wallis test with post-hoc Dunn's test and Benjamini Hochberg (BH) correction for significant main effects ($p < 0.05$). For reasons of clarity, only the global p-value is shown.

As these peripheral stimuli do not necessarily model infections as they only provide short-term stimulation while infections may last several days, mice were also i.v. infected with live bacteria (*Y. enterocolitica*, *S. aureus*) and the live attenuated vaccine Bacille-Calmette-Guerin (BCG). All three stimuli showed a general upregulation of cytokine production in the periphery and in the brain 1 day after infection and high levels of pro-inflammatory cytokines upon restimulation with LPS 4 weeks later. Interestingly, compared to acute stimuli (recombinant cytokines, LPS, Poly(I:C)), the immune response after live bacterial infections was prolonged, showing increasing cytokine production even after 3 dpi. In addition, for some cytokines, long-term effects were visible as lower or higher baseline levels compared to control animals 28 days after infection. For example, an infection with

Y. enterocolitica led to decreased baseline of certain cytokines such as IL-6, while BCG increased their levels (Fig. 21).

Taken together, these data suggest that not only isolated pro-inflammatory peripheral insults can lead to immune memory effects, but also infection with live pathogens, as well as pre-treatment with anti-inflammatory cytokines. Furthermore, these effects do not only depend on the number of applications, but also on the applied dose.

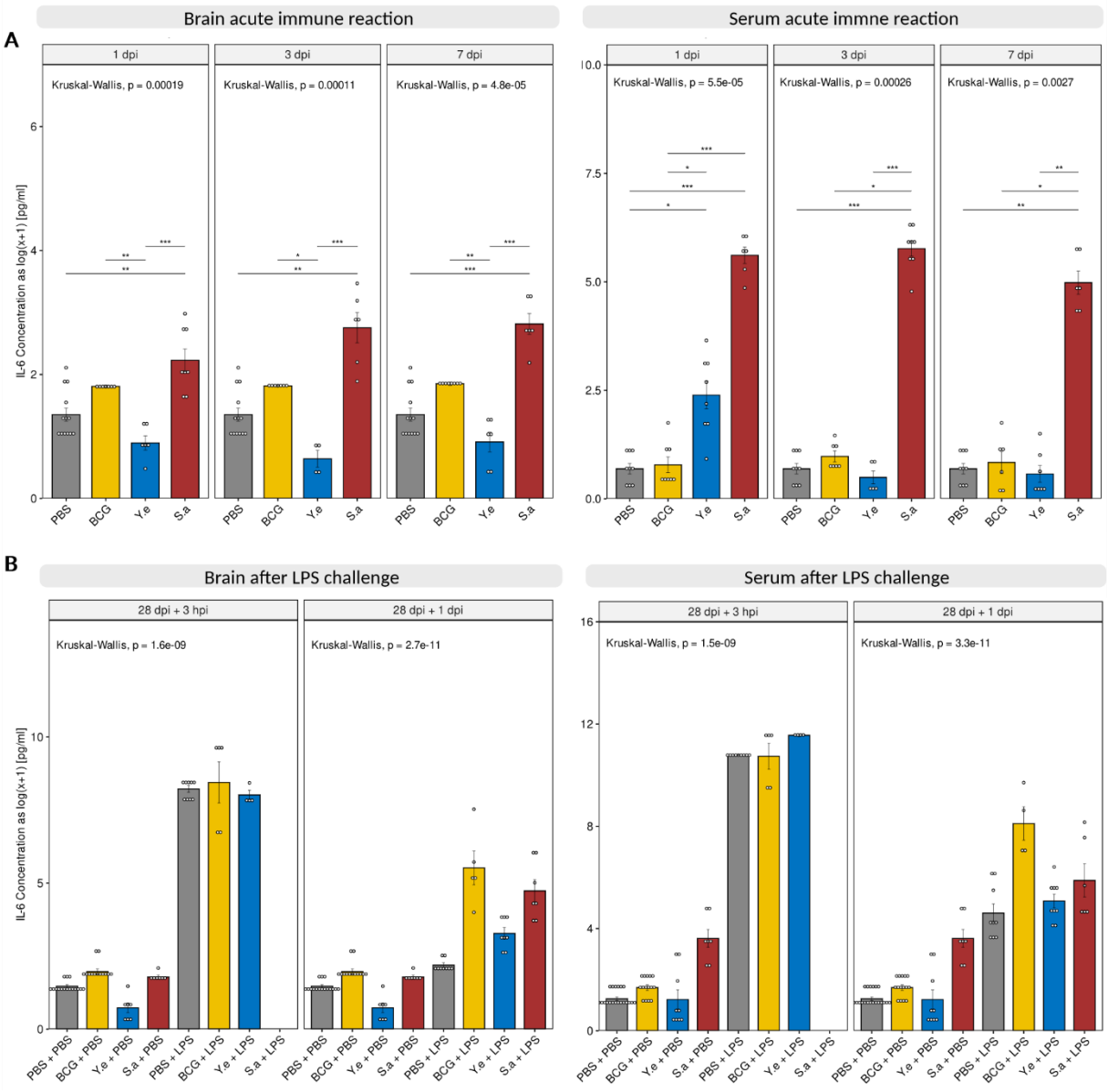

Fig. 21: Immune response after live infections. Barplots for IL-6 levels in serum (right panels) and brain homogenates (left panels) during acute immune response (A) and 3 hours and 24 hours after re-challenge with LPS 4 weeks later (B). Concentrations are shown as log(x+1). Single samples are shown as dots, error bars show standard error of the mean. Statistical comparison was performed using Kruskall-Wallis test with post-hoc Dunn's test and Benjamini Hochberg (BH) correction for significant main effects ($p < 0.05$). For reasons of clarity, only the global p-value is shown for challenge experiments.

5.2 Multi-omic characterization of cellular heterogeneity in AD

Any inflammatory event (e.g. bacterial infection or injury) results in the release of pro- and/or anti-inflammatory cytokines, allowing for immune memory formation in the periphery as well as in the brain. Whether such stimuli converge on similar signaling pathways is not yet clear and will be addressed in future work of this project, too. Therefore, different cortex samples of C57BL/6J mice that received the previously described peripheral inflammatory stimuli were chosen for transcriptomic and epigenetic analysis with SHARE-Seq. Unfortunately, at the time of submission, these experiments were not completed. Therefore, test data from method establishment is used here to provide proof-of-principle and show some types of analysis that will be done in the future.

5.2.1 Establishment of SHARE-Seq on PFA-fixed nuclei from frozen tissue

To generate joint profiles of gene expression and chromatin accessibility from frozen tissue (e.g. human post-mortem samples), a scalable and sensitive method is needed that can handle relatively small amounts of RNA, low input numbers and PFA-fixation. Therefore, we aimed to use a modified version of SHARE-Seq method (see 3.5.4). In the end, a fixation with 0.5 % FA for 5 min was chosen, which resulted in a good compromise between nuclei recovery and library/data quality. As the protocol is extremely long (3 whole days and additional 1-2 days of preparations), three different possible stopping-points were established that allow recovery periods for the experimenters while keeping duration of sample preparation as short as possible to minimize degradation and strand breaks due to FA-induced crosslinking:

1. After transposition of genomic DNA (at 4°C overnight, max. 10 hours)
2. After reverse crosslinking and first RT-PCR (before qPCR: 4°C overnight, after cleanup: -20°C for several days)
3. After library preparation (-20°C for several days)

In the end, the protocol was confirmed to be reproducible for 40-60.000 sorted nuclei in our hands, so that the qPCR step might be skipped in future experiments.

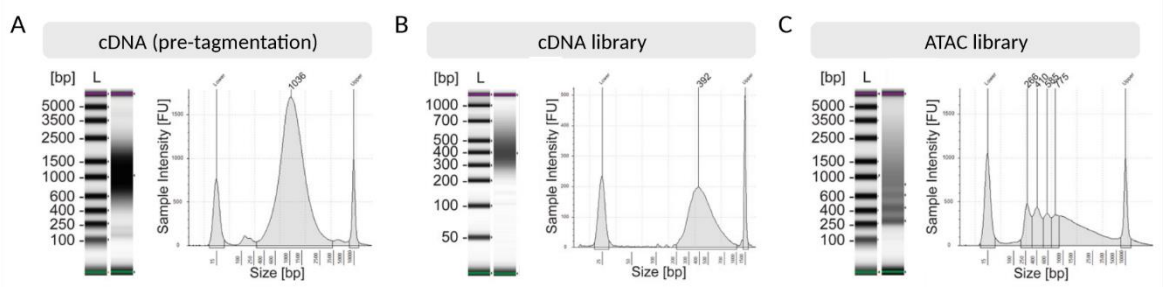

Fig. 22: Fragment size distribution of SHARE-seq libraries. Exemplary Agilent 4200 TapeStation profiles of **(A)** cDNA prior to tagmentation, **(B)** final snRNA-Seq library and **(C)** final snATAC-seq library. L = DNA ladder

5.2.2 Multi-omic analysis of AD-pathology

To validate data quality, we performed SHARE-Seq on a mixture of sorted PU.1-positive and NeuN-negative nuclei from mouse cortex from wildtype and APP transgenic animals. The different major cell types were well separated in both transcriptomic and chromatin profiles, resulting in 36,888 nuclei passing quality control. This represents about 15% recovery of the sorted nuclei populations, which is more than the authors of the original paper declared. With the sorting strategy chosen, all major cell types could be identified (Fig. 23A) with additional subpopulations in microglia (MG1-7), astrocytes (ASC_GFAP+, ASC_GFAP-) and border associated macrophages (BAM_Mrc1+, BAM_Cd11a+). Cell type identities of the co-embedded dataset were additionally confirmed by gene-activity and gene expression of some canonical marker genes (Fig. 23C,D). Interestingly, microglia subpopulations derived from nucleus sequencing cannot be identified by markers described in chapter 5, as the gene expression of nuclei differs from that of cells, which may be one of the reasons why it was not possible to fully integrate the datasets described previously.

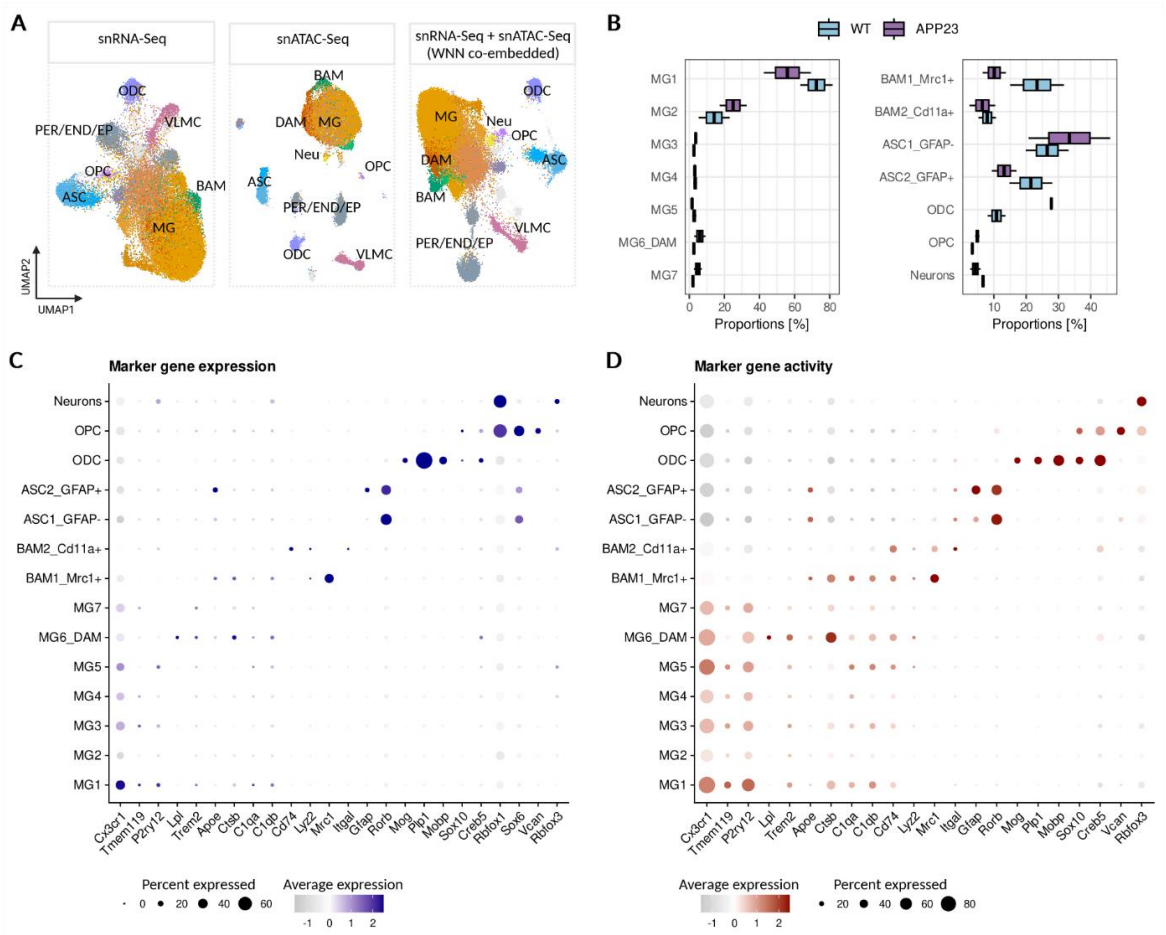

Fig. 23: Multi-omic characterization of cellular heterogeneity in AD. (A) UMAP plot of the 36,888 nuclei passing quality control (*n* = 4 cortices). Cells are colored according to clusters identified with Seurat's k-nearest neighbors (kNN) approach. MG = Microglia; ASC = Astrocytes; BAM = Border-associated macrophages; ODC = Oligodendrocytes; OPC = Oligodendrocyte Precursors; PER/END = Pericytes/endothelial; **(B)** Percentage of cells per cluster. Cells from WT animals are indicated in light blue, while cells from APP23+ mice are indicated in purple. **(C) + (D)** Dotplot of normalized expression **(C)** and gene activity **(D)** values of some cluster marker genes, according to snRNA-Seq. The size of the dot depicts the percentage of cells expressing this gene in this cluster. The color intensity corresponds to the normalized mean expression value of this gene over all cells within this cluster. Negative expression values (grey dots) correspond to expression values below the mean expression across the dataset.

To discover cell-type specific changes in Aβ-pathology, the composition of each cluster was examined by genotype. Several clusters showed significantly over- or underrepresentation (Fig. 23B) in APP23 vs WT animals. For example, MG1 significantly decreased with AD-pathology, while MG2 increased. Interestingly, the gene expression profile of MG2 did not overlap with the DAM signature in comparison to MG6. This could either be due to the fact that so far microglia populations were characterized by cellular transcriptomes or it could be a different disease-associated microglial phenotype. GFAP-expressing astrocytes (ASC2_GFAP+) decreased in proportion in APP23 positive microglia, while GFAP-negative astrocytes (ASC1_GFAP-) increased. However, consistent with a recent snRNA-seq study in 5x FAD-mice [220], GFAP-expression increased with Aβ-pathology.

Differentially accessible chromatin regions (DARs) and DEGs between APP23 and WT microglia and other brain immune cells resulted in cluster-specific GO-enrichment results (Fig. 24), corroborating our data in chapter 4 that Aβ-pathology leads to metabolic alterations and activation of the immune system. Interestingly, while DARs were selectively enriched in microglia from APP animals with Aβ-pathology, DEG analysis also showed downregulation of several genes, especially in the microglia population. Such a decrease in gene expression with simultaneous increase in chromatin accessibility may indicate repressive TF activity or other epigenetic alterations, e.g. histone modifications or DNA methylation that limit TF binding.

Therefore, to further examine the regulatory role of cell type-specific TFs in microglia exposed to Aβ-pathology, TF motif variability was calculated using `chromVAR` and the wilcoxauc function from presto, identifying several TFs enriched in microglia, astrocytes, oligodendrocytes and BAMs from APP transgenic animals. One of the top enriched TF in microglia was *Spi1* (also called *Pu.1*), the marker used for sorting microglia nuclei. Interestingly, while its motif was more highly represented in open chromatin regions of DAMs of APP23 mice, its gene expression was downregulated in APP23 mice. In addition, chromatin near the transcription start site of Spi1 also appeared to be more closed in APP23 compared to WT animals (Fig. 25B). Given its role in regulating neuroinflammatory responses, this provides insight into how SPI1 repression contributes to AD pathophysiology, in accordance with findings reported by Morabito *et al.* for human microglia nuclei [169].

Another TF that was highly enriched in APP23 mice was the astrocytic *Nrf1* (nuclear respiratory factor 1), which has previously been associated with mitochondrial function [221]. Here, data also suggests that it might work as a repressor in AD-pathology, as its motif variability was upregulated in astrocytes of APP23 animals, while its gene expression was downregulated (Fig. 25 D,F).

Taken together, the establishment of SHARE-Seq on frozen and FA-fixed nuclei was successful and can provide insight into how different cell populations and regulatory factors such as TFs contribute to immune response in AD-pathology or in future studies to innate immune responses in microglial cells.

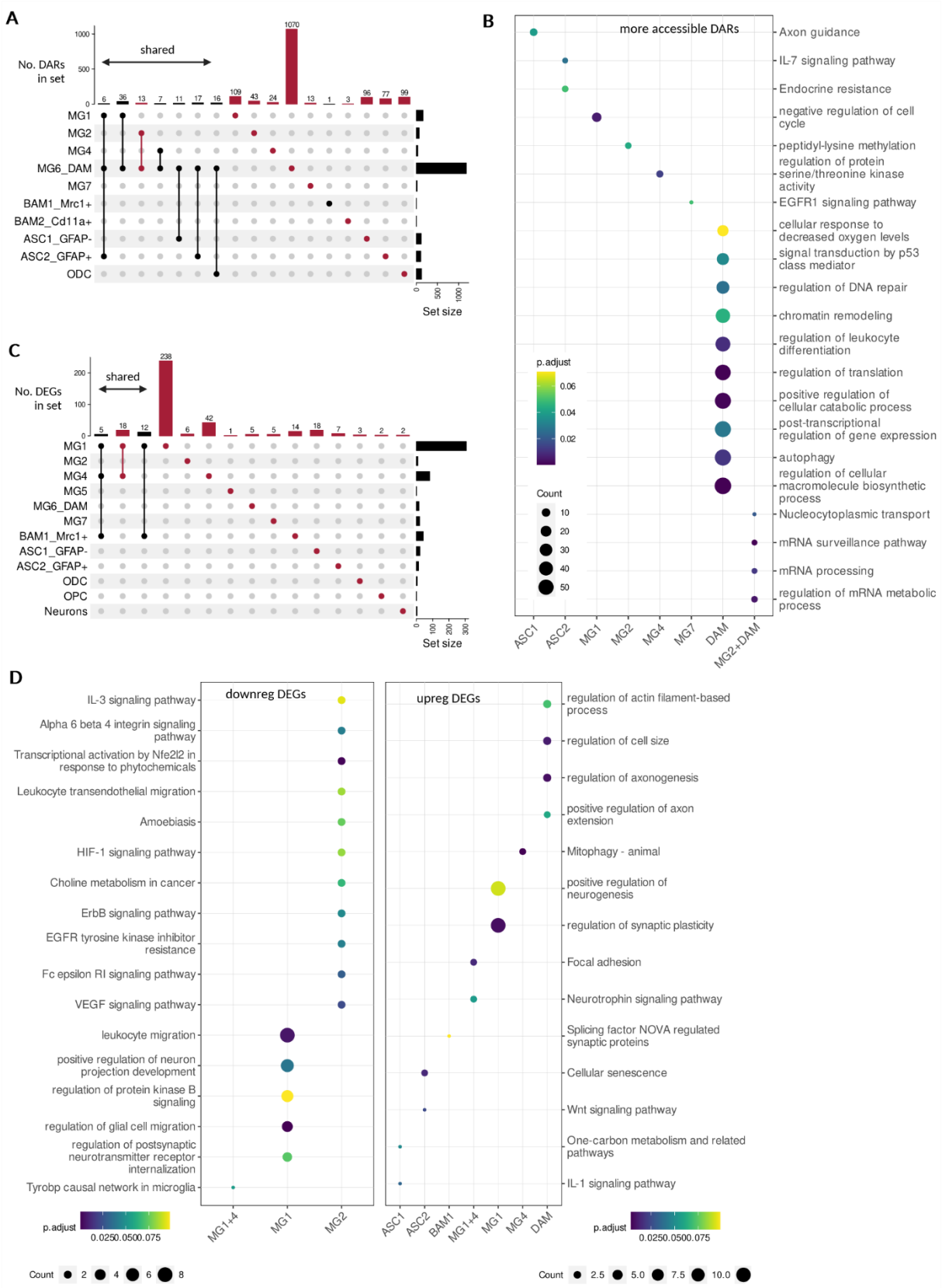

Fig. 24: Impact of Aβ-pathology on gene expression and chromatin accessibility. (A) UpSet plot showing closest genes to up-regulated DARs between APP23 and WT cells (FDR < 0.05, $|\log_2 FC| > 0.1$) unique for and shared between different cell populations. **(B)** Dotplot of GO and Pathway enrichment results for upregulated gene sets near DAR marked red in (A). The color indicates the significance value (Bonferroni adjusted p-value), the set size of dots refers to the gene counts. **(C)** UpSet plot of DEG sets (FDR < 0.05, $|\log_2 FC| > 0.1$) with associated GO and Pathway enrichment results **(D)** for up- and downregulated DEGs between APP23 and WT cells. The color indicates the significance value (Bonferroni adjusted p-value), the set size of dots refers to the gene counts.

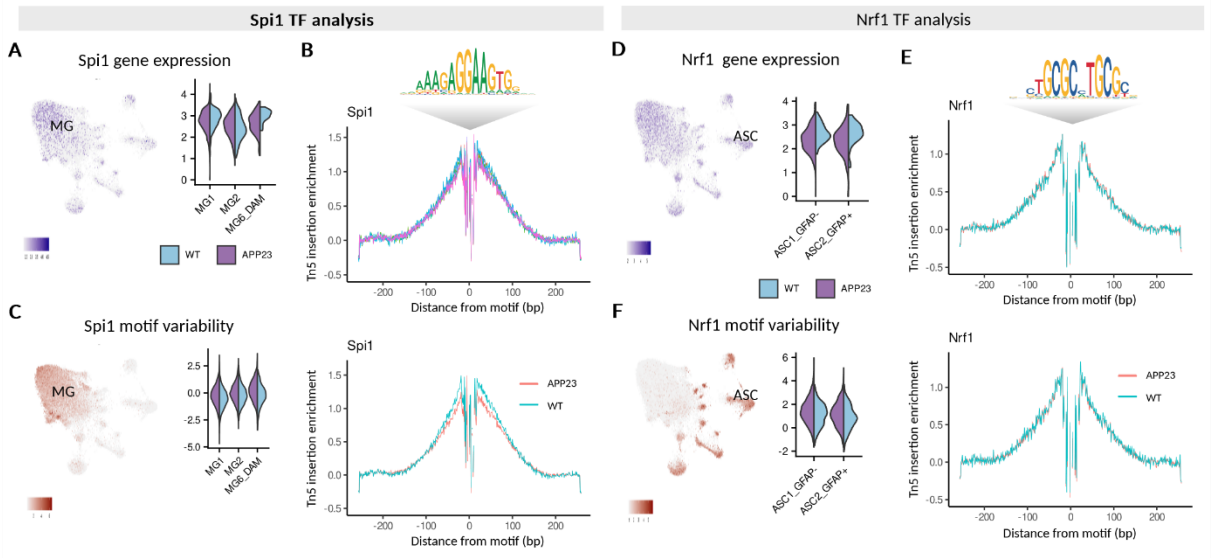

Fig. 25: Cell subpopulation-specific TF-analysis in AD-pathology. (A, D) Left: Coembedded UMAP plots colored by motif variability of *Spi1* and *Nrf1*. The cluster for which this TF was highly enriched is labeled. Right: Violin plots in snATAC-Seq for cell populations that showed a significant difference between APP23 and WT microglia, split by genotype. **(C, F)** Left: Coembedded UMAP plots colored by gene expression of *Spi1* and *Nrf1*. The cluster for which this TF was highly enriched is labeled. Right: Violin plots in snRNA-Seq for cell populations that showed a significant difference between APP23 and WT microglia, split by genotype. **(B, E)** Tn5-bias subtracted TF footprinting for cell subpopulation (top) and genotype (bottom). The according binding motifs are shown as motif logo above the footprints.

Discussion

Neurodegenerative diseases such as AD have been intensely studied on genetic level, demonstrating a significant contribution of non-neuronal cells and the innate immune system. However, it remains to be understood how environmental factors, such as peripheral inflammatory insults, influence the pathogenesis of neurodegenerative diseases (NDDs). Remarkably, even transient increases in inflammatory markers during midlife (e.g. due to infections or diseases) can increase the risk for developing NDDs, indicating that even short-term peripheral inflammation exerts negative long-term effects on the brain [222-225].

Using peripheral immune stimuli, including clinically-relevant insults such as live bacterial infections, and measuring a panel of cytokines in serum and brain, immune memory effects were identified. For example, BCG, a live attenuated vaccine against tuberculosis, was previously shown to induce immune training in peripheral macrophages [226] and also modulated cytokine levels in our experiment, indicating an immune memory effect in the brain. In addition, our data suggests that not only pro-inflammatory stimuli can induce immune memory effects, but also repeated applications of anti-inflammatory cytokines such as IL-10 or TGF-β. Effect sizes and, in some cases, large variances correspond to previous work [145] and with more sensitive methods such as cell-specific transcriptomics and epigenetics, more pronounced differences are to be expected. These experiments

will serve to examine if different immune stimuli induce immune training and tolerance through the same or through distinct pathways, broadening our current understanding of innate immune memory mechanisms. Moreover, in a separate part of this project, we aim to characterize the human brain's immune response to peripheral infections and validate the concept of innate immune memory in human brain cells; to this end, post-mortem human tissue will be used. For archived tissue analysis, a scalable and sensitive method is needed that can handle relatively little amounts of RNA, low input numbers and PFA-fixation. In addition, while single-cell chromatin accessibility profiling can provide insight into disease pathology, it is challenging to work with this data due to its inherent sparsity [169]. To circumvent this issue, transcriptomes and open-chromatin profiles of the same single-nucleus can be analyzed. Taking these considerations into account, SHARE-Seq was adapted to our needs [152, 153]. In a proof-of-principle experiment, a multi-omic analysis of major cell types in the mouse brain identified cell type-specific transcriptomic and epigenetic dysregulations in AD-pathology. For example, a dysregulation of *Nrf1* in astrocytes could contribute to disruption of mitochondrial function and myelination and hence neuronal dysfunction in AD [169, 221]. There are also indications that *Spi1* acts as a repressor in microglia in Aβ-pathology, providing insight into how different TFs contribute to AD-pathology.

Taken together, the data presented here shows a successful establishment of SHARE-Seq on FA-fixed nuclei, which will enable us to uncover transcriptomic and epigenetic changes in different cell populations on single-cell level. Using this technique will significantly improve our understanding of alterations in the human brain's immune response due to peripheral inflammatory insults and might be able to identify novel mechanisms that can be targeted to promote brain health.

6 CONCLUDING REMARKS AND FUTURE DIRECTIONS

In this thesis, an in-depth analysis of gene expression and chromatin accessibility in microglia subpopulations during aging and AD pathology was presented. Knowledge about microglia function in healthy aging is essential for the interpretation of their molecular responses in age-related NDDs. This work has enhanced our knowledge in this field by identifying shifts in microglia populations with age. While one subpopulation decreases with age, independent of pathology, another one increases in very old animals (Fig. 4D). This has not been described previously and could be highly relevant for brain aging and age-related NDDs. However, the role of these aging-associated microglia (AAM) in the brain is unclear, despite our findings that they can transition into disease-related phenotypes. Therefore, further studies, especially on functional characterization of this cell population, could be beneficial and highly informative for understanding the changes in microglia function in the aging and diseased brain.

Given the low turnover rate of microglia, age-related cellular senescence might contribute to the development of NDDs. Indeed, microglia from very old animals showed reduced expression of homeostatic marker genes and functions, similar to a previous report [38]. It is still not clear if and how transmission of epigenetic modifications in microglia take place and if the chronologically younger cells are also biologically younger. However, knowledge about rate and type of microglial proliferation (symmetric vs asymmetric) is crucial, as it can directly influence whether such changes are propagated throughout the lifespan. In addition, the proliferation mode may directly influence brain aging and disease. Therefore, understanding microglial turnover and mechanisms of self-renewal is essential to delineate the microglial aging process.

Streit *el al.* also identified a heterogenous microglial population in aged human brains, including senescent cells [36, 227]. Comparing our mouse with human data and to confirm these previously unrecognized microglia populations may provide insights into which microglia subtypes are relevant for human brain aging and disease. This would be especially important as the enhancer and transcriptional landscape of human and mouse microglia differ considerably, especially genes induced with aging [114, 116]. If a phenotype could be identified that is relevant to human pathology, this microglia population could directly be manipulated in transgenic mouse models to test their impact on brain aging and the development and progression of AD-pathology. This would help delineate the evolution of microglia subpopulations and their role in pathophysiology and may reveal novel molecular pathways as targets for therapeutic manipulation of the brain's immune system.

Considering the fact that sex is a risk factor for pathological aging as well as susceptibility and outcome of various NDDs, it should be considered in future studies. Indeed, numerous immune-related differences between men and women have been reported (reviewed in [228]). For example, women generally show a more active immune system, which could lead to alterations in the inflammatory

status of the brain. Furthermore, sex hormones have been shown to regulate cytokine production and microglial activation and are therefore important for neuronal protection (reviewed in [228]). Understanding the mechanisms behind sex differences and correlating them with pathological alterations in disease could lead to personalized medicine approaches with higher success rate in the treatment of various diseases.

Numerous studies have demonstrated a critical role for dysregulated metabolic functions in AD and in brain aging (reviewed in [229]), including alterations in glucose and cholesterol metabolism, oxidative phosphorylation and ATP biosynthesis. This work identified HIF-1 signaling and especially *Arnt* and *Hif1α*, the two subunits of the active TF, as key regulatory elements in AD pathology and related to these metabolic alterations. Transcriptomic analysis of a *Hif1α*-knockout model indicated shifts in microglia subpopulations to more homeostatic phenotypes and amelioration of these metabolic alterations. As metabolic dysregulation also affects cognitive performance, it would be interesting to see how *Hif1α*-ko animals perform in behavioral tasks (especially regarding learning and memory) compared to *Hif1α*-wt mice. This would provide further insight into whether *Hif1α* would be a good therapeutic target for the treatment of AD.

Various medical conditions that promote peripheral inflammation increase the risk of developing NDDs, with even a transient increase in inflammatory markers during midlife being sufficient for exerting negative long-term effects on the brain [222-225]. As we are exposed to infections or other inflammatory events (e.g. vaccinations) throughout life, it is crucial to understand how peripheral immune reactions affect the brain and if they can thereby modify our risk for developing neurological diseases. This could also highlight novel approaches to prevent age-related brain dysfunction. To develop any therapeutic intervention, a detailed understanding of the interplay of different cell types and the molecular targets driving detrimental cell states is important. Therefore, the second part of this thesis included the establishment of single-nucleus profiling of frozen post-mortem tissue to capture the transcriptomic and epigenetic heterogeneity of cellular responses in the brain. We aim to use this method to generate a molecular map of cellular responses to peripheral inflammation and to identify molecular fingerprints of previous pathogenic insults that led to immune memory effects in the brain's major cell populations. This will be of special interest in human post-mortem tissue, where transcriptomic analysis can only reveal the molecular phenotype at the time of death, whereas open chromatin profiling might yield information about the cells' past exposures to inflammatory signals.

Innate immune memory in the brain is a relatively new discovery [27, 145] and if we could confirm it by peripheral application of clinically relevant insults such as live bacterial infections or vaccines (here BCG), this could have significant implications for humans. It would mean that any infection, vaccination or other inflammatory event anywhere in the body could lead to long-term alterations in the brain's immune response and might influence onset and progression of neurological diseases.

LITERATURE

1. Río-Hortega, P., *El "Tercer elemento" de los centros nerviosos: poder fagocitario y movilidad de la microglia*. 1919.
2. Sierra, A., et al., *The "Big-Bang" for modern glial biology: Translation and comments on Pio del Rio-Hortega 1919 series of papers on microglia.* Glia, 2016. **64**(11): p. 1801-40.
3. Edler, M.K., I. Mhatre-Winters, and J.R. Richardson, *Microglia in Aging and Alzheimer's Disease: A Comparative Species Review.* Cells, 2021. **10**(5).
4. Uriarte Huarte, O., et al., *Microglia in Health and Disease: The Strength to Be Diverse and Reactive.* Front Cell Neurosci, 2021. **15**: p. 660523.
5. Lawson, L.J., et al., *Heterogeneity in the distribution and morphology of microglia in the normal adult mouse brain.* Neuroscience, 1990. **39**(1): p. 151-70.
6. Salter, M.W. and B. Stevens, *Microglia emerge as central players in brain disease.* Nat Med, 2017. **23**(9): p. 1018-1027.
7. Mittelbronn, M., et al., *Local distribution of microglia in the normal adult human central nervous system differs by up to one order of magnitude.* Acta Neuropathol, 2001. **101**(3): p. 249-55.
8. Ginhoux, F., et al., *Fate mapping analysis reveals that adult microglia derive from primitive macrophages.* Science, 2010. **330**(6005): p. 841-5.
9. Ginhoux, F. and M. Prinz, *Origin of microglia: current concepts and past controversies.* Cold Spring Harb Perspect Biol, 2015. **7**(8): p. a020537.
10. Zusso, M., et al., *Regulation of postnatal forebrain amoeboid microglial cell proliferation and development by the transcription factor Runx1.* J Neurosci, 2012. **32**(33): p. 11285-98.
11. Prinz, M. and A. Mildner, *Microglia in the CNS: immigrants from another world.* Glia, 2011. **59**(2): p. 177-187.
12. Schlegelmilch, T., K. Henke, and F. Peri, *Microglia in the developing brain: from immunity to behaviour.* Curr Opin Neurobiol, 2011. **21**(1): p. 5-10.
13. Ajami, B., et al., *Local self-renewal can sustain CNS microglia maintenance and function throughout adult life.* Nat Neurosci, 2007. **10**(12): p. 1538-43.
14. Hashimoto, D., et al., *Tissue-resident macrophages self-maintain locally throughout adult life with minimal contribution from circulating monocytes.* Immunity, 2013. **38**(4): p. 792-804.
15. Fuger, P., et al., *Microglia turnover with aging and in an Alzheimer's model via long-term in vivo single-cell imaging.* Nat Neurosci, 2017. **20**(10): p. 1371-1376.
16. Tay, T.L., et al., *A new fate mapping system reveals context-dependent random or clonal expansion of microglia.* Nat Neurosci, 2017. **20**(6): p. 793-803.

17. Grabert, K., et al., *Microglial brain region-dependent diversity and selective regional sensitivities to aging.* Nat Neurosci, 2016. **19**(3): p. 504-16.
18. Reu, P., et al., *The Lifespan and Turnover of Microglia in the Human Brain.* Cell Rep, 2017. **20**(4): p. 779-784.
19. Nimmerjahn, A., F. Kirchhoff, and F. Helmchen, *Resting microglial cells are highly dynamic surveillants of brain parenchyma in vivo.* Science, 2005. **308**(5726): p. 1314-8.
20. Hickman, S.E. and J. El Khoury, *Analysis of the Microglial Sensome.* Methods Mol Biol, 2019. **2034**: p. 305-323.
21. Azam, S., et al., *Microglial Turnover in Ageing-Related Neurodegeneration: Therapeutic Avenue to Intervene in Disease Progression.* Cells, 2021. **10**(1).
22. Kim, Y.S. and T.H. Joh, *Microglia, major player in the brain inflammation: their roles in the pathogenesis of Parkinson's disease.* Exp Mol Med, 2006. **38**(4): p. 333-47.
23. Ransohoff, R.M. and V.H. Perry, *Microglial physiology: unique stimuli, specialized responses.* Annu Rev Immunol, 2009. **27**: p. 119-45.
24. Tremblay, M.E., R.L. Lowery, and A.K. Majewska, *Microglial interactions with synapses are modulated by visual experience.* PLoS Biol, 2010. **8**(11): p. e1000527.
25. Schafer, D.P., et al., *Microglia sculpt postnatal neural circuits in an activity and complement-dependent manner.* Neuron, 2012. **74**(4): p. 691-705.
26. Parkhurst, C.N., et al., *Microglia promote learning-dependent synapse formation through brain-derived neurotrophic factor.* Cell, 2013. **155**(7): p. 1596-609.
27. Zhang, X., et al., *Epigenetic regulation of innate immune memory in microglia.* J Neuroinflammation, 2022. **19**(1): p. 111.
28. Hammond, T.R., et al., *Single-Cell RNA Sequencing of Microglia throughout the Mouse Lifespan and in the Injured Brain Reveals Complex Cell-State Changes.* Immunity, 2019. **50**(1): p. 253-271 e6.
29. Masuda, T., et al., *Spatial and temporal heterogeneity of mouse and human microglia at single-cell resolution.* Nature, 2019. **566**(7744): p. 388-392.
30. Yeh, H. and T. Ikezu, *Transcriptional and Epigenetic Regulation of Microglia in Health and Disease.* Trends Mol Med, 2019. **25**(2): p. 96-111.
31. Keren-Shaul, H., et al., *A Unique Microglia Type Associated with Restricting Development of Alzheimer's Disease.* Cell, 2017. **169**(7): p. 1276-1290 e17.
32. Yeh, F.L., D.V. Hansen, and M. Sheng, *TREM2, Microglia, and Neurodegenerative Diseases.* Trends Mol Med, 2017. **23**(6): p. 512-533.
33. Sibille, E., *Molecular aging of the brain, neuroplasticity, and vulnerability to depression and other brain-related disorders.* Dialogues Clin Neurosci, 2013. **15**(1): p. 53-65.

34. NIH. *Cognitive super agers defy typical age-related decline in brainpower*. July 31, 2020 [cited 2023 January 04]; Available from: https://www.nia.nih.gov/news/cognitive-super-agers-defy-typical-age-related-decline-brainpower#.
35. Angelova, D.M. and D.R. Brown, *Microglia and the aging brain: are senescent microglia the key to neurodegeneration?* J Neurochem, 2019. **151**(6): p. 676-688.
36. Streit, W.J., et al., *Dystrophic microglia in the aging human brain.* Glia, 2004. **45**(2): p. 208-12.
37. Damani, M.R., et al., *Age-related alterations in the dynamic behavior of microglia.* Aging Cell, 2011. **10**(2): p. 263-76.
38. Hefendehl, J.K., et al., *Homeostatic and injury-induced microglia behavior in the aging brain.* Aging Cell, 2014. **13**(1): p. 60-9.
39. Chan, T.E., et al., *Cell-Type Specific Changes in Glial Morphology and Glucocorticoid Expression During Stress and Aging in the Medial Prefrontal Cortex.* Front Aging Neurosci, 2018. **10**: p. 146.
40. Yegla, B., et al., *Partial microglial depletion is associated with impaired hippocampal synaptic and cognitive function in young and aged rats.* Glia, 2021. **69**(6): p. 1494-1514.
41. Mouton, P.R., et al., *Age and gender effects on microglia and astrocyte numbers in brains of mice.* Brain Res, 2002. **956**(1): p. 30-5.
42. Brawek, B., M. Skok, and O. Garaschuk, *Changing Functional Signatures of Microglia along the Axis of Brain Aging.* Int J Mol Sci, 2021. **22**(3).
43. Marschallinger, J., et al., *Lipid-droplet-accumulating microglia represent a dysfunctional and proinflammatory state in the aging brain.* Nat Neurosci, 2020. **23**(2): p. 194-208.
44. Krenning, L., et al., *Transient activation of p53 in G2 phase is sufficient to induce senescence.* Mol Cell, 2014. **55**(1): p. 59-72.
45. Chinta, S.J., et al., *Cellular senescence and the aging brain.* Exp Gerontol, 2015. **68**: p. 3-7.
46. Streit, W.J. and Q.S. Xue, *The Brain's Aging Immune System.* Aging Dis, 2010. **1**(3): p. 254-261.
47. Alzheimer Europe. *Prevalence of dementia in Europe*. 2021 [cited 2023 January 12]; Available from: https://www.alzheimer-europe.org/dementia/prevalence-dementia-europe.
48. World Health Organisation (WHO). *Dementia*. September 20, 2022 [cited 2023 January 12]; Available from: https://www.who.int/news-room/fact-sheets/detail/dementia.
49. McKhann, G.M., et al., *The diagnosis of dementia due to Alzheimer's disease: recommendations from the National Institute on Aging-Alzheimer's Association workgroups on diagnostic guidelines for Alzheimer's disease.* Alzheimers Dement, 2011. **7**(3): p. 263-9.
50. Alzheimer, A., *Über eine eigenartige Erkrankung der Hirnrinde.* Allgemeine Zeitschrift für Psychiatrie und Psychisch-gerichtliche Medizin, 1907. **64**: p. 146-148.
51. Heneka, M.T., et al., *Neuroinflammation in Alzheimer's disease.* Lancet Neurol, 2015. **14**(4): p. 388-405.

52. Jack, C.R., Jr., et al., *Hypothetical model of dynamic biomarkers of the Alzheimer's pathological cascade.* Lancet Neurol, 2010. **9**(1): p. 119-28.
53. Ma, C., F. Hong, and S. Yang, *Amyloidosis in Alzheimer's Disease: Pathogeny, Etiology, and Related Therapeutic Directions.* Molecules, 2022. **27**(4).
54. Reitz, C., C. Brayne, and R. Mayeux, *Epidemiology of Alzheimer disease.* Nat Rev Neurol, 2011. **7**(3): p. 137-52.
55. Sun, X., W.D. Chen, and Y.D. Wang, *beta-Amyloid: the key peptide in the pathogenesis of Alzheimer's disease.* Front Pharmacol, 2015. **6**: p. 221.
56. Hardy, J.A. and G.A. Higgins, *Alzheimer's disease: the amyloid cascade hypothesis.* Science, 1992. **256**(5054): p. 184-5.
57. Liu, C.C., et al., *Apolipoprotein E and Alzheimer disease: risk, mechanisms and therapy.* Nat Rev Neurol, 2013. **9**(2): p. 106-18.
58. Piaceri, I., B. Nacmias, and S. Sorbi, *Genetics of familial and sporadic Alzheimer's disease.* Front Biosci (Elite Ed), 2013. **5**(1): p. 167-77.
59. Aizenstein, H.J., et al., *Frequent amyloid deposition without significant cognitive impairment among the elderly.* Arch Neurol, 2008. **65**(11): p. 1509-17.
60. Edison, P., et al., *Microglia, amyloid, and cognition in Alzheimer's disease: An [11C](R)PK11195-PET and [11C]PIB-PET study.* Neurobiol Dis, 2008. **32**(3): p. 412-9.
61. Philippens, I.H., et al., *Acceleration of Amyloidosis by Inflammation in the Amyloid-Beta Marmoset Monkey Model of Alzheimer's Disease.* J Alzheimers Dis, 2017. **55**(1): p. 101-113.
62. Leng, F. and P. Edison, *Neuroinflammation and microglial activation in Alzheimer disease: where do we go from here?* Nat Rev Neurol, 2021. **17**(3): p. 157-172.
63. Zhang, F. and L. Jiang, *Neuroinflammation in Alzheimer's disease.* Neuropsychiatr Dis Treat, 2015. **11**: p. 243-56.
64. El Khoury, J.B., et al., *CD36 mediates the innate host response to beta-amyloid.* J Exp Med, 2003. **197**(12): p. 1657-66.
65. Stewart, C.R., et al., *CD36 ligands promote sterile inflammation through assembly of a Toll-like receptor 4 and 6 heterodimer.* Nat Immunol, 2010. **11**(2): p. 155-61.
66. Lee, C.Y. and G.E. Landreth, *The role of microglia in amyloid clearance from the AD brain.* J Neural Transm (Vienna), 2010. **117**(8): p. 949-60.
67. Baik, S.H., et al., *Microglia contributes to plaque growth by cell death due to uptake of amyloid beta in the brain of Alzheimer's disease mouse model.* Glia, 2016. **64**(12): p. 2274-2290.
68. Morimoto, K., et al., *Expression profiles of cytokines in the brains of Alzheimer's disease (AD) patients compared to the brains of non-demented patients with and without increasing AD pathology.* J Alzheimers Dis, 2011. **25**(1): p. 59-76.

69. Hong, S., et al., *Complement and microglia mediate early synapse loss in Alzheimer mouse models.* Science, 2016. **352**(6286): p. 712-716.
70. Petrisko, T.J., A. Gomez-Arboledas, and A.J. Tenner, *Complement as a powerful "influencer" in the brain during development, adulthood and neurological disorders.* Adv Immunol, 2021. **152**: p. 157-222.
71. Shi, Q., et al., *Complement C3 deficiency protects against neurodegeneration in aged plaque-rich APP/PS1 mice.* Sci Transl Med, 2017. **9**(392).
72. Fonseca, M.I., et al., *Absence of C1q leads to less neuropathology in transgenic mouse models of Alzheimer's disease.* J Neurosci, 2004. **24**(29): p. 6457-65.
73. Liddelow, S.A., et al., *Neurotoxic reactive astrocytes are induced by activated microglia.* Nature, 2017. **541**(7638): p. 481-487.
74. Walker, D.G., et al., *Decreased expression of CD200 and CD200 receptor in Alzheimer's disease: a potential mechanism leading to chronic inflammation.* Exp Neurol, 2009. **215**(1): p. 5-19.
75. Wu, Y., et al., *Mild traumatic brain injury induces microvascular injury and accelerates Alzheimer-like pathogenesis in mice.* Acta Neuropathol Commun, 2021. **9**(1): p. 74.
76. Cunningham, C., *Microglia and neurodegeneration: the role of systemic inflammation.* Glia, 2013. **61**(1): p. 71-90.
77. Drake, C., et al., *Brain inflammation is induced by co-morbidities and risk factors for stroke.* Brain Behav Immun, 2011. **25**(6): p. 1113-22.
78. Dunn, N., et al., *Association between dementia and infectious disease: evidence from a case-control study.* Alzheimer Dis Assoc Disord, 2005. **19**(2): p. 91-4.
79. Lotz, S.K., et al., *Microbial Infections Are a Risk Factor for Neurodegenerative Diseases.* Front Cell Neurosci, 2021. **15**: p. 691136.
80. Rogers, J., et al., *Clinical trial of indomethacin in Alzheimer's disease.* Neurology, 1993. **43**(8): p. 1609-11.
81. Weggen, S., et al., *A subset of NSAIDs lower amyloidogenic Abeta42 independently of cyclooxygenase activity.* Nature, 2001. **414**(6860): p. 212-6.
82. Aisen, P.S., et al., *Effects of rofecoxib or naproxen vs placebo on Alzheimer disease progression: a randomized controlled trial.* JAMA, 2003. **289**(21): p. 2819-26.
83. Meyer, P.F., et al., *INTREPAD: A randomized trial of naproxen to slow progress of presymptomatic Alzheimer disease.* Neurology, 2019. **92**(18): p. e2070-e2080.
84. Guerreiro, R., et al., *TREM2 variants in Alzheimer's disease.* N Engl J Med, 2013. **368**(2): p. 117-27.
85. Bradshaw, E.M., et al., *CD33 Alzheimer's disease locus: altered monocyte function and amyloid biology.* Nat Neurosci, 2013. **16**(7): p. 848-50.

86. Griciuc, A. and R.E. Tanzi, *The role of innate immune genes in Alzheimer's disease.* Curr Opin Neurol, 2021. **34**(2): p. 228-236.

87. McQuade, A. and M. Blurton-Jones, *Microglia in Alzheimer's Disease: Exploring How Genetics and Phenotype Influence Risk.* J Mol Biol, 2019. **431**(9): p. 1805-1817.

88. Liu, X., B. Jiao, and L. Shen, *The Epigenetics of Alzheimer's Disease: Factors and Therapeutic Implications.* Front Genet, 2018. **9**: p. 579.

89. Marciani, D.J., *Promising Results from Alzheimer's Disease Passive Immunotherapy Support the Development of a Preventive Vaccine.* Research (Wash D C), 2019. **2019**: p. 5341375.

90. Song, C., et al., *Immunotherapy for Alzheimer's disease: targeting beta-amyloid and beyond.* Transl Neurodegener, 2022. **11**(1): p. 18.

91. Sanchez-Varo, R., et al., *Transgenic Mouse Models of Alzheimer's Disease: An Integrative Analysis.* Int J Mol Sci, 2022. **23**(10).

92. Alzforum. *Alzheimer's Disease Research Models*. [cited 2023 February 11]; Available from: https://www.alzforum.org/research-models/alzheimers-disease.

93. Dawson, T.M., T.E. Golde, and C. Lagier-Tourenne, *Animal models of neurodegenerative diseases.* Nat Neurosci, 2018. **21**(10): p. 1370-1379.

94. Jankowsky, J.L. and H. Zheng, *Practical considerations for choosing a mouse model of Alzheimer's disease.* Mol Neurodegener, 2017. **12**(1): p. 89.

95. Trujillo-Estrada, L., et al., *Animal and Cellular Models of Alzheimer's Disease: Progress, Promise, and Future Approaches.* Neuroscientist, 2022. **28**(6): p. 572-593.

96. Radde, R., et al., *Abeta42-driven cerebral amyloidosis in transgenic mice reveals early and robust pathology.* EMBO Rep, 2006. **7**(9): p. 940-6.

97. Oakley, H., et al., *Intraneuronal beta-amyloid aggregates, neurodegeneration, and neuron loss in transgenic mice with five familial Alzheimer's disease mutations: potential factors in amyloid plaque formation.* J Neurosci, 2006. **26**(40): p. 10129-40.

98. Johnson, K.A., et al., *Tau positron emission tomographic imaging in aging and early Alzheimer disease.* Ann Neurol, 2016. **79**(1): p. 110-9.

99. Andorfer, C., et al., *Hyperphosphorylation and aggregation of tau in mice expressing normal human tau isoforms.* J Neurochem, 2003. **86**(3): p. 582-90.

100. Oddo, S., et al., *Triple-transgenic model of Alzheimer's disease with plaques and tangles: intracellular Abeta and synaptic dysfunction.* Neuron, 2003. **39**(3): p. 409-21.

101. Sturchler-Pierrat, C., et al., *Two amyloid precursor protein transgenic mouse models with Alzheimer disease-like pathology.* Proc Natl Acad Sci U S A, 1997. **94**(24): p. 13287-92.

102. Alzforum. *APP23*. Nov 25, 2013 [cited 2023 February 12]; Available from: https://www.alzforum.org/research-models/app23.

103. Kelly, P.H., et al., *Progressive age-related impairment of cognitive behavior in APP23 transgenic mice.* Neurobiol Aging, 2003. **24**(2): p. 365-78.
104. Hickman, S., et al., *Microglia in neurodegeneration.* Nat Neurosci, 2018. **21**(10): p. 1359-1369.
105. Lucin, K.M. and T. Wyss-Coray, *Immune activation in brain aging and neurodegeneration: too much or too little?* Neuron, 2009. **64**(1): p. 110-22.
106. Gao, C., et al., *Pathogenesis, therapeutic strategies and biomarker development based on "omics" analysis related to microglia in Alzheimer's disease.* J Neuroinflammation, 2022. **19**(1): p. 215.
107. Lowe, R., et al., *Transcriptomics technologies.* PLoS Comput Biol, 2017. **13**(5): p. e1005457.
108. Velculescu, V.E., et al., *Serial analysis of gene expression.* Science, 1995. **270**(5235): p. 484-7.
109. Schena, M., et al., *Quantitative monitoring of gene expression patterns with a complementary DNA microarray.* Science, 1995. **270**(5235): p. 467-70.
110. Gautier, E.L., et al., *Gene-expression profiles and transcriptional regulatory pathways that underlie the identity and diversity of mouse tissue macrophages.* Nat Immunol, 2012. **13**(11): p. 1118-28.
111. Wang, Z., M. Gerstein, and M. Snyder, *RNA-Seq: a revolutionary tool for transcriptomics.* Nat Rev Genet, 2009. **10**(1): p. 57-63.
112. Hickman, S.E., et al., *The microglial sensome revealed by direct RNA sequencing.* Nat Neurosci, 2013. **16**(12): p. 1896-905.
113. Gerrits, E., et al., *Transcriptional profiling of microglia; current state of the art and future perspectives.* Glia, 2020. **68**(4): p. 740-755.
114. Galatro, T.F., et al., *Transcriptomic analysis of purified human cortical microglia reveals age-associated changes.* Nat Neurosci, 2017. **20**(8): p. 1162-1171.
115. Guneykaya, D., et al., *Transcriptional and Translational Differences of Microglia from Male and Female Brains.* Cell Rep, 2018. **24**(10): p. 2773-2783 e6.
116. Gosselin, D., et al., *An environment-dependent transcriptional network specifies human microglia identity.* Science, 2017. **356**(6344).
117. Kolodziejczyk, A.A., et al., *The technology and biology of single-cell RNA sequencing.* Mol Cell, 2015. **58**(4): p. 610-20.
118. Tang, F., et al., *mRNA-Seq whole-transcriptome analysis of a single cell.* Nat Methods, 2009. **6**(5): p. 377-82.
119. Haque, A., et al., *A practical guide to single-cell RNA-sequencing for biomedical research and clinical applications.* Genome Med, 2017. **9**(1): p. 75.
120. Sala Frigerio, C., et al., *The Major Risk Factors for Alzheimer's Disease: Age, Sex, and Genes Modulate the Microglia Response to Abeta Plaques.* Cell Rep, 2019. **27**(4): p. 1293-1306 e6.

121. Mathys, H., et al., *Single-cell transcriptomic analysis of Alzheimer's disease.* Nature, 2019. **570**(7761): p. 332-337.

122. Olah, M., et al., *Single cell RNA sequencing of human microglia uncovers a subset associated with Alzheimer's disease.* Nat Commun, 2020. **11**(1): p. 6129.

123. Del-Aguila, J.L., et al., *A single-nuclei RNA sequencing study of Mendelian and sporadic AD in the human brain.* Alzheimers Res Ther, 2019. **11**(1): p. 71.

124. Habib, N., et al., *Massively parallel single-nucleus RNA-seq with DroNc-seq.* Nat Methods, 2017. **14**(10): p. 955-958.

125. NHGRI. *Epigenomics Fact Sheet*. August 16, 2020 [cited 2023 March 10]; Available from: https://www.genome.gov/about-genomics/fact-sheets/Epigenomics-Fact-Sheet.

126. Cantone, I. and A.G. Fisher, *Epigenetic programming and reprogramming during development.* Nat Struct Mol Biol, 2013. **20**(3): p. 282-9.

127. Rodriguez-Rodero, S., et al., *Epigenetic regulation of aging.* Discov Med, 2010. **10**(52): p. 225-33.

128. Creighton, S.D., et al., *Epigenetic Mechanisms of Learning and Memory: Implications for Aging.* Int J Mol Sci, 2020. **21**(18).

129. Petralla, S., et al., *Epigenetics and Communication Mechanisms in Microglia Activation with a View on Technological Approaches.* Biomolecules, 2021. **11**(2).

130. Rodriguez-Gomez, J.A., et al., *Microglia: Agents of the CNS Pro-Inflammatory Response.* Cells, 2020. **9**(7).

131. Cho, S.H., et al., *SIRT1 deficiency in microglia contributes to cognitive decline in aging and neurodegeneration via epigenetic regulation of IL-1beta.* J Neurosci, 2015. **35**(2): p. 807-18.

132. Matt, S.M., M.A. Lawson, and R.W. Johnson, *Aging and peripheral lipopolysaccharide can modulate epigenetic regulators and decrease IL-1beta promoter DNA methylation in microglia.* Neurobiol Aging, 2016. **47**: p. 1-9.

133. Kannan, V., et al., *Histone deacetylase inhibitors suppress immune activation in primary mouse microglia.* J Neurosci Res, 2013. **91**(9): p. 1133-42.

134. Suh, H.S., et al., *Histone deacetylase inhibitors suppress the expression of inflammatory and innate immune response genes in human microglia and astrocytes.* J Neuroimmune Pharmacol, 2010. **5**(4): p. 521-32.

135. Datta, M., et al., *Histone Deacetylases 1 and 2 Regulate Microglia Function during Development, Homeostasis, and Neurodegeneration in a Context-Dependent Manner.* Immunity, 2018. **48**(3): p. 514-529 e6.

136. Guedes, J.R., et al., *Early miR-155 upregulation contributes to neuroinflammation in Alzheimer's disease triple transgenic mouse model.* Hum Mol Genet, 2014. **23**(23): p. 6286-301.

137. Lopez-Ramirez, M.A., et al., *MicroRNA-155 negatively affects blood-brain barrier function during neuroinflammation.* FASEB J, 2014. **28**(6): p. 2551-65.

138. Ponomarev, E.D., et al., *MicroRNA-124 promotes microglia quiescence and suppresses EAE by deactivating macrophages via the C/EBP-alpha-PU.1 pathway.* Nat Med, 2011. **17**(1): p. 64-70.

139. Yang, Z., et al., *miR-203 protects microglia mediated brain injury by regulating inflammatory responses via feedback to MyD88 in ischemia.* Mol Immunol, 2015. **65**(2): p. 293-301.

140. Zhou, T., et al., *alpha-synuclein accumulation in SH-SY5Y cell impairs autophagy in microglia by exosomes overloading miR-19a-3p.* Epigenomics, 2019. **11**(15): p. 1661-1677.

141. Zhou, Y., et al., *MicroRNA-7 targets Nod-like receptor protein 3 inflammasome to modulate neuroinflammation in the pathogenesis of Parkinson's disease.* Mol Neurodegener, 2016. **11**: p. 28.

142. Sharma, S., et al., *Presymptomatic change in microRNAs modulates Tau pathology.* Sci Rep, 2018. **8**(1): p. 9251.

143. Liu, H.C., et al., *N9 microglial cells polarized by LPS and IL4 show differential responses to secondary environmental stimuli.* Cell Immunol, 2012. **278**(1-2): p. 84-90.

144. Schwarz, J.M., M.R. Hutchinson, and S.D. Bilbo, *Early-life experience decreases drug-induced reinstatement of morphine CPP in adulthood via microglial-specific epigenetic programming of anti-inflammatory IL-10 expression.* J Neurosci, 2011. **31**(49): p. 17835-47.

145. Wendeln, A.C., et al., *Innate immune memory in the brain shapes neurological disease hallmarks.* Nature, 2018. **556**(7701): p. 332-338.

146. Heneka, M.T., et al., *NLRP3 is activated in Alzheimer's disease and contributes to pathology in APP/PS1 mice.* Nature, 2013. **493**(7434): p. 674-8.

147. Gerlach, J.P., et al., *Combined quantification of intracellular (phospho-)proteins and transcriptomics from fixed single cells.* Sci Rep, 2019. **9**(1): p. 1469.

148. Gierahn, T.M., et al., *Seq-Well: portable, low-cost RNA sequencing of single cells at high throughput.* Nat Methods, 2017. **14**(4): p. 395-398.

149. Picelli, S., et al., *Smart-seq2 for sensitive full-length transcriptome profiling in single cells.* Nat Methods, 2013. **10**(11): p. 1096-8.

150. Genomics, X., *Nuclei Isolation for Single Cell ATAC Sequencing.* 2021. **Rev E**.

151. Genomics, X., *Chromium Next GEM Single Cell ATAC Reagent Kits v1.1.* 2021. **Rev D**.

152. Ma, S., et al., *Chromatin Potential Identified by Shared Single-Cell Profiling of RNA and Chromatin.* Cell, 2020. **183**(4): p. 1103-1116 e20.

153. Scholz, R., et al., *Combined Analysis of mRNA Expression and Open Chromatin in Microglia.* Methods Mol Biol, 2024. **2713**: p. 543-571.

154. Bray, N.L., et al., *Near-optimal probabilistic RNA-seq quantification.* Nat Biotechnol, 2016. **34**(5): p. 525-7.

155. Stuart, T., et al., *Comprehensive Integration of Single-Cell Data.* Cell, 2019. **177**(7): p. 1888-1902 e21.

156. Hafemeister, C. and R. Satija, *Normalization and variance stabilization of single-cell RNA-seq data using regularized negative binomial regression.* Genome Biol, 2019. **20**(1): p. 296.

157. Aran, D., et al., *Reference-based analysis of lung single-cell sequencing reveals a transitional profibrotic macrophage.* Nat Immunol, 2019. **20**(2): p. 163-172.

158. Yu, G., et al., *clusterProfiler: an R package for comparing biological themes among gene clusters.* OMICS, 2012. **16**(5): p. 284-7.

159. Morabito, S., et al., *High dimensional co-expression networks enable discovery of transcriptomic drivers in complex biological systems.* bioRxiv, 2022: p. 2022.09.22.509094.

160. Kuleshov, M.V., et al., *Enrichr: a comprehensive gene set enrichment analysis web server 2016 update.* Nucleic Acids Res, 2016. **44**(W1): p. W90-7.

161. Trapnell, C., et al., *The dynamics and regulators of cell fate decisions are revealed by pseudotemporal ordering of single cells.* Nat Biotechnol, 2014. **32**(4): p. 381-386.

162. Stuart, T., et al., *Single-cell chromatin state analysis with Signac.* Nat Methods, 2021. **18**(11): p. 1333-1341.

163. Consortium, F., et al., *A promoter-level mammalian expression atlas.* Nature, 2014. **507**(7493): p. 462-70.

164. Tan, G. and B. Lenhard, *TFBSTools: an R/bioconductor package for transcription factor binding site analysis.* Bioinformatics, 2016. **32**(10): p. 1555-6.

165. Schep, A.N., et al., *chromVAR: inferring transcription-factor-associated accessibility from single-cell epigenomic data.* Nat Methods, 2017. **14**(10): p. 975-978.

166. Castro-Mondragon, J.A., et al., *JASPAR 2022: the 9th release of the open-access database of transcription factor binding profiles.* Nucleic Acids Res, 2022. **50**(D1): p. D165-D173.

167. Cusanovich, D.A., et al., *A Single-Cell Atlas of In Vivo Mammalian Chromatin Accessibility.* Cell, 2018. **174**(5): p. 1309-1324 e18.

168. Pliner, H.A., et al., *Cicero Predicts cis-Regulatory DNA Interactions from Single-Cell Chromatin Accessibility Data.* Mol Cell, 2018. **71**(5): p. 858-871 e8.

169. Morabito, S., et al., *Single-nucleus chromatin accessibility and transcriptomic characterization of Alzheimer's disease.* Nat Genet, 2021. **53**(8): p. 1143-1155.

170. Allen Mouse Brain Atlas. *Allen Mouse Brain Atlas*. 2023 [cited 2023 Oct.]; Available from: http://mouse.brain-map.org/.

171. Lehmann, J.S., et al., *LEGENDplex: Bead-assisted multiplex cytokine profiling by flow cytometry.* Methods Enzymol, 2019. **629**: p. 151-176.

172. Butovsky, O., et al., *Identification of a unique TGF-beta-dependent molecular and functional signature in microglia.* Nat Neurosci, 2014. **17**(1): p. 131-43.

173. Corder, E.H., et al., *Gene dose of apolipoprotein E type 4 allele and the risk of Alzheimer's disease in late onset families.* Science, 1993. **261**(5123): p. 921-3.

174. Paz, Y.M.C.A., et al., *Positive Association of the Cathepsin D Ala224Val Gene Polymorphism With the Risk of Alzheimer's Disease.* Am J Med Sci, 2015. **350**(4): p. 296-301.

175. Scacchi, R., et al., *The H+ allele of the lipoprotein lipase (LPL) HindIII intronic polymorphism and the risk for sporadic late-onset Alzheimer's disease.* Neurosci Lett, 2004. **367**(2): p. 177-80.

176. Pottier, C., et al., *TYROBP genetic variants in early-onset Alzheimer's disease.* Neurobiol Aging, 2016. **48**: p. 222 e9-222 e15.

177. Klunk, W.E., et al., *Imaging Abeta plaques in living transgenic mice with multiphoton microscopy and methoxy-X04, a systemically administered Congo red derivative.* J Neuropathol Exp Neurol, 2002. **61**(9): p. 797-805.

178. Ayata, P., et al., *Epigenetic regulation of brain region-specific microglia clearance activity.* Nat Neurosci, 2018. **21**(8): p. 1049-1060.

179. Ulrich, J.D., et al., *ApoE facilitates the microglial response to amyloid plaque pathology.* J Exp Med, 2018. **215**(4): p. 1047-1058.

180. Smith, L.K., et al., *beta2-microglobulin is a systemic pro-aging factor that impairs cognitive function and neurogenesis.* Nat Med, 2015. **21**(8): p. 932-7.

181. Zhao, Y., et al., *beta(2)-Microglobulin coaggregates with Abeta and contributes to amyloid pathology and cognitive deficits in Alzheimer's disease model mice.* Nat Neurosci, 2023. **26**(7): p. 1170-1184.

182. Li, Q., et al., *Developmental Heterogeneity of Microglia and Brain Myeloid Cells Revealed by Deep Single-Cell RNA Sequencing.* Neuron, 2019. **101**(2): p. 207-223 e10.

183. Sankowski, R., et al., *Mapping microglia states in the human brain through the integration of high-dimensional techniques.* Nat Neurosci, 2019. **22**(12): p. 2098-2110.

184. Kluever, V., et al., *Protein lifetimes in aged brains reveal a proteostatic adaptation linking physiological aging to neurodegeneration.* Sci Adv, 2022. **8**(20): p. eabn4437.

185. Skariah, G. and P.K. Todd, *Translational control in aging and neurodegeneration.* Wiley Interdiscip Rev RNA, 2021. **12**(4): p. e1628.

186. Van Muiswinkel, F.L., R. Veerhuis, and P. Eikelenboom, *Amyloid beta protein primes cultured rat microglial cells for an enhanced phorbol 12-myristate 13-acetate-induced respiratory burst activity.* J Neurochem, 1996. **66**(6): p. 2468-76.

187. Wilkinson, B., et al., *Fibrillar beta-amyloid-stimulated intracellular signaling cascades require Vav for induction of respiratory burst and phagocytosis in monocytes and microglia.* J Biol Chem, 2006. **281**(30): p. 20842-20850.

188. Wilkinson, B.L. and G.E. Landreth, *The microglial NADPH oxidase complex as a source of oxidative stress in Alzheimer's disease.* J Neuroinflammation, 2006. **3**: p. 30.

189. Gedam, M., et al., *Complement C3aR depletion reverses HIF-1alpha-induced metabolic impairment and enhances microglial response to Abeta pathology.* J Clin Invest, 2023. **133**(12).

190. Grubman, A., et al., *Transcriptional signature in microglia associated with Abeta plaque phagocytosis.* Nat Commun, 2021. **12**(1): p. 3015.

191. Johnson, E.C.B., et al., *Large-scale proteomic analysis of Alzheimer's disease brain and cerebrospinal fluid reveals early changes in energy metabolism associated with microglia and astrocyte activation.* Nat Med, 2020. **26**(5): p. 769-780.

192. Mosconi, L., *Glucose metabolism in normal aging and Alzheimer's disease: Methodological and physiological considerations for PET studies.* Clin Transl Imaging, 2013. **1**(4).

193. Zhang, H., et al., *Rho Signaling in Synaptic Plasticity, Memory, and Brain Disorders.* Front Cell Dev Biol, 2021. **9**: p. 729076.

194. Candeias, E., et al., *The impairment of insulin signaling in Alzheimer's disease.* IUBMB Life, 2012. **64**(12): p. 951-7.

195. Holscher, C., *Insulin Signaling Impairment in the Brain as a Risk Factor in Alzheimer's Disease.* Front Aging Neurosci, 2019. **11**: p. 88.

196. Kumar, V., S.H. Kim, and K. Bishayee, *Dysfunctional Glucose Metabolism in Alzheimer's Disease Onset and Potential Pharmacological Interventions.* Int J Mol Sci, 2022. **23**(17).

197. Kyrtata, N., et al., *A Systematic Review of Glucose Transport Alterations in Alzheimer's Disease.* Front Neurosci, 2021. **15**: p. 626636.

198. Kheiri, G., et al., *Role of p38/MAPKs in Alzheimer's disease: implications for amyloid beta toxicity targeted therapy.* Rev Neurosci, 2018. **30**(1): p. 9-30.

199. Nagamoto-Combs, K. and C.K. Combs, *Microglial phenotype is regulated by activity of the transcription factor, NFAT (nuclear factor of activated T cells).* J Neurosci, 2010. **30**(28): p. 9641-6.

200. Manocha, G.D., et al., *NFATc2 Modulates Microglial Activation in the AbetaPP/PS1 Mouse Model of Alzheimer's Disease.* J Alzheimers Dis, 2017. **58**(3): p. 775-787.

201. Castro-Sanchez, S., et al., *CX3CR1-deficient microglia shows impaired signalling of the transcription factor NRF2: Implications in tauopathies.* Redox Biol, 2019. **22**: p. 101118.

202. Lastres-Becker, I., et al., *Fractalkine activates NRF2/NFE2L2 and heme oxygenase 1 to restrain tauopathy-induced microgliosis.* Brain, 2014. **137**(Pt 1): p. 78-91.

203. Jain, M., et al., *Role of JAK/STAT in the Neuroinflammation and its Association with Neurological Disorders.* Ann Neurosci, 2021. **28**(3-4): p. 191-200.

204. Lee, S., et al., *APOE modulates microglial immunometabolism in response to age, amyloid pathology, and inflammatory challenge.* Cell Rep, 2023. **42**(3): p. 112196.

205. Liu, H., et al., *Distinct conformers of amyloid beta accumulate in the neocortex of patients with rapidly progressive Alzheimer's disease.* J Biol Chem, 2021. **297**(5): p. 101267.

206. Luo, Z., et al., *Hypoxia signaling in human health and diseases: implications and prospects for therapeutics.* Signal Transduct Target Ther, 2022. **7**(1): p. 218.

207. Audrain, M., et al., *Reactive or transgenic increase in microglial TYROBP reveals a TREM2-independent TYROBP-APOE link in wild-type and Alzheimer's-related mice.* Alzheimers Dement, 2021. **17**(2): p. 149-163.

208. Masuda, T., et al., *Microglia Heterogeneity in the Single-Cell Era.* Cell Rep, 2020. **30**(5): p. 1271-1281.

209. Hu, Y., et al., *Replicative senescence dictates the emergence of disease-associated microglia and contributes to Abeta pathology.* Cell Rep, 2021. **35**(10): p. 109228.

210. Miklossy, G., T.S. Hilliard, and J. Turkson, *Therapeutic modulators of STAT signalling for human diseases.* Nat Rev Drug Discov, 2013. **12**(8): p. 611-29.

211. Natarajan, C., et al., *Signaling through JAK2-STAT5 pathway is essential for IL-3-induced activation of microglia.* Glia, 2004. **45**(2): p. 188-96.

212. Sayed, F.A., et al., *AD-linked R47H-TREM2 mutation induces disease-enhancing microglial states via AKT hyperactivation.* Sci Transl Med, 2021. **13**(622): p. eabe3947.

213. Ehehalt, R., et al., *Amyloidogenic processing of the Alzheimer beta-amyloid precursor protein depends on lipid rafts.* J Cell Biol, 2003. **160**(1): p. 113-23.

214. Ghribi, O., et al., *High cholesterol content in neurons increases BACE, beta-amyloid, and phosphorylated tau levels in rabbit hippocampus.* Exp Neurol, 2006. **200**(2): p. 460-7.

215. Mori, T., et al., *Cholesterol accumulates in senile plaques of Alzheimer disease patients and in transgenic APP(SW) mice.* J Neuropathol Exp Neurol, 2001. **60**(8): p. 778-85.

216. Zhang, X., N. Alshakhshir, and L. Zhao, *Glycolytic Metabolism, Brain Resilience, and Alzheimer's Disease.* Front Neurosci, 2021. **15**: p. 662242.

217. Ma, J., et al., *TYROBP in Alzheimer's disease.* Mol Neurobiol, 2015. **51**(2): p. 820-6.

218. Deng, H., et al., *Molecular mechanism responsible for the priming of macrophage activation.* J Biol Chem, 2013. **288**(6): p. 3897-906.

219. Zhang, X. and D.C. Morrison, *Lipopolysaccharide-induced selective priming effects on tumor necrosis factor alpha and nitric oxide production in mouse peritoneal macrophages.* J Exp Med, 1993. **177**(2): p. 511-6.

220. Habib, N., et al., *Disease-associated astrocytes in Alzheimer's disease and aging.* Nat Neurosci, 2020. **23**(6): p. 701-706.

221. Satoh, J., N. Kawana, and Y. Yamamoto, *Pathway Analysis of ChIP-Seq-Based NRF1 Target Genes Suggests a Logical Hypothesis of their Involvement in the Pathogenesis of Neurodegenerative Diseases.* Gene Regul Syst Bio, 2013. **7**: p. 139-52.

222. Bu, X.L., et al., *A study on the association between infectious burden and Alzheimer's disease.* Eur J Neurol, 2015. **22**(12): p. 1519-25.

223. Douros, A., et al., *Infectious Disease Burden and the Risk of Alzheimer's Disease: A Population-Based Study.* J Alzheimers Dis, 2021. **81**(1): p. 329-338.

224. Eidson, L.N., et al., *Candidate inflammatory biomarkers display unique relationships with alpha-synuclein and correlate with measures of disease severity in subjects with Parkinson's disease.* J Neuroinflammation, 2017. **14**(1): p. 164.

225. Rail, D., C. Scholtz, and M. Swash, *Post-encephalitic Parkinsonism: current experience.* J Neurol Neurosurg Psychiatry, 1981. **44**(8): p. 670-6.

226. Arts, R.J.W., et al., *BCG Vaccination Protects against Experimental Viral Infection in Humans through the Induction of Cytokines Associated with Trained Immunity.* Cell Host Microbe, 2018. **23**(1): p. 89-100 e5.

227. Streit, W.J., et al., *Dystrophic (senescent) rather than activated microglial cells are associated with tau pathology and likely precede neurodegeneration in Alzheimer's disease.* Acta Neuropathol, 2009. **118**(4): p. 475-85.

228. Hanamsagar, R. and S.D. Bilbo, *Sex differences in neurodevelopmental and neurodegenerative disorders: Focus on microglial function and neuroinflammation during development.* J Steroid Biochem Mol Biol, 2016. **160**: p. 127-33.

229. Yan, X., et al., *Metabolic Dysregulation Contributes to the Progression of Alzheimer's Disease.* Front Neurosci, 2020. **14**: p. 530219.

APPENDIX

A1 Statement of Contributions

As these studies are collaborative projects and were partially started already before I joined the lab, there were other people involved in every part of them.

A1.1 Microglial Reprogramming during Healthy Aging and AD

scRNA-Seq (SeqWell, SmartSeq2)

I took over this project in 2019 and was from then on responsible for microglia isolation and library preparations of SeqWell and SmartSeq2.

The people doing the first batches of microglia isolation for scRNA-Seq were Dr. Ann-Christin Wendeln, Dr. Jessica Wagner, Lisa Steinbrecher, and Katleen Wild. Ann-Christin also did the first batches of Library-Preparation for SeqWell before I took over the project in 2019. Lisa Steinbrecher was also responsible for the HIF-1α knockout animals (breeding, Tamoxifen injections).

Our collaboration partners from DZNE Bonn also took care of library preparation, sequencing and alignment of all scRNA-Seq libraries. Namely, Dr. Collins Osei-Sarpong prepared the beads, membranes and arrays for SeqWell that Ann-Christin and I needed for the first steps of library preparation (Bead and cell loading, membrane sealing, cell lysis and hybridization, bead removal, reverse transcription and exonuclease digestion), before sending the cDNA to them for further processing. Collins then did the other steps of library preparation.

SmartSeq2-plates were prepared by Heidi Theis using an automatic system. Sequencing, demultiplexing and alignment for all samples was done at PRECISE by Dr. Kristian Händler.

scATAC-Seq

Every step of the scATAC-Seq workflow (animal preparation, nuclei isolation, library preparation) was done by myself, except for Cortex isolation which was done by Dr. Jonas Neher, and sequencing which was done at PRECISE by Dr. Kristian Händler.

Data analysis

Data analysis of all datasets was mainly done by myself, with help of different people from the Beyer and Schultze labs at the DZNE Bonn. Nico Reusch started the analysis of the first SeqWell-batches (before 2019). Other support regarding questions and/or issues that came up during analysis came from Jonas Schulte-Schrepping and Dr. Kristian Händler.

Marker gene validation

I selected different marker genes according to the scRNA-Seq data. Nina Hermann then mainly did the staining and image quantification during her Master's thesis under my supervision. Cutting of the PFA-fixed brains was done by Katleen Wild and Nina Hermann. Statistical analysis was done by myself.

A1.2 Influence of Peripheral Inflammatory Insults on the Brains Immune Response

The establishment of SHARE-Seq was done in parallel in two labs: In Tübingen by myself (later on together with Dr. Xidi Yuan) and in Bonn by Rebekka Scholz, whereby we were always in close contact and coordinated our work.

Brain Homogenization was mainly done by myself with some help of Nina Hermann and Dr. Xidi Yuan. Cytokine Measurements in Serum and Brain Homogenates were carried out and analyzed exclusively by myself. I was also responsible for the C57BL/6J mice (breeding, injections, dissections). At a later time in the project, I had help of Dr. Xidi Yuan for injections and dissections.

A2 Related Publications

Book Chapter:

Scholz R., **Brösamle D.**, Yuan X., Neher J., Beyer M. (2023), *Combined analysis of mRNA expression and open chromatin in microglia*, in *Tissue-resident macrophages: Methods and Protocols*. Methods in Molecular Biology [148].

A3 Abbreviations

AAM	**A**ging-**a**ssociated **m**icroglia
AD	**A**lzheimer's **D**isease
Apoe	**Apo**lipoprotein **E**
APP	**A**myloid **p**recursor **p**rotein
ARM	**A**ctivated **r**esponse **m**icroglia
Arnt	**A**ryl Hydrocarbon **R**eceptor **N**uclear **T**ranslocator
ASC	**As**troc**y**te
Aβ	**A**myloid-**β**
B2m	**B2**-**m**icroglobulin
BAM	**B**order **a**ssociated **m**acrophages
BBB	**B**lood **B**rain **B**arrier
BCG	***B**acillus **C**almette-**G**uérin*
BH	**B**enjamini **H**ochberg
CAA	**C**erebral **a**myloid **a**ngiopathy
Cbm	**C**ere**b**ellu**m**
CCA	**C**anonical **c**orrelation **a**nalysis
CCAN	***C**is*-**C**o-**a**ccessibility **N**etworks
cCRE	***C**is*-**C**o-**r**egulatory-**e**lement
CMRglc	**C**erebral **m**etabolic **r**ate of **gl**u**c**ose
CNS	**C**entral **n**ervous **s**ystem
Ctx	**C**or**te**x
DAM	**D**isease **a**ssociated **m**icroglia
DAR	**D**ifferentially **a**ccessible **r**egion
DEG	**D**ifferentially **e**xpressed **g**ene
DME	**D**ifferential **m**odule **e**igenenes
dpi	**D**ays **p**ost **i**nfection
FA	**F**orm**a**ldehyde
FACS	**F**luorescent-**a**ctivated **c**ell **s**orting
FAD	**F**amilial **A**lzheimer's **D**isease
FDR	**F**alse **d**iscovery **r**ate
GO	**G**ene **o**ntology
GWAS	**G**enome-**w**ide **a**ssociation **s**tudies
HDAC	**H**istone **dea**cetylase
hdWGCNA	**H**igh-**d**imensional **w**eighted **g**ene **c**o-expression **n**etwork **a**nalysis

HIF	**H**ypoxia **i**nducible **f**actor
HM	**H**omeostatic **m**icroglia
Hp	**Hip**pocampus
hpi	**H**ours **p**ost **i**nfection
IL	**I**nter**l**eukin
ImmGen	**Imm**unological **Gen**ome
IRM	**I**nterferon **r**esponse **m**icroglia
KEGG	**K**yoto **E**nzyclopedia of **G**enes and **G**enomes
KNN	**K**-**n**earest **n**eighbor
KO	**K**nock**o**ut
LOAD	**L**ate **o**nset **A**lzheimer's **D**isease
LPS	**L**ipo**p**oly**s**accharide
lsi	**L**atent **s**emantic **i**ndexing
MAPT	**M**icrotubule-**a**ssociated **p**rotein **t**au
ME	**M**odule **e**igengenes
MG	**M**icro**g**lia
MHC	**M**ajor **H**istocompatibility **c**omplex
MX04	**M**ethxy-**XO4**
NDD	**N**euro**d**egenerative **D**isease
Nfat	**N**uclear **f**actor of **a**ctivated **T** cells
Nfe2l2	**N**uclear **f**actor 2 **e**rythroid **2** **l**ike **2**
NFT	**N**euro**f**ibrillary **t**angle
NGS	**N**ext **g**eneration **s**equencing
Nrf	**N**uclear **r**espiratory **f**actor
NSAID	**N**on-**s**teroidal **a**nti-**i**nflammatory **d**rugs
ODC	**O**ligo**d**endro**c**yte
OPC	**O**ligodendro**c**yte **p**recursor
PAM	**P**laque-**a**ssociated **m**icroglia
PCA	**P**rincipal **c**omponent **a**nalysis
PCR	**P**olymarease **c**hain **r**eaction
PFA	**P**ara**f**orm**a**ldehyde
Poly(I:C)	**Poly**inosinic-polycytidylic acid
PSEN	**P**re**sen**ilin
RI	**R**Nase **I**nhibitor
RNA-seq	**RNA**-**seq**uencing
ROS	**R**eactive **o**xygen **s**pecies

RT	**R**everse **T**ranscription
S.a.	***S**taphylococcus **a**ureus*
SAGE	**S**erial **a**nalysis of **g**ene **e**xpression
SASP	**S**enescence-**a**ssociated **s**ecretory **p**henotype
scATAC-Seq	**S**ingle-**c**ell **a**ssay for **t**ransposase-**a**ccessible **c**hromatin with **seq**uencing
scRNA-Seq	**S**ingle-**c**ell **RNA seq**uencing
SHARE-Seq	**S**imultaneous high-throughput ATAC and RNA expression with sequencing
snRNA-seq	**S**ingle-**n**uclei **RNA**-**seq**uencing
SS2	**S**mart**S**eq **2**
Stat	**Stat**in
TF	**T**ranscription **f**actor
TFIDF	**T**erm-**f**requency **i**nverse-**d**ocument-**f**requency
Tg	**T**rans**g**enic
TGF-β	**T**ransforming **g**rowth **f**actor **β**
TLR	**T**oll-**l**ike **r**eceptor
TNF-α	**T**umor **n**ecrosis **f**actor **α**
Trem2	**T**riggering **r**eceptor **e**xpressed on **m**yeloid cells **2**
TRM	**T**NF-α **r**esponse **m**icroglia
tSNE	**S**tochastic **n**eighbor **e**mbedding
TSS	**T**ranscription **s**tart **s**ite
UMAP	**U**niform **m**anifold **a**pproximation and **p**rojection
UTR	**U**n**t**ranslated **r**egion
WT	**W**ild**t**ype
WTA	**W**hole **t**ranscriptome **a**mplification
Y.e.	***Y**ersinia **e**nterocolitica*